Supplementary Information

A halide methyltransferase family unites methyl-donor regeneration and methylation in a single scaffold

Junxi Chi[1,2,3,#], Peishan Li[4,#], Shaixiao Tian[5,#], Zhi-Min Zhang*[4], Jian-bo Wang*[1,2,3,5]

[1]Department of Microbiology, Zhejiang University School of Medicine, Hangzhou, 310058, P. R. China. [2]Key Laboratory of Multiple Organ Failure (Zhejiang University), Ministry of Education, Department of General Intensive Care Unit of the Second Affiliated Hospital (Zhejiang University), Zhejiang University School of Medicine, Hangzhou, 310058, P. R. China. [3]Institute of Pharmaceutical Biotechnology Zhejiang University School of Medicine, Hangzhou, 310058, P. R. China. [4]State Key Laboratory of Bioactive Molecules and Draggability Assessment, Jinan University, Guangzhou, 511436, P. R. China. [5]Key Laboratory of Chemical Biology and Traditional Chinese Medicine Research (Ministry of Education) and Key Laboratory of Phytochemistry R&D of Hunan Province, College of Chemistry and Chemical Engineering, Hunan Normal University, Changsha, 410081, P. R. China.

[#]These authors contributed equally: Junxi Chi, Peishan Li, and Shaixiao Tian.

***Correspondence:** jwang2023@zju.edu.cn; zhangzm@jnu.edu.cn

Table of Contents

Supplementary Tables

Supplementary Table 1 | Mutants in this study.

Variants	Mutations
***Ate*HMT**	
*Ate*HMT-VG	M11V/V264G
*Ate*HMT-VVG	K4V/M11V/V264G
*Ate*HMT-VLVG	K4V/A5L/M11V/V264G
*Ate*HMT-C167A	C167A
***Acl*HMT**	
*Acl*HMT^{mut}	P4V/S5L/V264G
***Aho*HMT**	
*Aho*HMT^{mut}	K6V/A7L
***Ati*HMT**	
*Ati*HMT^{mut}	K5V/A6L
***Ale*HMT**	
*Ale*HMT^{mut}	K5V/A6L
***Aam*HMT**	
*Aam*HMT^{mut}	K4V/A5L/V264G

Supplementary Table 2 | Strains and plasmids in this study.

Strain or plasmid	Characteristics
Strains	
E. coli TOP 10	General cloning host strain
E. coli BL21 (DE3)	Protein production host strain
Plasmids	
pET28a	Km, vector for protein expression
pET28a-atehmt	Km, plasmid for *Ate*HMT-WT expression
pET28a-*aphmt*	Km, plasmid for *Ap*HMT-WT expression
pET28a-*athhmt*	Km, plasmid for *Ath*HMT-WT expression
pET28a-*anahmt*	Km, plasmid for *Ana*HMT-WT expression
pET28a-*pphmt*	Km, plasmid for *Pp*HMT-WT expression
pET28a-*sghmt*	Km, plasmid for *Sg*HMT-WT expression
pET28a-*atehmt*-C167A	Km, plasmid for *Ate*HMT-C167A expression
pET28a-*atehmt*-M11V	Km, plasmid for *Ate*HMT-M11V expression
pET28a-*atehmt*-V264G	Km, plasmid for *Ate*HMT-V264G expression
pET28a-*atehmt*-VG	Km, plasmid for *Ate*HMT-VG expression
pET28a-*atehmt*-VVG	Km, plasmid for *Ate*HMT-VVG expression
pET28a-*atehmt*-VLVG	Km, plasmid for *Ate*HMT-VLVG expression
pET28a-*ainhmt*	Km, plasmid for *Ain*HMT-WT expression

pET28a-*auvhmt*	Km, plasmid for *Auv*HMT-WT expression
pET28a-*alehmt*	Km, plasmid for *Ale*HMT-WT expression
pET28a-*abrhmt*	Km, plasmid for *Abr*HMT-WT expression
pET28a-*atihmt*	Km, plasmid for *Ati*HMT-WT expression
pET28a-*afihmt*	Km, plasmid for *Afi*HMT-WT expression
pET28a-*avihmt*	Km, plasmid for *Avi*HMT-WT expression
pET28a-*ajahmt*	Km, plasmid for *Aja*HMT-WT expression
pET28a-*ahohmt*	Km, plasmid for *Aho*HMT-WT expression
pET28a-*aamhmt*	Km, plasmid for *Aam*HMT-WT expression
pET28a-*aclhmt-mut*	Km, plasmid for *Acl*HMT-MUT expression
pET28a-*ahohmt-mut*	Km, plasmid for *Aho*HMT-MUT expression
pET28a-*atihmt-mut*	Km, plasmid for *Ati*HMT-MUT expression
pET28a-*alehmt-mut*	Km, plasmid for *Ale*HMT-MUT expression
pET28a-*aamhmt-mut*	Km, plasmid for *Aam*HMT-MUT expression
pApr-*g*RNA(*mtn*)	Apr, plasmid for a *g*RNA guiding CRISPR/Cas9 to *mtn* locus on *E. coli* genome expression
pRedCas9	Km, plasmid for CRISPR/Cas9 system and λ-RED proteins expression

Supplementary Table 3 | Primers used in this study.

Primer	Sequence (5'-3')
*Ate*HMT-F	TCGCGGATCCATGCCGCCGAAAGCGGTGG
*Ate*HMT-R	TGCTCGAGAGGTTAGCGACGGCGCCACAC
P210A-F	CCGGGCCCGGCGTGGGGCAGCAGTAGCG
P210A-R	GCCCCACGCCGGGCCCGGTTTGCTC
W40A-F	CGGCGATTGCCTGCCGGCGGATCGCGGCGTGCCGAACCC
W40A-R	TCGGCACGCCGCGATCCGCCGGCAGGCAATCGCCGCCTTTC
C167A-F	ACCTTTTTTGCGGCGCTGAACCCGAGCATG
C167A-R	GTTCAGCGCCGCAAAAAAGGTATAATCATAAATCAGATCAAAGC
R200A-F	GAATTTCCGGCGCATAAAGATCCGAGCAAACCGG
R200A-R	TTTATGCGCCGGAAATTCCAGGCAAATCAGG
T164A-F	TATGATTATGCGTTTTTTTGCGCGCTGAACCCG
T164A-R	GCAAAAAAACGCATAATCATAAATCAGATCAAAGCAGTTCAGC
F198A-F	TGCCTGGAAGCGCCGCGCCATAAAGATCCG
F198A-R	TTTATGGCGCGGCGCTTCCAGGCAAATCAGGTTGC
C167NNK-F	ACCTTTTTTTNNKGCGCTGAACCCGAGCATG
C167NNK-R	GTTCAGCGCMNNAAAAAAGGTATAATCATAAATCAGATCAAAGC
A168NNK-F	TTTTTTGCNNKCTGAACCCGAGCATGC
A168NNK-R	CTCGGGTTCAGMNNGCAAAAAAAGGTATAATC
W27NNK-F	TTGATGGCNNKGAAGAACTGTGGCAGAAAGGC
W27NNK-R	CCACAGTTCTTCMNNGCCATCAAACACGCGATC
M11NNK-F	CGCAAGAANNKCTGGATACCCTGGGCAAATATCAAGGC

M11NNK-R	AGGGTATCCAGMNNTTCTTGCGGCGCCACCG
P39NNK-F	ATTGCCTGNNKTGGGATCGCGGCGTGCC
P39NNK-R	GCGATCCCAMNNCAGGCAATCGCCGCCTTTC
W40NNK-F	TTGCCTGCCGNNKGATCGCGGCGTGCCGAACC
W40NNK-R	CCGCGATCMNNCGGCAGGCAATCGCCGC
L38NNK-F	GGCGATTGCNNKCCGTGGGATCGCGGCGTG
L38NNK-R	ATCCCACGGMNNGCAATCGCCGCCTTTCTGCC
V264NNK-F	ACCCATGAANNKGGCAAAGATGCGGAAGGCG
V264NNK-R	CTTTGCCMNNTTCATGGGTGCGCGCCG
T164NNK-F	TATGATTATNNKTTTTTTTGCGCGCTGAACCCG
T164NNK-R	GCAAAAAAAMNNATAATCATAAATCAGATCAAAGCAGTTCAGC
P209NNK-F	ACCGGGCNNKCCGTGGGGCAGCAGTAGC
P209NNK-R	TGCTGCCCCACGGMNNGCCCGGTTTGCTCGGATC
P210NNK-F	GGCCCGNNKTGGGGCAGCAGTAGCGAAG
P210NNK-R	CTGCTGCCCCAMNNCGGGCCCGGTTTGCTCG
R200NNK-F	GAATTTCCGNNKCATAAAGATCCGAGCAAACCGG
R200NNK-R	TTTATGMNNCGGAAATTCCAGGCAAATCAGG
F165NNK-F	CGCGCAAAANNKGGTATAATCATAAATCAGATCAAAGCAGTTC
F165NNK-R	GATTATACCMNNTTTTGCGCGCTGAACCCG
Y163NNK-F	ATTTATGATNNKACCTTTTTTTGCGCGCTGAACC
Y163NNK-R	AAAAAAGGTMNNATCATAAATCAGATCAAAGCAGTTCAGC
L196NNK-F	CTGATTTGCNNKGAATTTCCGCGCCATAAAGATCCG
L196NNK-R	CGGAAATTCMNNGCAAATCAGGTTGCCGTTCGG
F198NNK-F	TGCCTGGAANNKCCGCGCCATAAAGATCCGAG
F198NNK-R	ATGGCGCGGMNNTTCCAGGCAAATCAGGTTGCCG
Q273NNK-F	GGCGAAATTNNKGATCGCGTGAGCGTGTGGCG
Q273NNK-R	CACGCGATCMNNAATTTCGCCTTCCGCATCTTTGC
D274NNK-F	GAAATTCAANNKCGCGTGAGCGTGTGGCGC
D274NNK-R	GCTCACGCGMNNTTGAATTTCGCCTTCCGCATCTTTG
G265NNK-F	CATGAAGTGNNKAAAGATGCGGAAGGCGAAATTC
G265NNK-R	CGCATCTTTMNNCACTTCATGGGTGCGCGC
N46NNK-F	GGCGTGCCGNNKCCGGCGCTGGAAGATACCC
N46NNK-R	CAGCGCCGGMNNCGGCACGCCGCGATCC
H262NNK-F	GCGCGCACCNNKGAAGTGGGCAAAGATGCGGAAG
H262NNK-R	ATCTTTGCCCACTTCMNNGGTGCGCGCCGGCTGC
T261NNK-F	CCGGCGCGCNNKCATGAAGTGGGCAAAGATGCG
T261NNK-R	CACTTCATGMNNGCGCGCCGGCTGCCAATACG
K4NNK-F	ATGCCGCCGNNKGCGGTGGCGCCGCAAGAAATG
K4NNK-R	CGCCACCGCMNNCGGCGGCATGGATCCGCG
V6NNK-F	CCGAAAGCGNNKGCGCCGCAAGAAATGCTGG
V6NNK-R	TTGCGGCGCMNNCGCTTTCGGCGGCATGGATC
A7NNK-F	AAAGCGGTGNNKCCGCAAGAAATGCTGGATACC
A7NNK-R	TTCTTGCGGMNNCACCGCTTTCGGCGGTCATG

P8NNK-F	GCGGTGGCGNNKCAAGAAATGCTGGATACCCTGGG
P8NNK-R	CATTTCTTGMNNCGCCACCGCTTTCGGCG
L15NNK-F	CTGGATACCNNKGGCAAATATCAAGGCGATCGC
L15NNK-R	ATATTTGCCMNNGGTATCCAGCATTTCTTGCGG
C37NNK-F	GGCGGCGATNNKCTGCCGTGGGATCGCGG
C37NNK-R	CCACGGCAGMNNATCGCCGCCTTTCTGCC
D41NNK-F	CTGCCGTGGNNKCGCGGCGTGCCGAACCCG
D41NNK-R	CACGCCGCGMNNCCACGGCAGGCAATCGC
R42NNK-F	CCGTGGGATNNKGGCGTGCCGAACCCGGCG
R42NNK-R	CGGCACGCCMNNATCCCACGGCAGGCAATC
L169NNK-F	TTTTGCGCGNNKAACCCGAGCATGCGCCCGG
L169NNK-R	GCTCGGGTTMNNCGCGCAAAAAAAGGTATAATC
E197NNK-F	ATTTGCCTGNNKTTTCCGCGCCATAAAGATCC
E197NNK-R	GCGCGGAAAMNNCAGGCAAATCAGGTTGCC
G208NNK-F	AGCAAACCGNNKCCGCCGTGGGGCAGCAGTAG
G208NNK-R	CCACGGCGGMNNCGGTTTGCTCGGATCTTTATGG
W211NNK-F	GGCCCGCCGNNKGGCAGCAGTAGCGAAGCG
W211NNK-R	ACTGCTGCCMNNCGGCGGGCCCGGTTTGCTC
E263NNK-F	CGCACCCATNNKGTGGGCAAAGATGCGGAAG
E263NNK-R	TTTGCCCACMNNATGGGTGCGCGCCGGCTG
K266NNK-F	GAAGTGGGCNNKGATGCGGAAGGCGAAATTC
K266NNK-R	TTCCGCATCMNNGCCCACTTCATGGGTGCG
R275NNK-F	ATTCAAGATNNKGTGAGCGTGTGGCGCCGTC
R275NNK-R	CACGCTCACMNNATCTTGAATTTCGCCTTCCGC
*g*RNA-*mtn*-up-F	ATTAAGTGTATCCAGTAATTTAAGCTCTTTC
*g*RNA-*mtn*-up-R	CAGAGATAAGCGCAACCTCGGTTCC
*g*RNA-*mtn*-down-F	GGCAAATAAGCCCATGTCTGCCACAATTTCAAC
*g*RNA-*mtn*-down-R	ACTTCGAAGCATTTGTTC AATGCTTGTCGCATC
N20-F	GGGATCGGTAAAGTCGCTGGTTTTAGAGCTAGAAATAGCAAGTTAAAATAAGGC
N20-R	CAGCGACTTTACCGATGCCCACCGAGATCTGACTCCATAACAGAG

Supplementary Table 4 | General conditions for PCR.

Step	Condition	Cycle index
1	98 °C, 3 min	×1
2~4	98 °C, 10 sec; (Tm-5) °C, 5 sec; 68 °C, 10 sec/kb.	×28
5	68 °C, 10 min	×1

Supplementary Table 5 | HPLC methods used in this study.

Method	Solvent A	Solvent B	Gradient	Analysis substrates
A	Water containing 0.1% formic acid	Acetonitrile	20% B, 0.1-3.0 min; 20%-80% B, 3.1-8.0 min; 80% B, 8.1-14.0 min; 80%-20% B, 14.1-15.0 min; 20% B, 15.1-18.0 min.	**1A**, **1B-1H**
B	Water containing 0.1% formic acid	Acetonitrile	20% B, 0.1-3.0 min; 20%-90% B, 3.1-6.0 min; 90% B, 6.1-11.0 min; 90%-20% B, 11.1-12.0 min; 20% B, 12.1-15.0 min.	**1a**, **1b-1ad**

Supplementary Table 6 | Yields of *Ate*HMT Catalyzed 1A and 1a Reactions from Different Organisms

Enzyme	Organism	Ratio of 2A (%)	Ratio of 2a (%)
*Ap*HMT	*Aspergillus pseudoviridinutans*	N.D.	N.D.
*Ath*HMT	*Aspergillus thermomutatus*	N.D.	N.D.
*Ana*HMT	*Aspergillus nanangensis*	N.D.	N.D.
*Ate*HMT	*Aspergillus terreus*	2.54±0.52%	0.54±0.07%
*Pp*HMT	*Penicillium polonicum*	N.D.	N.D.
*Sg*HMT	*Sporisorium graminicola*	N.D.	N.D.

Supplementary Table 7 | The yield of *Ate*HMT mutants in the catalytic reaction of 1A and 1a.

	Yield of 2A (%)	Error bar	Yield of 2a (%)	Error bar
WT	2.54	0.52	0.45	0.07
C167A	41.33	1.08		
M11V			1.96	0.45
VG			10.21	0.93
VVG			19.71	1.24
VLVG			32.04	1.77

Supplementary Table 8 | Kinetic parameters

	STEP 1			STEP 2		
Enzyme	K_m (mM)	k_{cat} (min^{-1})	k_{cat}/K_m (min^{-1}* mM^{-1})	K_m (mM)	k_{cat} (min^{-1})	k_{cat}/K_m (min^{-1}* mM^{-1})
***Ate*HMT-WT**	2.71 ± 0.91	83.30 ± 8.80	30.74	N.D.	N.D.	N.D.
***Ate*HMT-C167A**	8.23 ± 1.31	323.80 ± 26.76	39.34	0.24 ± 0.03	0.09 ± 0.003	0.38
***Ate*HMT-VLVG**	3.64 ± 0.78	157.18 ± 15.84	43.18	0.05 ± 0.01	0.05 ± 0.002	1.00

Supplementary Table 9 | TON for 1A/1a Catalyzed by *Ate*HMT-C167A/*Ate*HMT-VLVG.

entry	reaction	enzyme	TON
1	**1A→2A**	*Ate*HMT-WT	<1
2	**1A→2A**	*Ate*HMT-VLVG	25
3	**1a→2a**	*Ate*HMT-WT	1
4	**1a→2a**	*Ate*HMT-C167A	19

Supplementary Table 10 | Data collection and refinement statistics.

	*Ate*HMT-VLVG-SAH-**1a** **(23CH)**	*Ate*HMT-C167A-SAH-**1A** **(23BZ)**	*Ate*HMT-C167A-SAH-CH_3I **(23CM)**	*Ate*HMT-SAH-**1A** **(23EE)**	*Ate*HMT-SAH-CH_3I **(23DI)**	*Ate*HMT-SAH **(23DH)**
Data collection						
Space group	$P2_1$	P1	P1	P1	P1	P1
Cell dimensions						
a, *b*, *c* (Å)	41.96 71.68 48.32	39.38 42.10 47.48	39.25 42.02 47.45	39.65 42.22 47.60	38.98 41.88 47.40	39.36 42.15 47.87
a, *b*, *γ* (°)	90 105.82 90	72.9 72.78 83.29	72.66 73.02 83.17	73.14 72.77 83.57	73.62 73.14 82.94	72.31 72.16 83.77
Resolution (Å)	71.68-1.85	40.22-2.00	43.60-2.00	43.77-2.20	43.81-2.50	33.62-1.97
*R*merge	0.069(0.306)	0.053(0.134)	0.119(0.288)	0.328(0.361)	0.120(0.427)	0.037(0.088)
$I/\sigma(I)$	18.54(5.13)	15.05 (7.06)	5.72 (2.71)	18.79 (4.66)	9.31 (2.58)	24.94 (14.80)
CC1/2	0.998(0.884)	0.996(0.972)	0.974(0.864)	0.873(0.821)	0.992(0.864)	0.997(0.970)
Completeness (%)	99.55(96.07)	93.65 (94.44)	91.05 (92.17)	98.52 (98.11)	90.32 (83.85)	95.76 (92.95)
Redundancy	6.2(3.8)	3.6(3.7)	2.3(2.3)	3.6 (3.5)	2.2(2.2)	3.5(3.0)
Refinement						
Resolution (Å)	35.84-1.85	40.22-2.00	43.60-2.00	37.85-2.25	43.81-2.50	37.46-1.97
No. reflections	23457	17605	17015	14098	8603	18902
*R*work / *R*free	0.1548/0.1972	0.1654/0.2030	0.1708/0.2240	0.1833/0.2383	0.1831/0.2233	0.1565/0.1977
No. atoms						
Protein	2200	2166	2174	2164	2165	2211
Ligand	53	44	34	44	28	32
Water	287	194	181	118	57	263
B factors						
Protein	14.90	17.10	18.94	29.08	33.41	7.42
Ligand	16.90	18.89	24.58	38.20	37.38	6.67
Water	23.26	22.70	23.90	33.48	29.50	15.31
R.m.s.deviations						
Bond lengths (Å)	0.007	0.003	0.008	0.003	0.002	0.007
Bond angles (°)	1.10	0.82	1.11	0.71	0.64	1.14

Supplementary Table 11 | BLASTP *Ate*HMT homologs in NCBI databases.

Description	Max Score	Total Score	Query Cover	Per. Ident	Accession
putative thiol methyltransferase ***Aam*HMT** [*Aspergillus ambiguus*]	540	540	100%	89.36%	XP_073551594.1
putative thiol methyltransferase ***Afi*HMT** [*Aspergillus fijiensis*]	458	458	97%	79.20%	XP_040800137.1
putative thiol methyltransferase ***Auv*HMT** [*Aspergillus melleus*]	456	456	100%	76.87%	XP_025494331.1
thiol methyltransferase ***Ain*HMT** [*Aspergillus indologenus*]	454	454	100%	76.51%	PYI30707.1
putative thiol methyltransferase ***Ale*HMT** [*Aspergillus aculeatus*]	461	461	99%	78.85%	XP_020054291.1
putative thiol methyltransferase ***Ati*HMT** [*Aspergillus aculeatinus*]	459	459	99%	78.49%	XP_025506030.1
putative thiol methyltransferase ***Aja*HMT** [*Aspergillus japonicus*]	450	450	100%	76.16%	XP_025532990.1
thiol methyltransferase **AviHMT** [*Aspergillus violaceofuscus*]	449	449	100%	75.80%	PYI22734.1
putative thiol methyltransferase ***Acl*HMT** [*Aspergillus clavatus*]	426	426	100%	72.34%	XP_001272206.1
putative thiol methyltransferase ***Aho*HMT** [*Aspergillus homomorphus*]	463	463	100%	77.94%	XP_025547253.1
putative thiol methyltransferase ***Abr*HMT** [*Aspergillus brunneoviolaceus*]	461	461	97%	79.93%	XP_025442544.1

Supplementary Figures

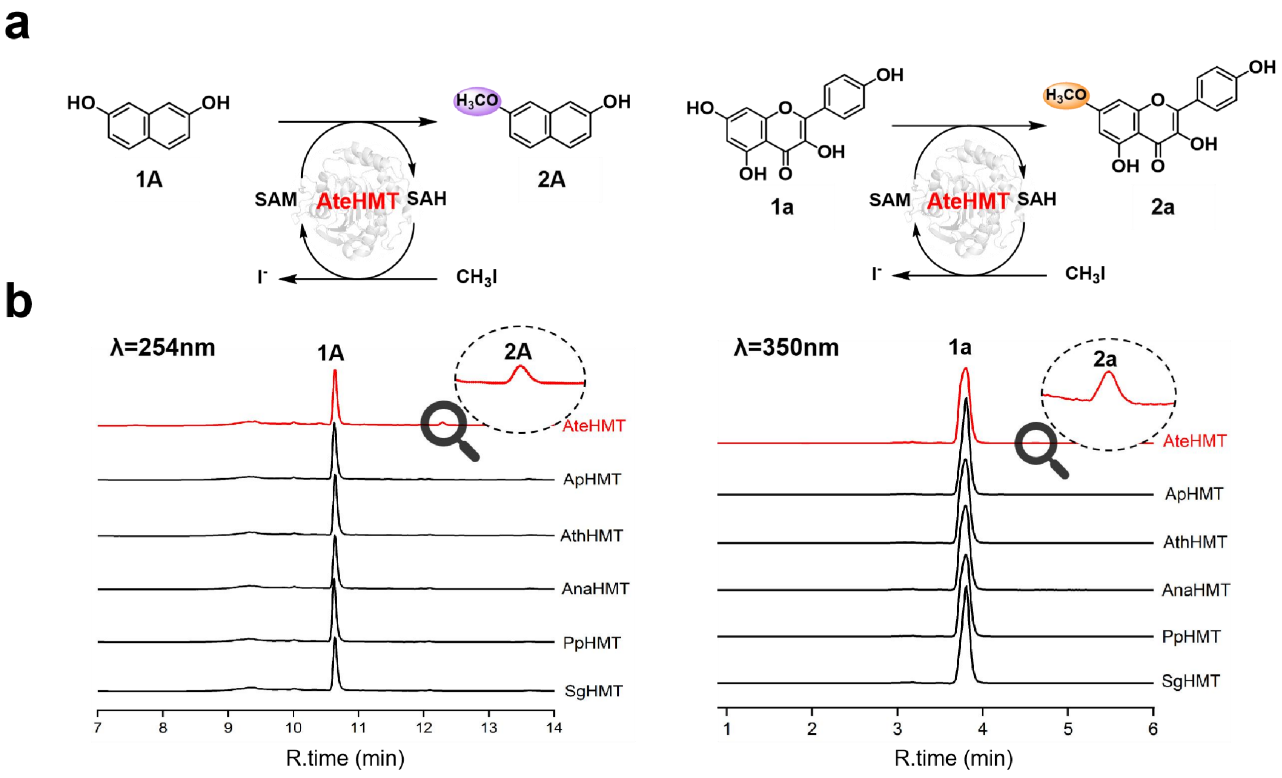

Supplementary Fig. 1 | Methylation of 1A and 1a catalyzed by the whole cell harboring HMTs from different organisms. a, Model reactions. **b**, HPLC chromatograms of substrates **1A** and **1a** and the corresponding methylated products **2A** and **2a**. Whole cells were resuspended in 100 mM potassium phosphate (KPi) buffer (pH 7.0) containing 3% (v/v) DMSO, and the cell density was adjusted to an OD_{600} of 40. Substrates **1A** or **1a**, SAH, and MeI were added to the reaction mixture at final concentrations of 1 mM, 1 mM, and 15 mM, respectively, in a total volume of 0.3 mL. Bioconversion reactions were conducted with shaking at 25 °C for 24 h.

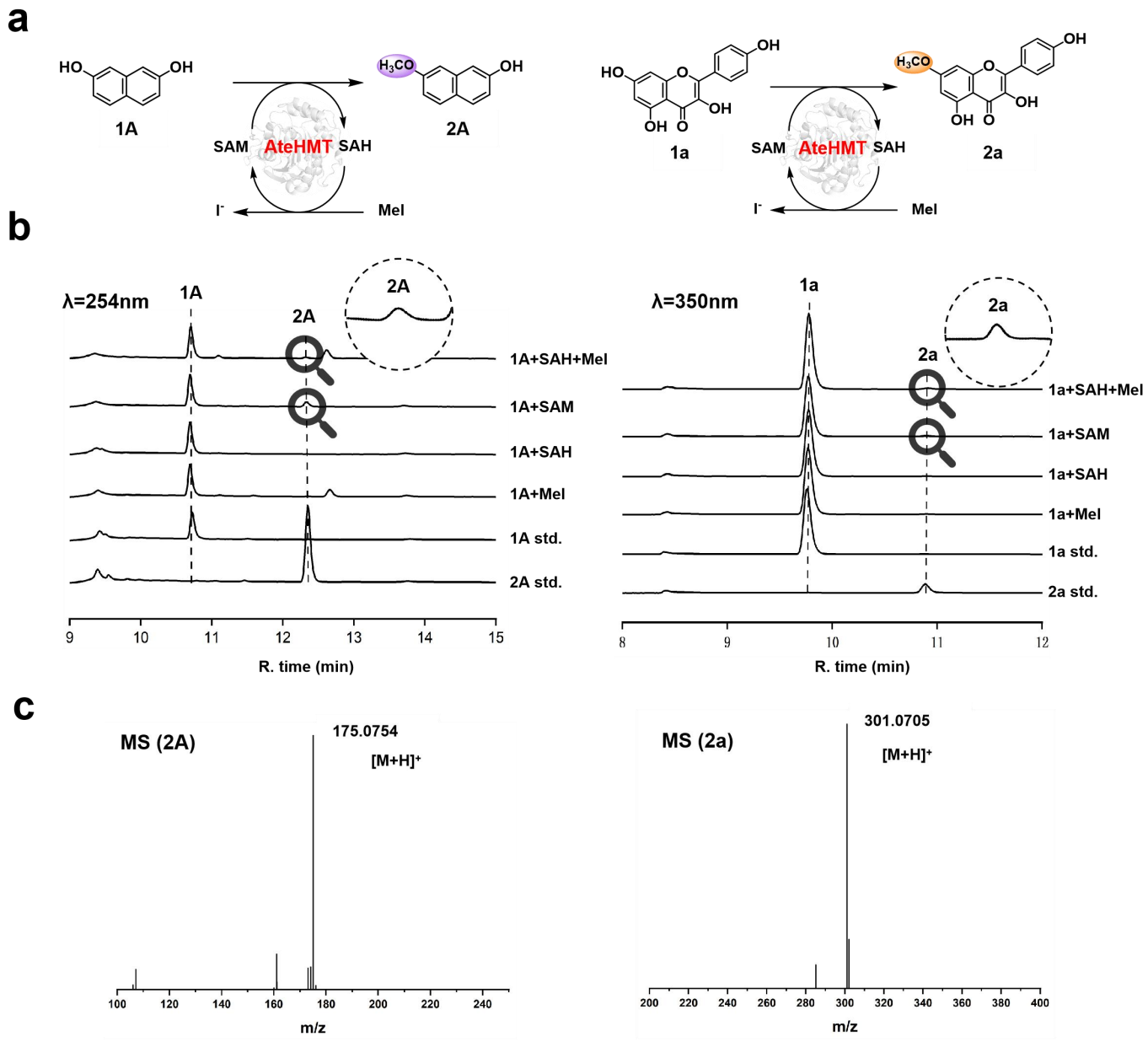

Supplementary Fig. 2 | *Ate*HMT mediated MeI-coupled substrate methylation. a, Model reactions: Conversion of 2,7-dihydroxynaphthalene (**1A**) to 7-methoxy-2-naphthol (**2A**) and kaempferol (**1a**) to rhamnocitrin (**2a**). **b**, HPLC analysis of methylation products from model reactions. **c**, (+)-ESI-MS confirming **2A** and **2a**.

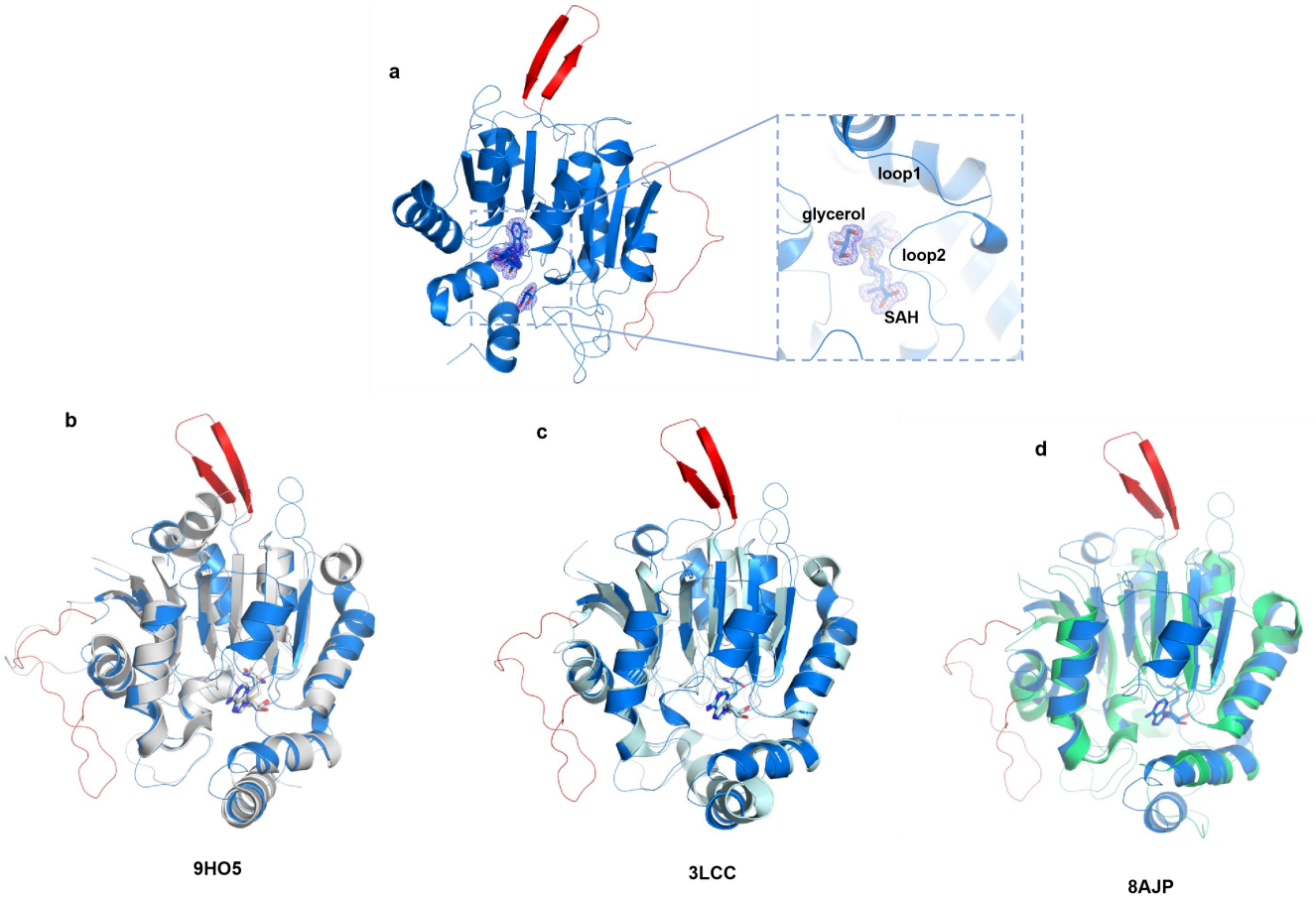

Supplementary Fig. 3 | Crystal structural of *Ate*HMT-WT-SAH complex(a) and structural comparison of *Ate*HMT with KIO (9HO5), *Ath*MT (PDB: 3LCC) and BXE (PDB: 8AJP). The two segments in *Ate*HMT that have no equivalent in other halide methyltransferases are colored in red. SAH and glycerol in all the structures are shown as stick. Blue mesh: The 2Fo-Fc omit map of SAH and glycerol is contoured at the σ-level = 1.0.[1-3]

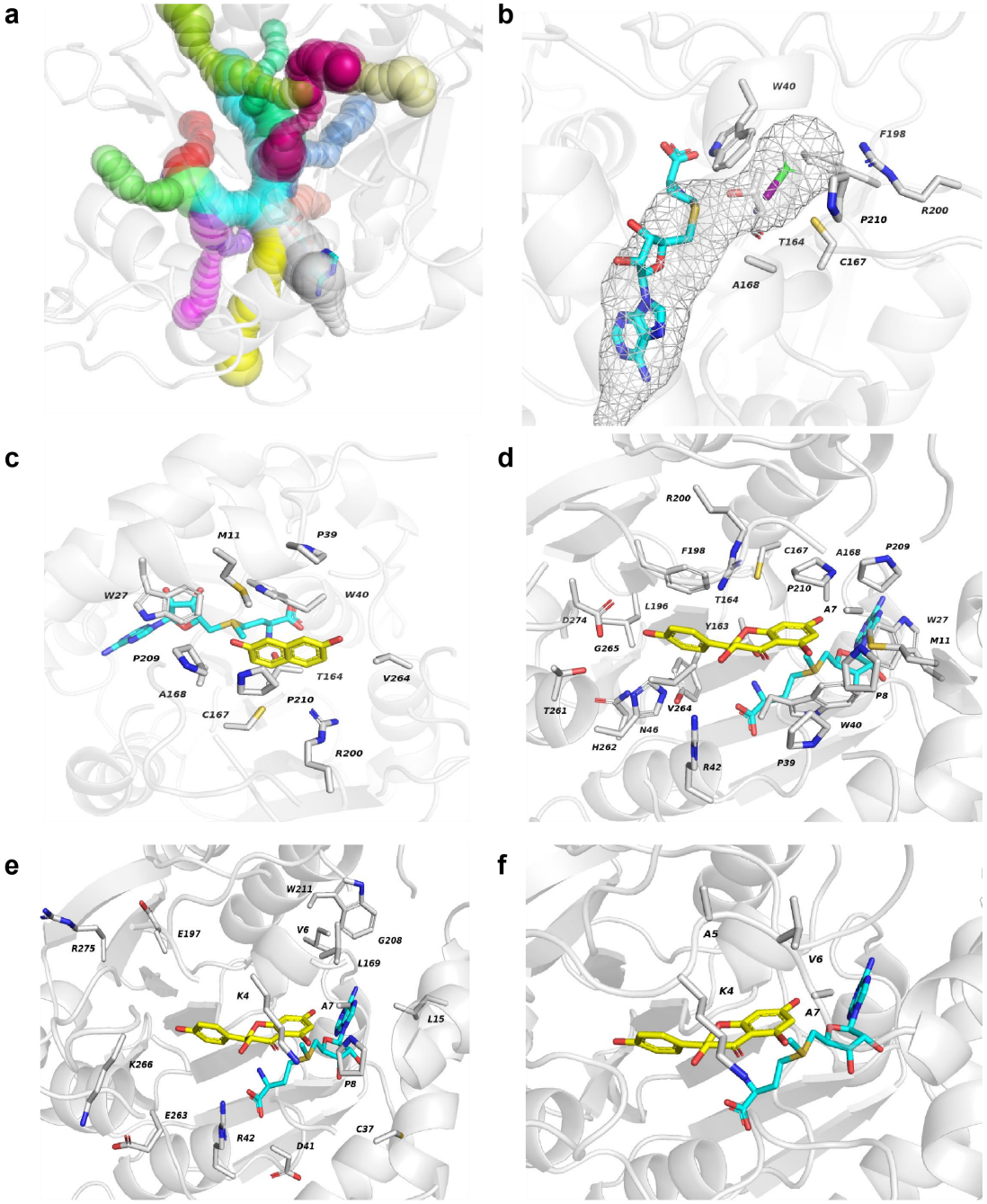

Supplementary Fig. 4 | Prediction of *Ate*HMT-WT substrate channel and molecular docking conformation of substrate 1A and 1a. a, CAVER 3.0.3[4] was used to predict tunnels for MeI entry into and exit from the enzyme active site, yielding a total of 15 potential tunnels. **b**, The shortest tunnel capable of accommodating both MeI and SAH was selected and is shown in grey. Amino acid residues located within 5 Å of this tunnel, in proximity to MeI, include P210, W40, C167, R200, T164, F198, and A168. **c**, Amino acid residues within the 5 Å range near substrate **1A**, including C167, A168, W27, M11, P39, W40, L38, V264, T164, P209, P210, R200 and F165. **d**, Amino acid residues within the 5 Å range near substrate **1a**, including A168, W27, M11, P39, W40, L38, C167, V264, T164, P209, P210, R200, F165, Y163, L196, F198, Q273, D274, G265, N46, H262 and T261. **e**, Amino acid residues within the 7 Å range near substrate **1a**, including K4, V6, A7, P8, L15, C37, D41, R42, L169, E197, G208, W211, E263, K266 and R275. **f**, Partial amino acid residues in the N-terminal loop region, including K4, A5, V6, and A7.

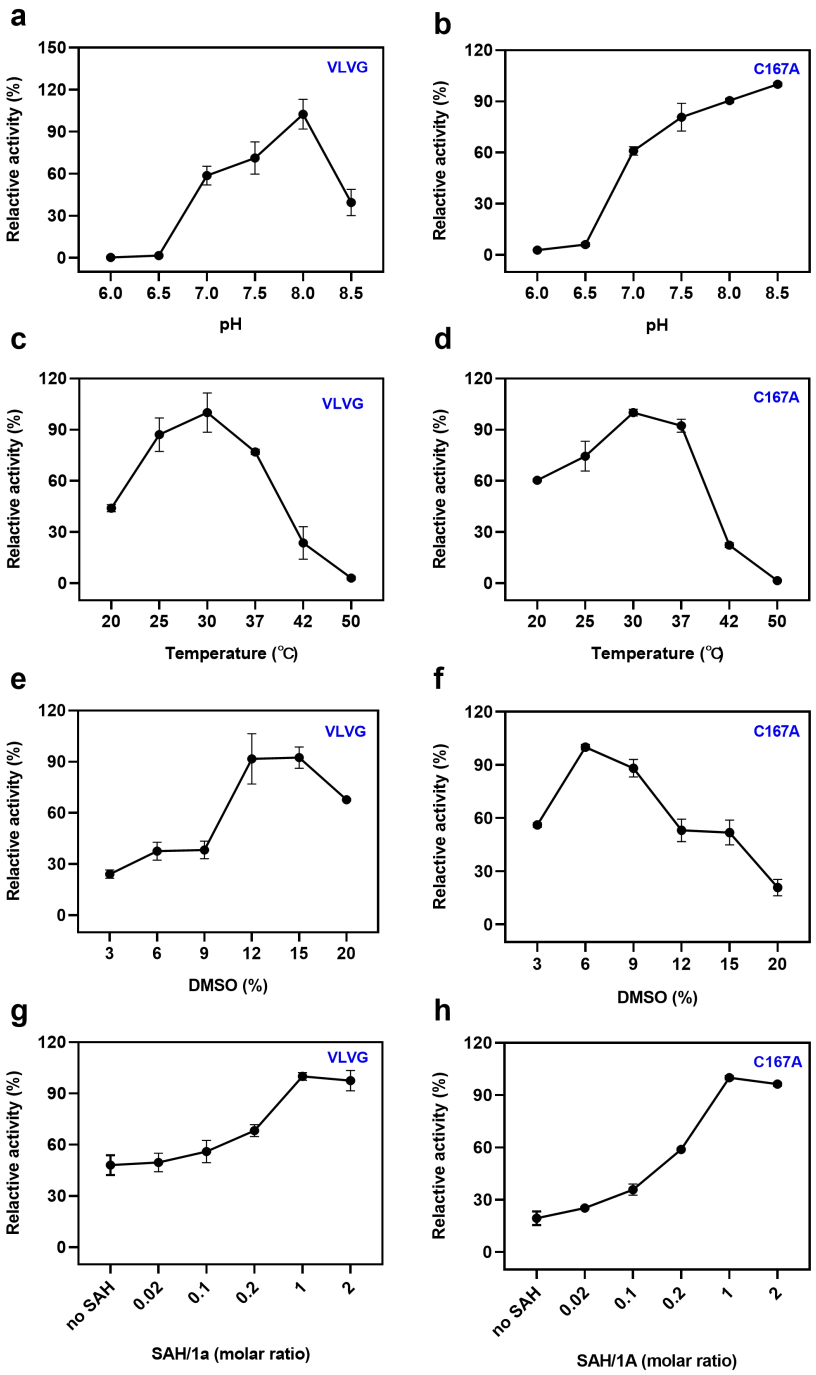

Supplementary Fig. 5 | Optimization of reaction conditions for 1A and 1a methylation catalysed by *Ate*HMT variants. a-b, Effect of pH in KPi buffer on enzymatic activity. **c-d,** Effect of reaction temperature on enzymatic activity. **e-f,** Effect of cosolvent (DMSO) concentration on enzymatic activity. **g-h**, Effect of the molar ratio of SAH to acceptor substrate on enzymatic activity (**1a**, kaempferol; **1A**, 2,7-dihydroxynaphthalene). When compound **1a** was used as the acceptor substrate, the optimal reaction conditions were identified as a 1:1 molar ratio of **1a** to SAH, pH 8.0, temperature 30 °C, and 15% (v/v) DMSO. When compound **1A** was used as the acceptor substrate, the optimal conditions were a 1:1 molar ratio of **1A** to SAH, pH 8.5, temperature 30 °C, and 6% (v/v) DMSO. All reactions were performed with whole cells adjusted to an OD_{600} of 40. Relative activities are reported as mean ± s.d. from three independent biological replicates (n = 3).

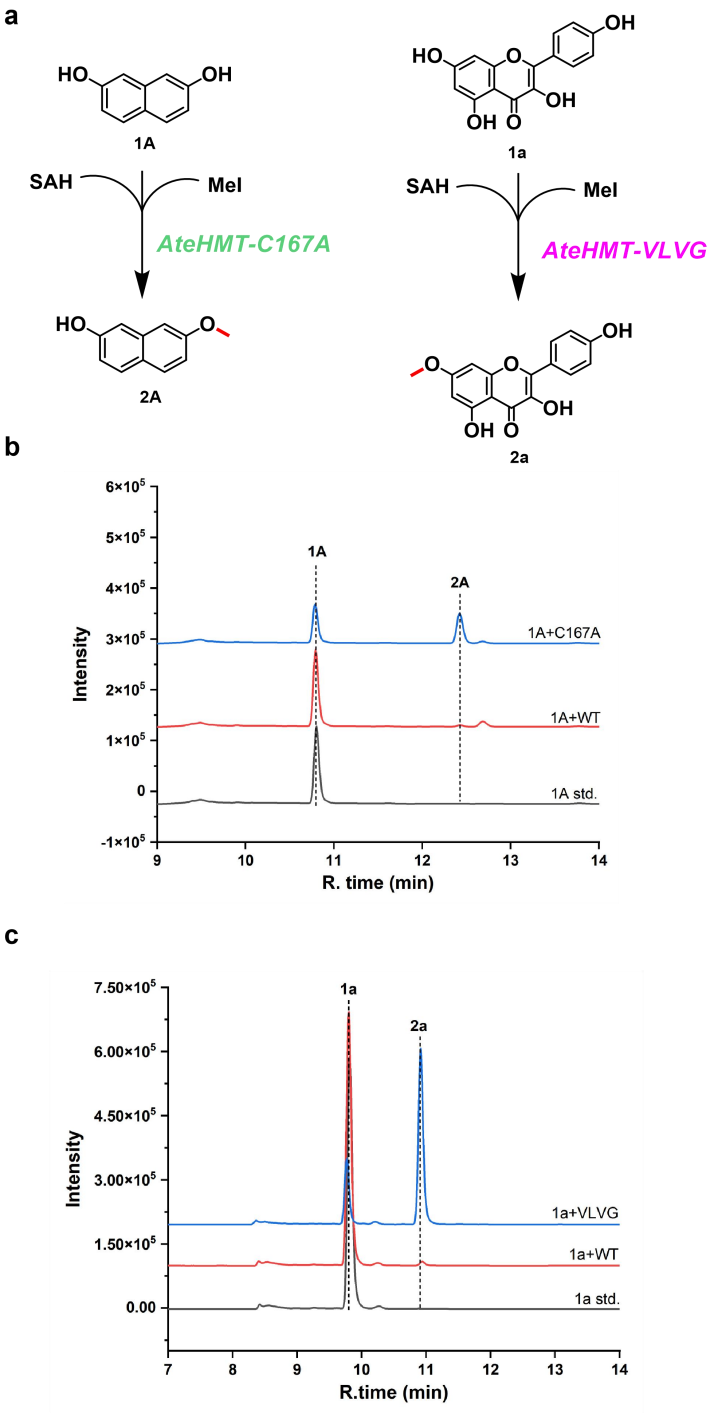

Supplementary Fig. 6 | Methylation activity of *Ate*HMT variants toward model substrates 1A and 1a for the production of 2A and 2a. Whole cells expressing *Ate*HMT variants were resuspended in 100 mM KPi buffer (pH 8.0) containing 6% or 15% (v/v) DMSO, with the cell density adjusted to an OD_{600} of 40. Substrates **1A** or **1a**, SAH, and MeI were added at final concentrations of 1 mM, 1 mM, and 15 mM, respectively, in a total reaction volume of 300 µL. Bioconversion reactions were carried out at 30 °C with shaking at 1,200 rpm for 24 h. Relative activities are reported as mean ± s.d. from three independent biological replicates (n = 3). WT: *Ate*HMT-WT; C167A: *Ate*HMT-C167A; VLVG: K4V/A5L/M11V/V264G or *Ate*HMT-VLVG.

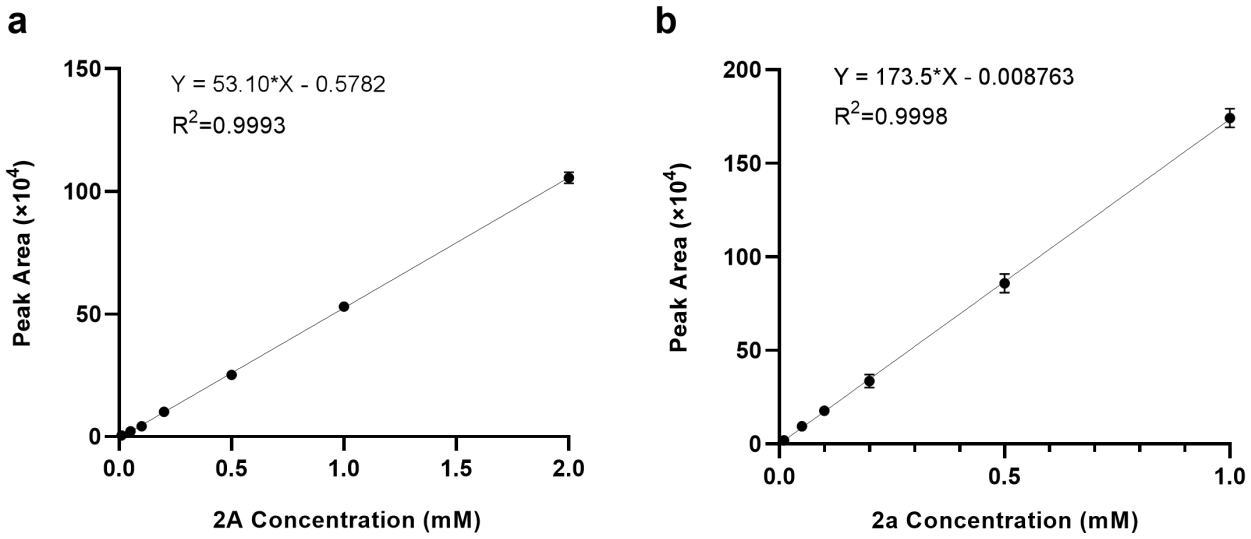

Supplementary Fig. 7 | Establishment of standard calibration curves for methyl products 2A and 2a.

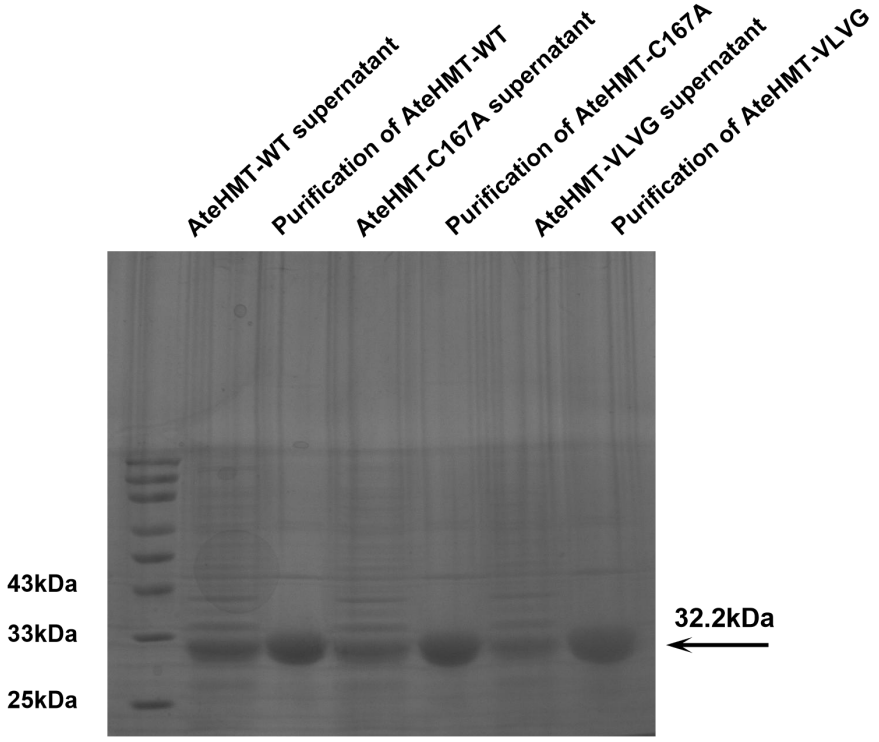

(uncropped image)

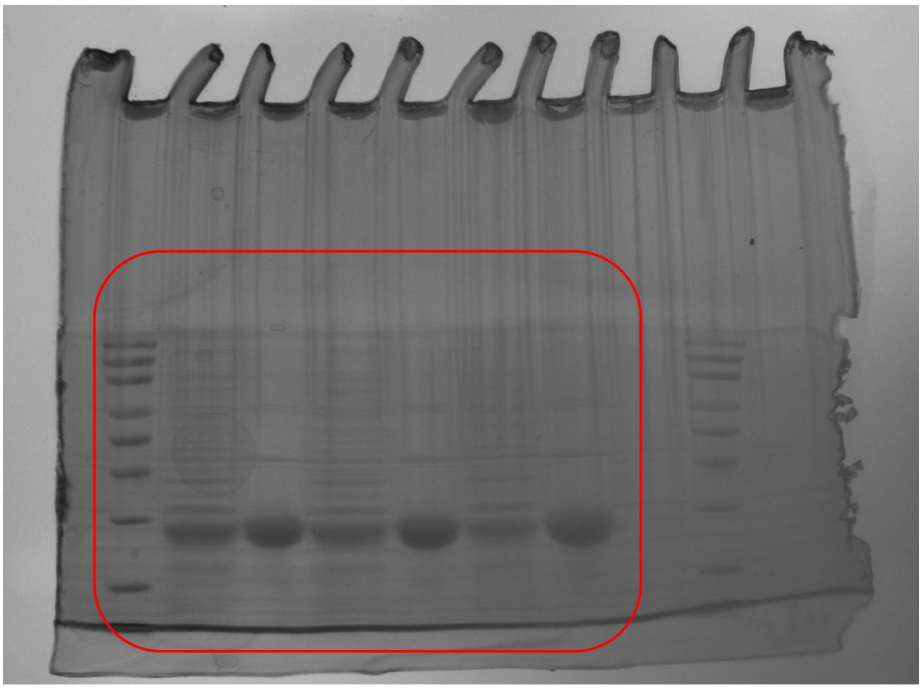

Supplementary Fig. 8 | SDS-PAGE analysis of purified recombinant 6His-tagged *Ate*HMT and its mutants.

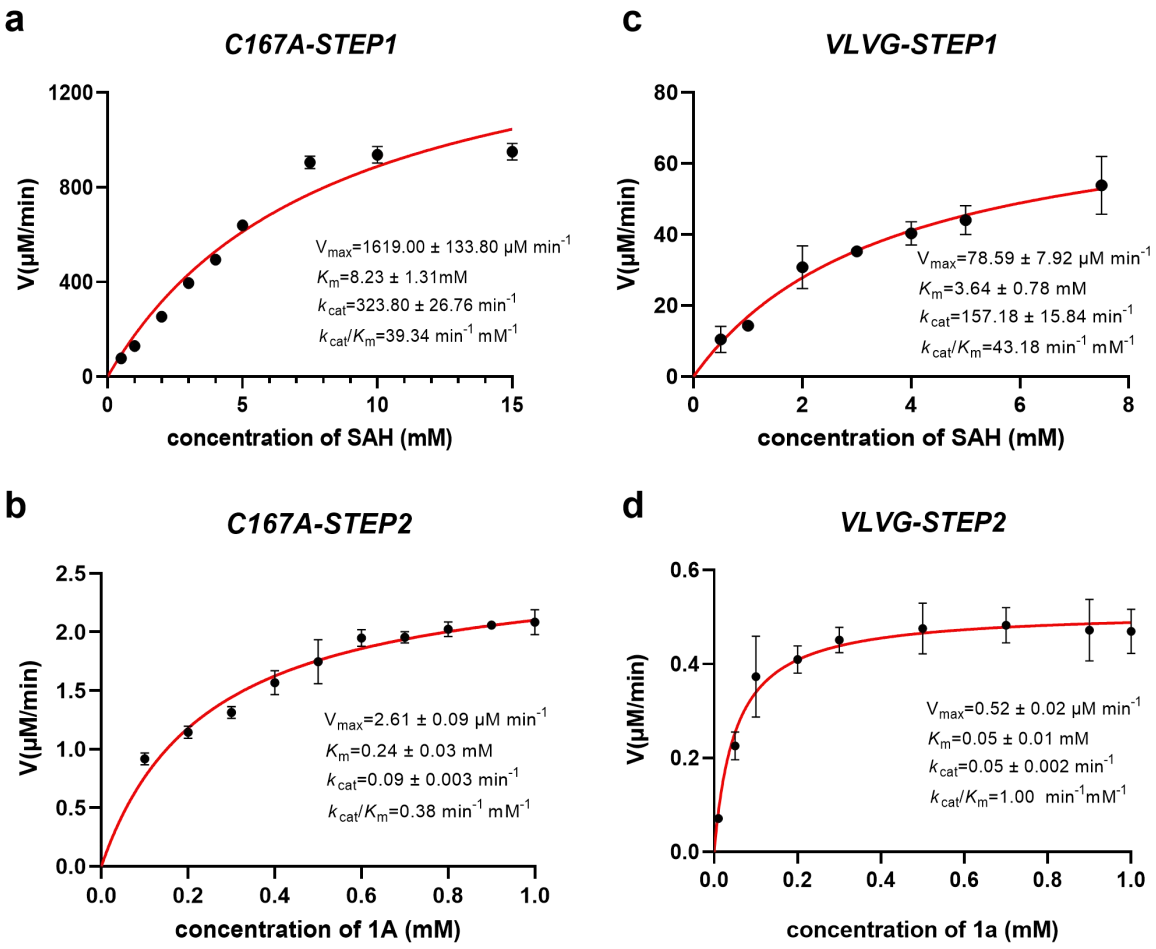

Supplementary Fig. 9 | Determination of kinetic parameters for the two sequential catalytic steps catalysed by *Ate*HMT-C167A and *Ate*HMT-VLVG. a–c, Step 1: MeI + SAH → SAM + I^-. Kinetic parameters were determined using SAH as the acceptor and MeI as the methyl donor at 30 °C, pH 8.0, with shaking at 1,200 rpm. **b–d**, Step 2: SAM + **1A** or **1a** → SAH + methylated product. Kinetic parameters were determined using **1A** or **1a** as the acceptor and SAM as the methyl donor under the same conditions. Data are presented as mean ± s.d. from three independent biological replicates (n = 3).

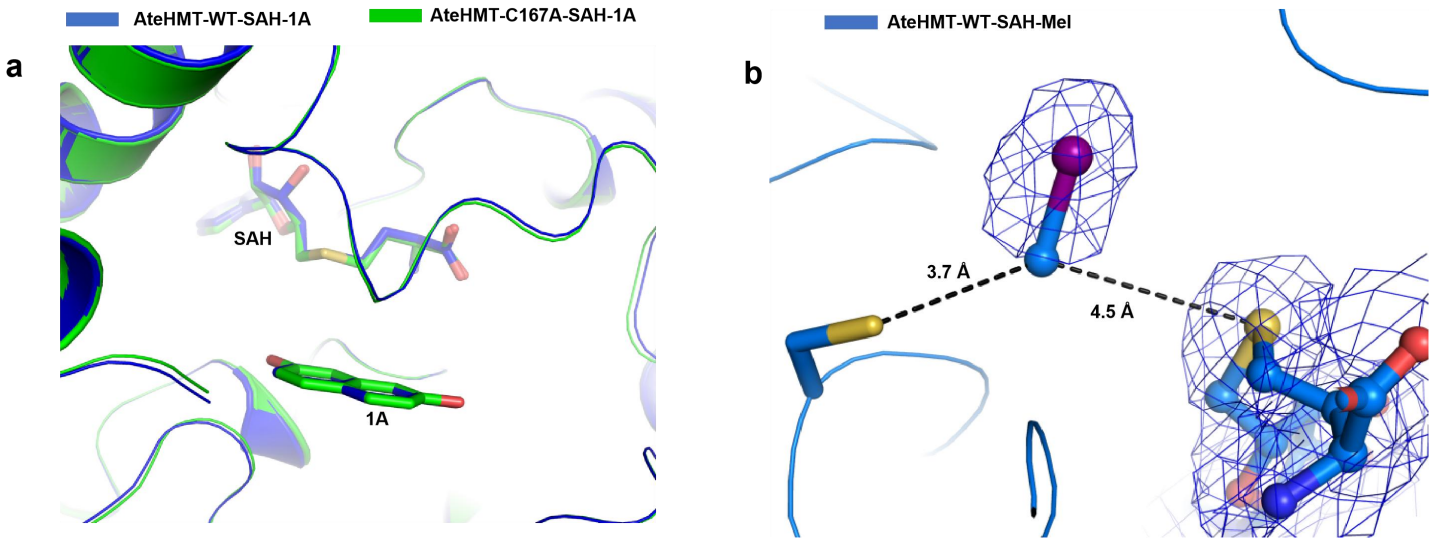

Supplementary Fig. 10 | The active site of *Ate*HMT in different complex structures. a, Overlap of the active site of *Ate*HMT-C167A-SAH-**1A** complex with that of *Ate*HMT-WT-SAH-**1A** complex. **b**, The binding sites of MeI in *Ate*HMT-WT-SAH-MeI complex. The distances are shown as black dashes.

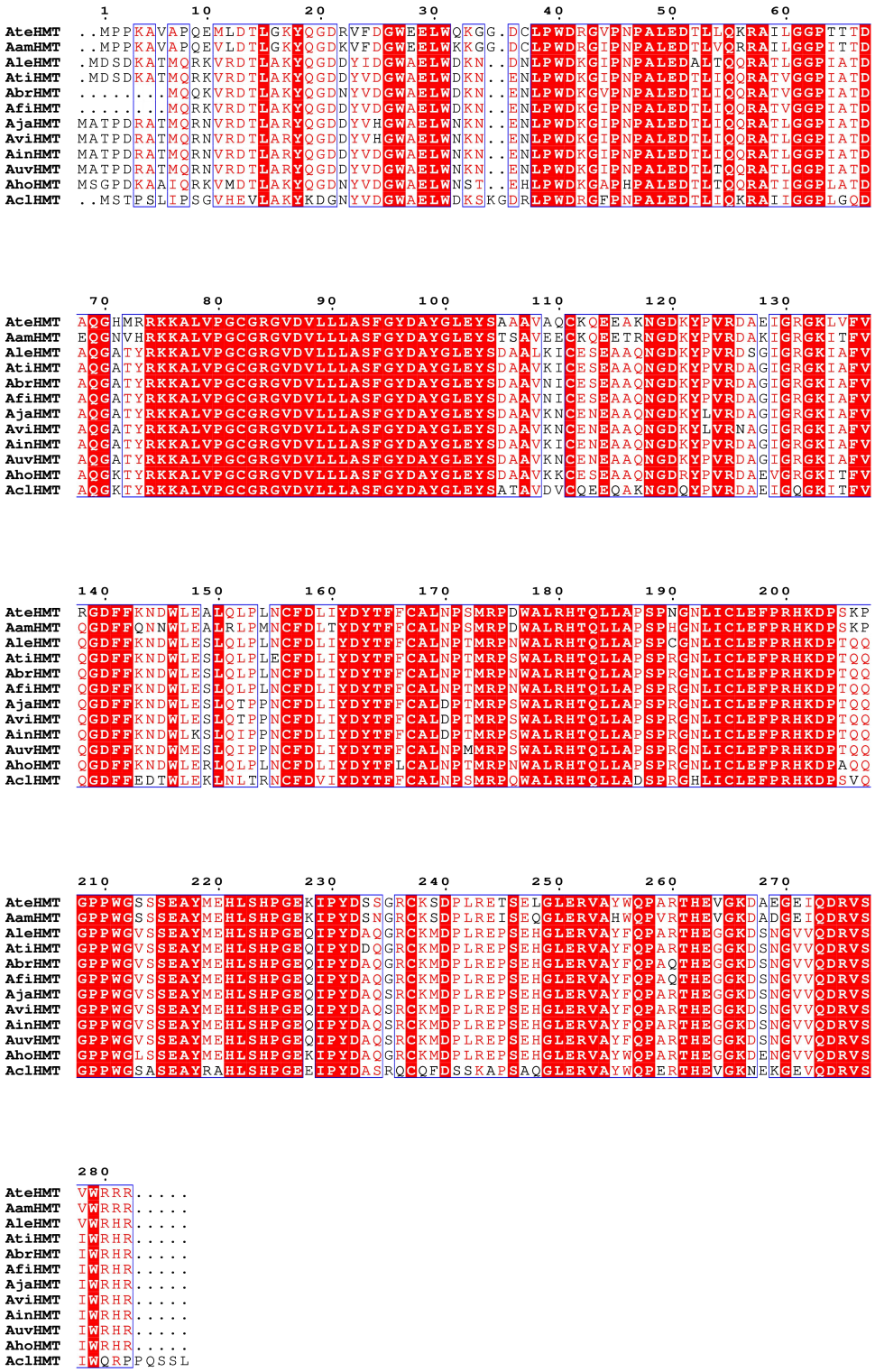

Supplementary Fig. 11 | Sequence alignments of *Ate*HMT with *Aam*HMT, *Aho*HMT, *Aja*HMT, *Avi*HMT, *Afi*HMT, *Ati*HMT, *Abr*HMT, *Ale*HMT, *Auv*HMT, *Ain*HMT and *Acl*HMT.

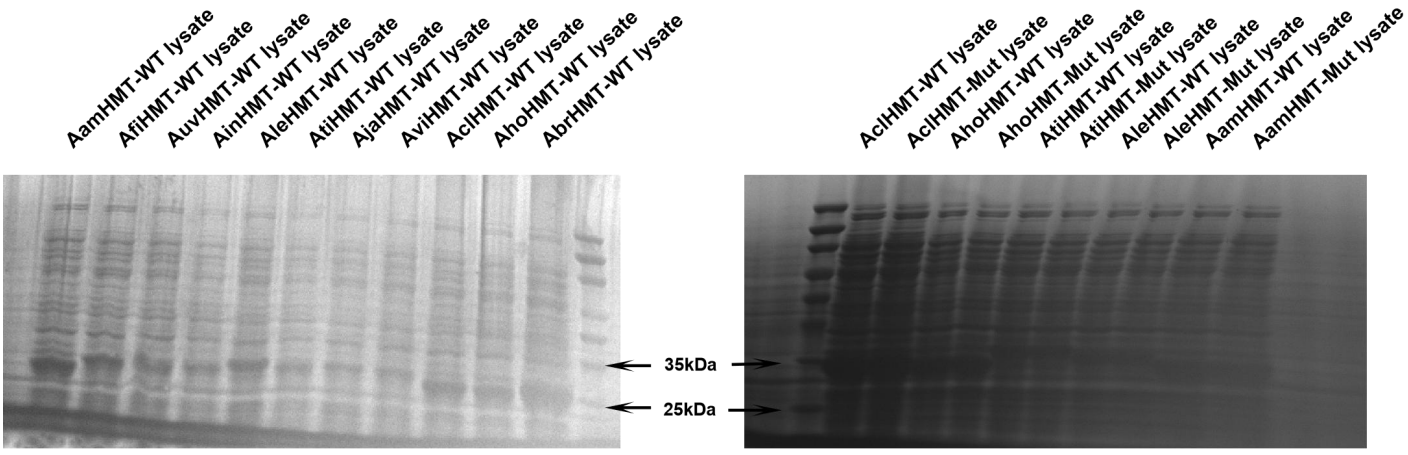

(uncropped image)

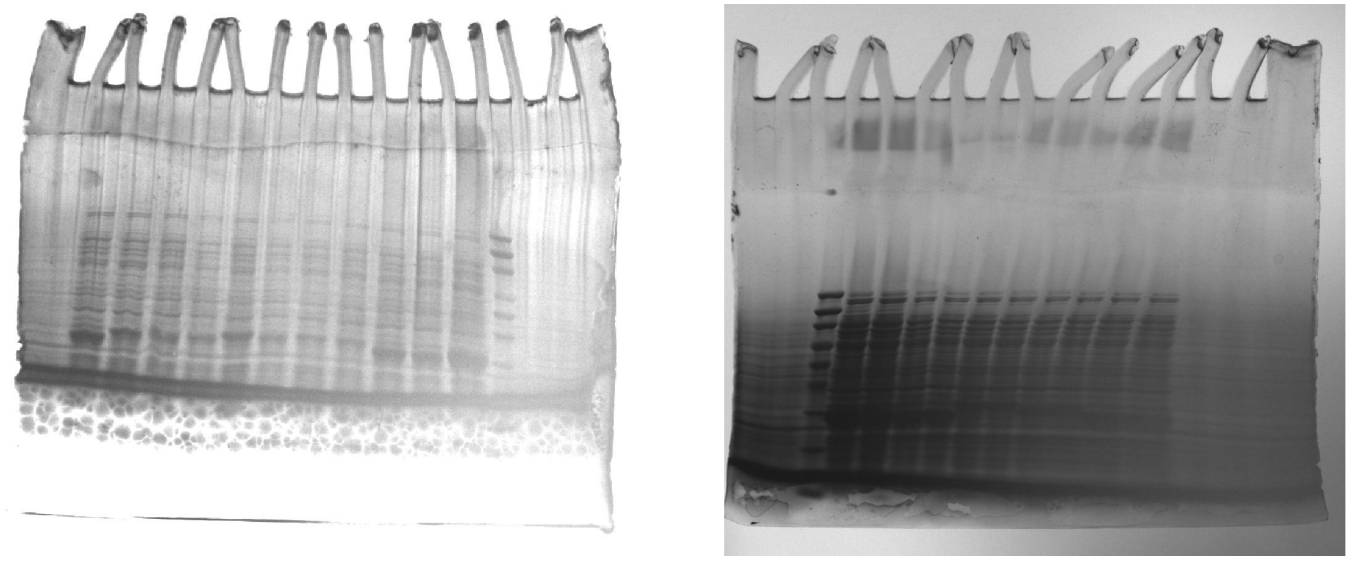

Supplementary Fig. 12 | SDS-PAGE analysis of *Aam*HMT, *Afi*HMT, *Auv*HMT, *Ain*HMT, *Ale*HMT, *Ati*HMT, *Aja*HMT, *Avi*HMT, *Acl*HMT, *Aho*HMT, *Abr*HMT and some of mutants.

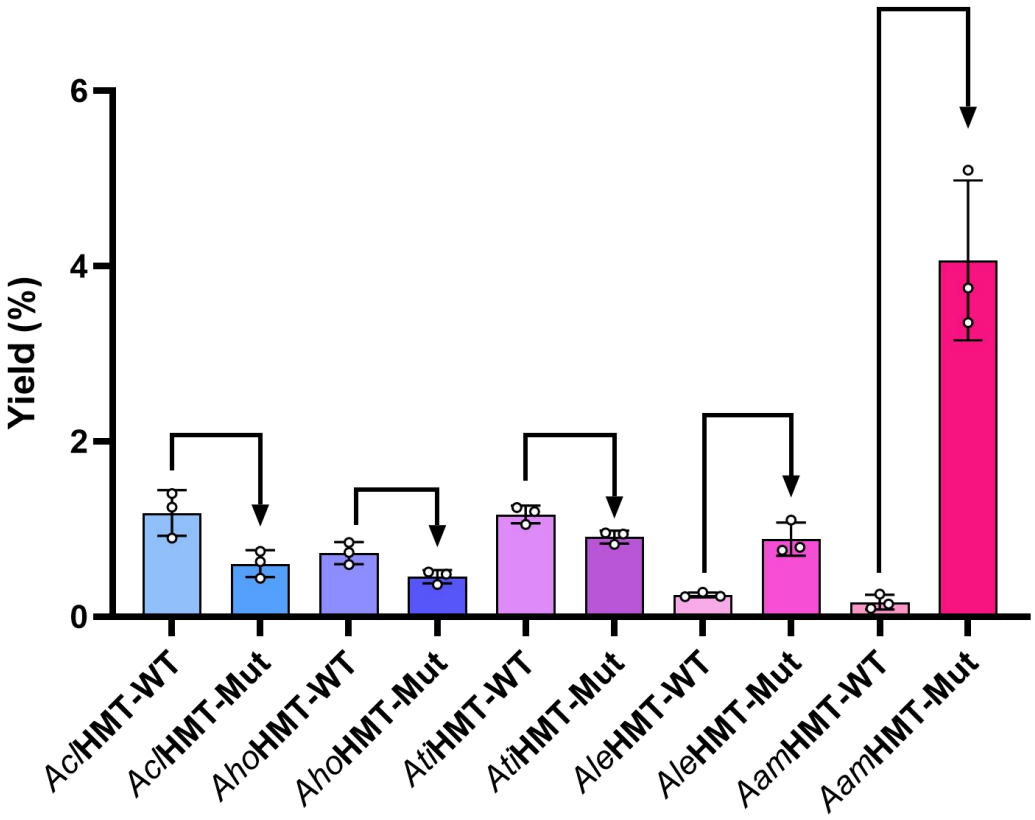

Supplementary Fig. 13 | Activity assays of additional HMT variants. Activity assays of *Acl*HMT, *Aho*HMT, *Ati*HMT, *Ale*HMT and *Aam*HMT in their wild-type (WT) and engineered forms. Whole cells expressing HMTs or their mutant variants were resuspended in 100 mM KPi buffer (pH 8.0) containing 15% (v/v) DMSO, and the cell density was adjusted to OD_{600} = 40. Substrate **1a**, SAH and MeI were added at final concentrations of 1 mM, 1 mM and 15 mM, respectively, in a total reaction volume of 300 µL. Bioconversion reactions were carried out at 30 °C with shaking at 1,200 rpm for 24 h. WT, wild-type; *Acl*HMT-Mut, P4V/S5L/V264G; *Aho*HMT-Mut, K6V/A7L; *Ati*HMT-Mut, K5V/A6L; *Ale*HMT-Mut, K5V/A6L; *Aam*HMT-Mut, K4V/A5L/V264G. Relative activities are reported as mean ± s.d. from three independent biological replicates (n = 3).

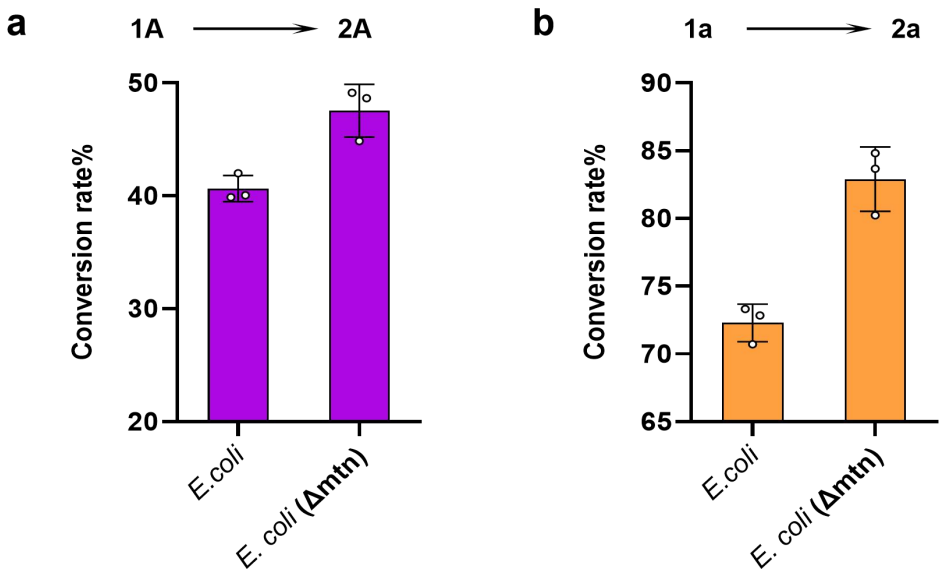

Supplementary Fig. 14 | Functional assay of *mtn*-knockout *E. coli* Cells. a, Conversion of **1A** to **2A** catalyzed by *E. coli* expressing *Ate*HMT-C167A. **b**, Conversion of **1a** to **2a** catalyzed by *E. coli* expressing *Ate*HMT-VLVG. Whole cells harboring *Ate*HMT mutants were resuspended in 100 mM KPi buffer (pH 8.0) containing 6% or 15% (v/v) DMSO, with the cell density adjusted to OD_{600} = 40. Substrate **1A**/**1a**, SAH, and MeI were added at final concentrations of 1 mM, 1 mM, and 15 mM, respectively, in a total reaction volume of 300 µL. Bioconversion reactions were carried out at 30 °C with shaking at 1,200 rpm for 24 h. Relative activities are presented as mean ± s.d. from three independent biological replicates (n = 3).

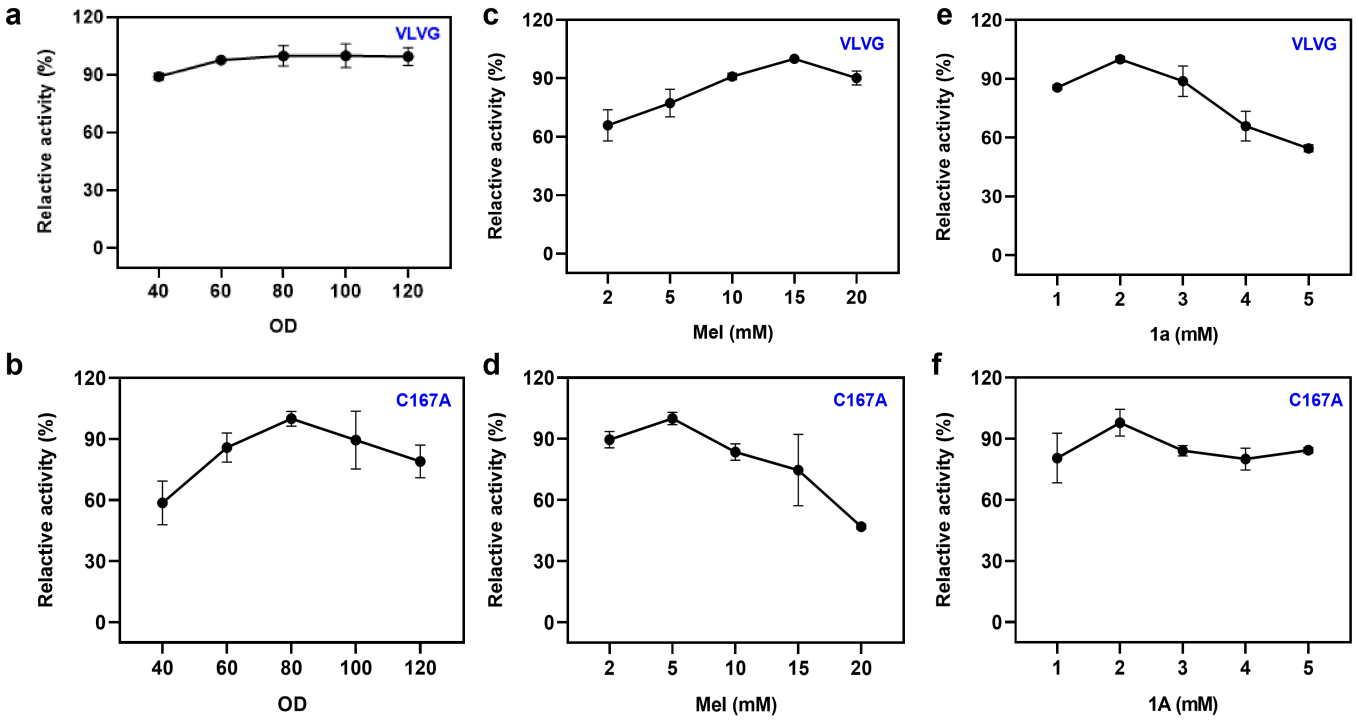

Supplementary Fig. 15 | Optimization of scale-up reactions using cell lysate. a-b, Effect of cell lysate concentration (OD_{600}) on reaction efficiency. **c-d**, Effect of MeI addition on methylation activity. **e-f**, Effect of substrate (**1A** or **1a**) concentration on product formation. Relative activities are shown as mean ± s.d. from three independent biological replicates (n = 3).

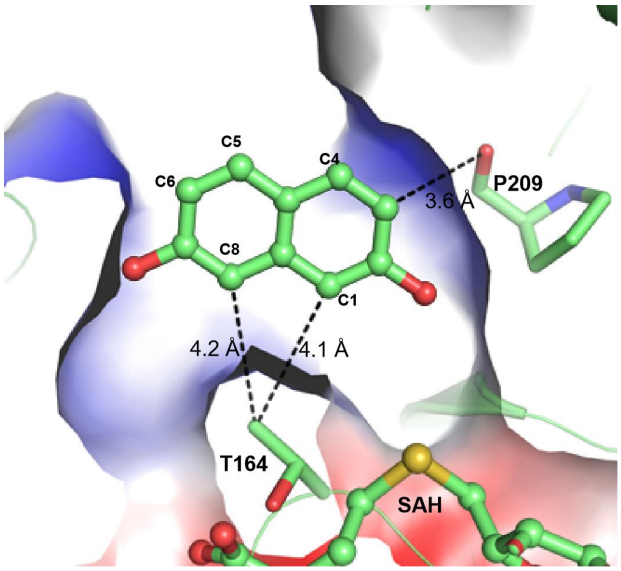

Supplementary Fig. 16 | Structural insights into the local environment of 1A in *Ate*HMT-C167A-SAH-1A complex. Distances between atoms of **1A** and surrounding residues are indicated by black dashed lines.

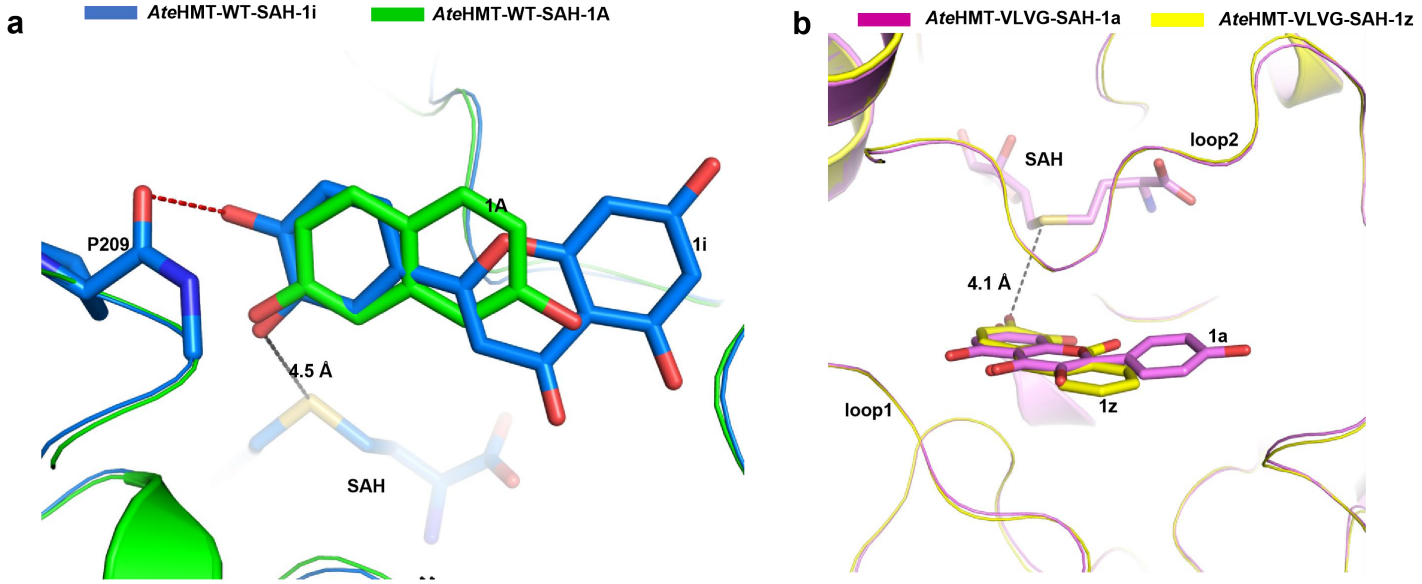

Supplementary Fig. 17 | Comparison of docking models with crystal structures. a, Overlap of *Ate*HMT-WT-SAH-**1i** docking model with the structure of *Ate*HMT-WT-SAH-**1A** complex. **b**, Overlap of *Ate*HMT-VLVG-SAH-**1z** docking model with the structure of *Ate*HMT-VLVG-SAH-**1a** complex. The distances between target hydroxyl group on **1i** and **1z** to the SAH sulfur are indicated by black dashed lines.

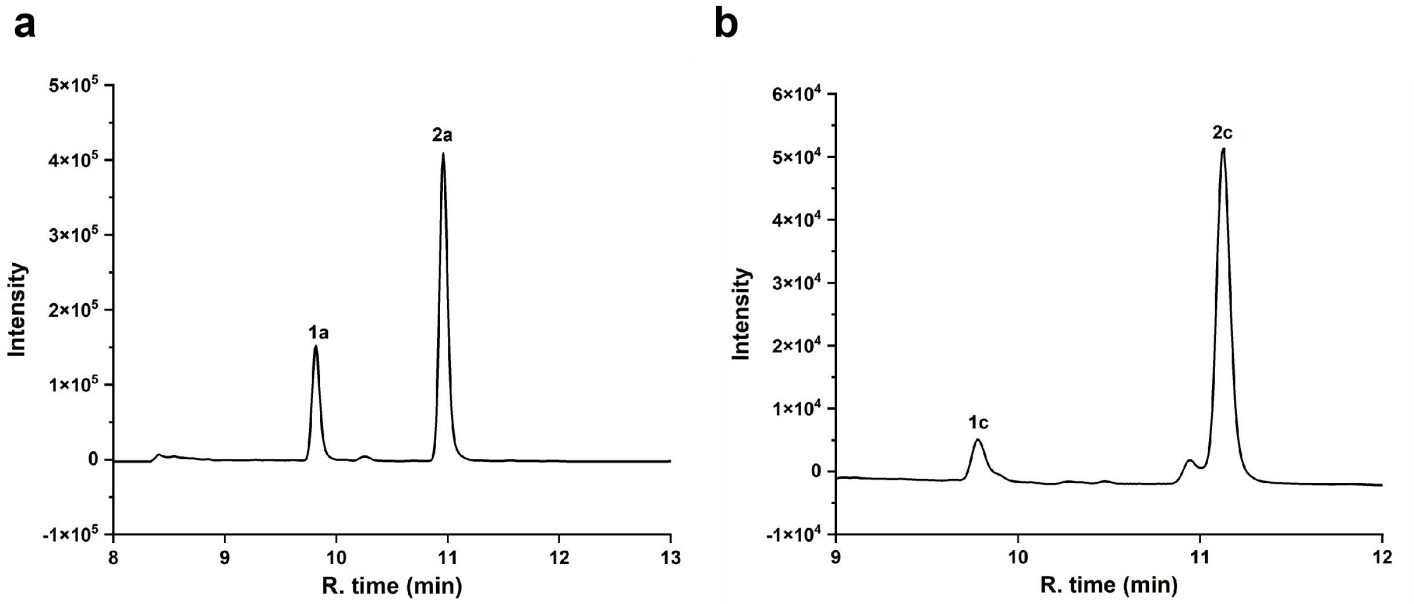

Supplementary Fig. 18 | Preparative-scale methylation of substrates 1a and 1c using AteHMT-VLVG Whole cells were resuspended in 100 mM KPi buffer (pH 8.0) to an OD_{600} of 120 and lysed. Substrates **1a** or **1c**, SAH, and MeI were added to final concentrations of 2 mM, 2 mM, and 15 mM, respectively, in a total volume of 0.5 L. Reactions were conducted under optimized conditions for preparative-scale conversion.

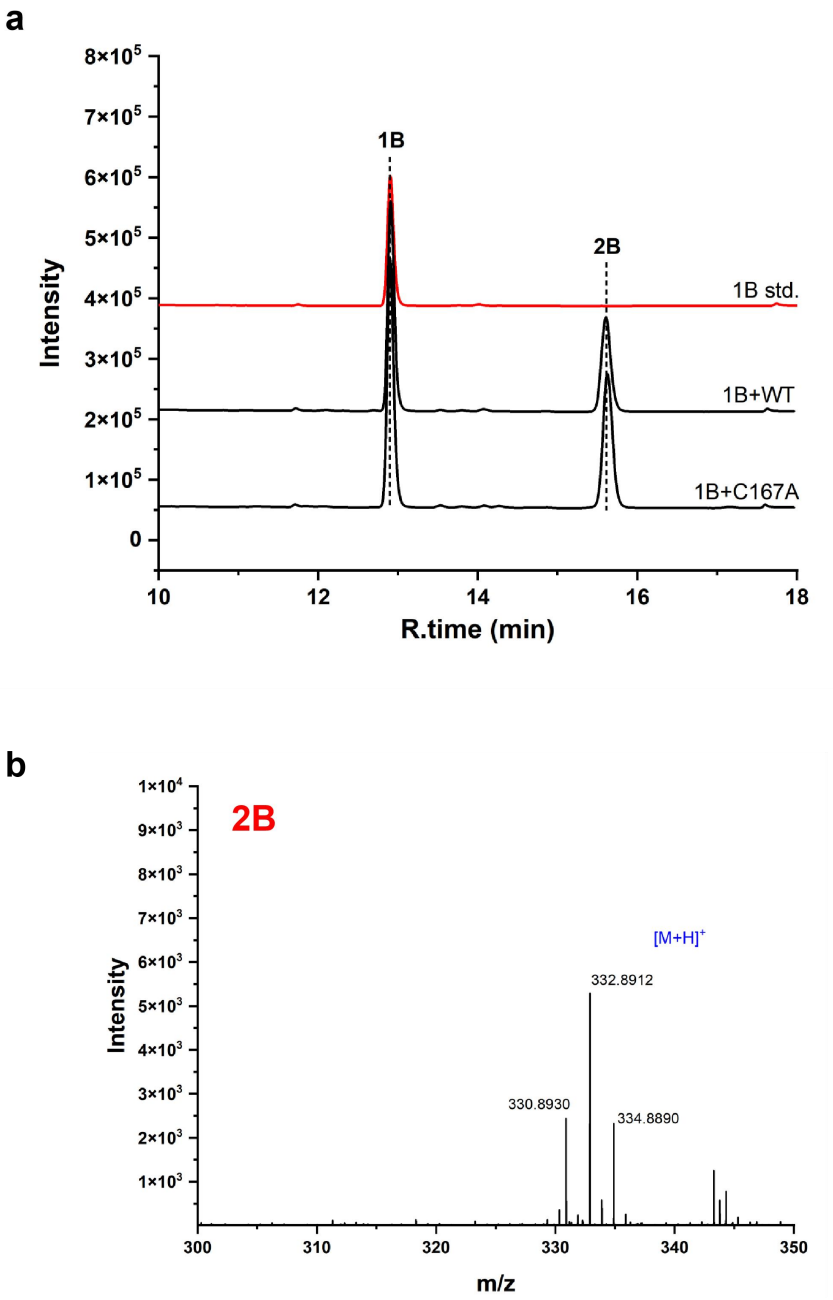

Supplementary Fig. 19 | HPLC-DAD and HRMS analysis of 1B methylation by *Ate*HMT mutants. a, HPLC chromatogram showing substrate **1B** and its methylated products **2B**. **b**, Representative positive-ion HRMS spectra of **2B**. Molecular weights: **1B** =317; **2B** = 331. Detection wavelength: 254 nm.

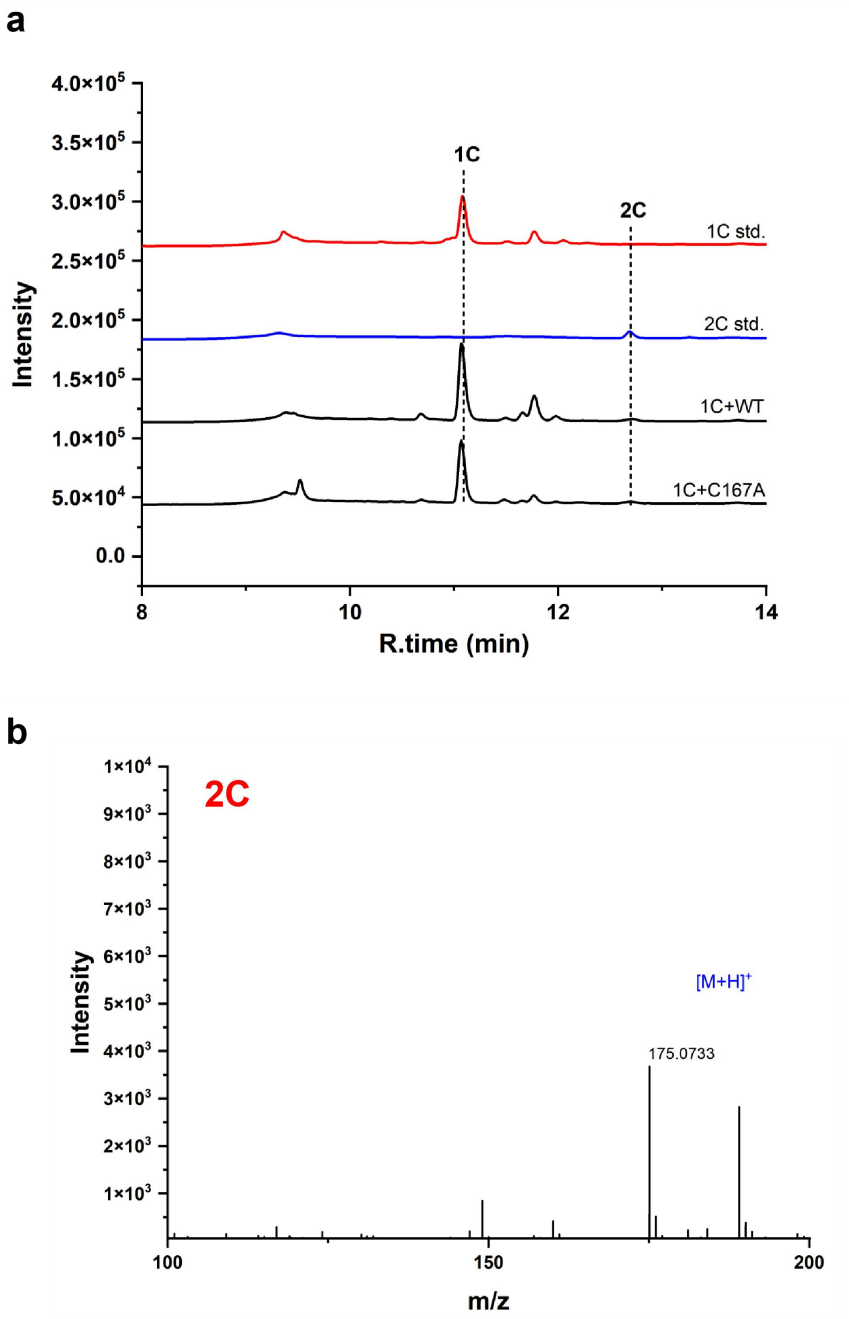

Supplementary Fig. 20 | HPLC-DAD and HRMS analysis of 1C methylation by *Ate*HMT mutants. a, HPLC chromatogram showing substrate **1C** and its methylated products **2C**. **b**, Representative positive-ion HRMS spectra of **2C**. Molecular weights: **1C** =160; **2C** = 174. Detection wavelength: 254 nm.

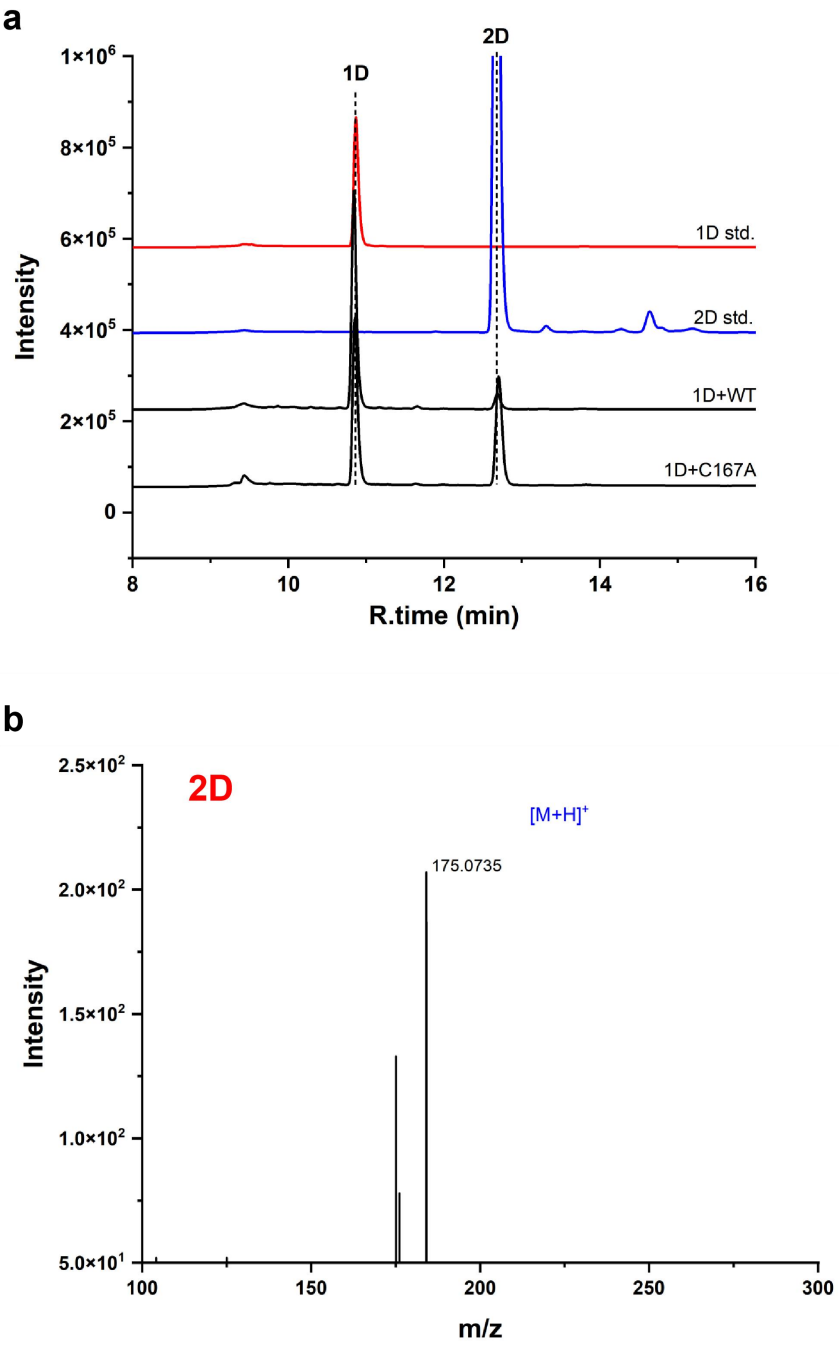

Supplementary Fig. 21 | HPLC-DAD and HRMS analysis of 1D methylation by *Ate*HMT mutants. a, HPLC chromatogram showing substrate **1D** and its methylated products **2D**. **b**, Representative positive-ion HRMS spectra of **2D**. Molecular weights: **1D** =160; **2D** = 174. Detection wavelength: 254 nm.

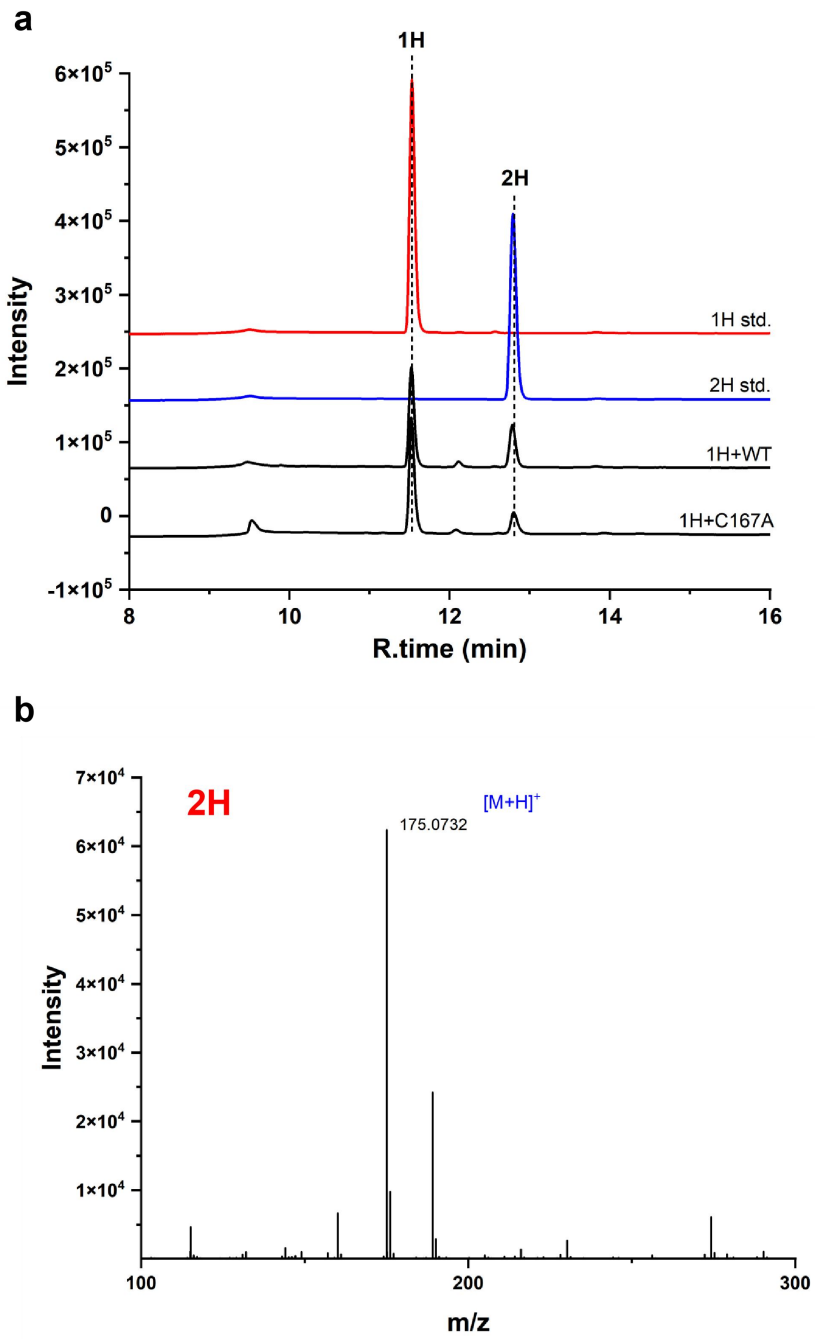

Supplementary Fig. 22 | HPLC-DAD and HRMS analysis of 1H methylation by *Ate*HMT mutants. a, HPLC chromatogram showing substrate **1H** and its methylated products **2H**. **b**, Representative positive-ion HRMS spectra of **2H**. Molecular weights: **1H** =160; **2H** = 174. Detection wavelength: 254 nm.

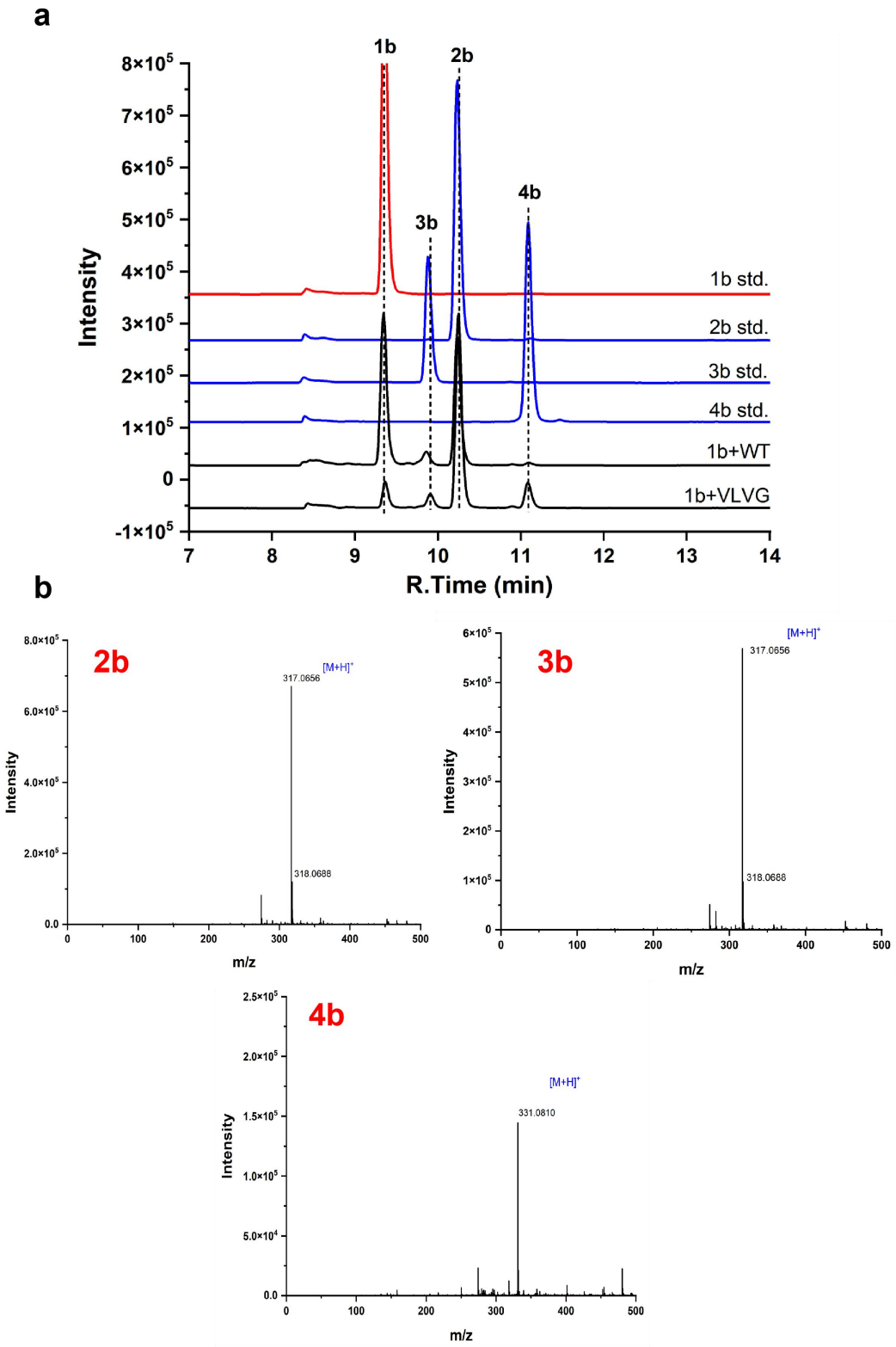

Supplementary Fig. 23 | HPLC-DAD and HRMS analysis of 1b methylation by *Ate*HMT mutants. a, HPLC chromatogram showing substrate **1b** and its methylated products **2b**, **3b**, and **4b**. **b**, Representative positive-ion HRMS spectra of **2b**, **3b**, and **4b**. Molecular weights: **1b** =302; **2b**, **3b** = 316; **4b** = 330. Detection wavelength: 370 nm.

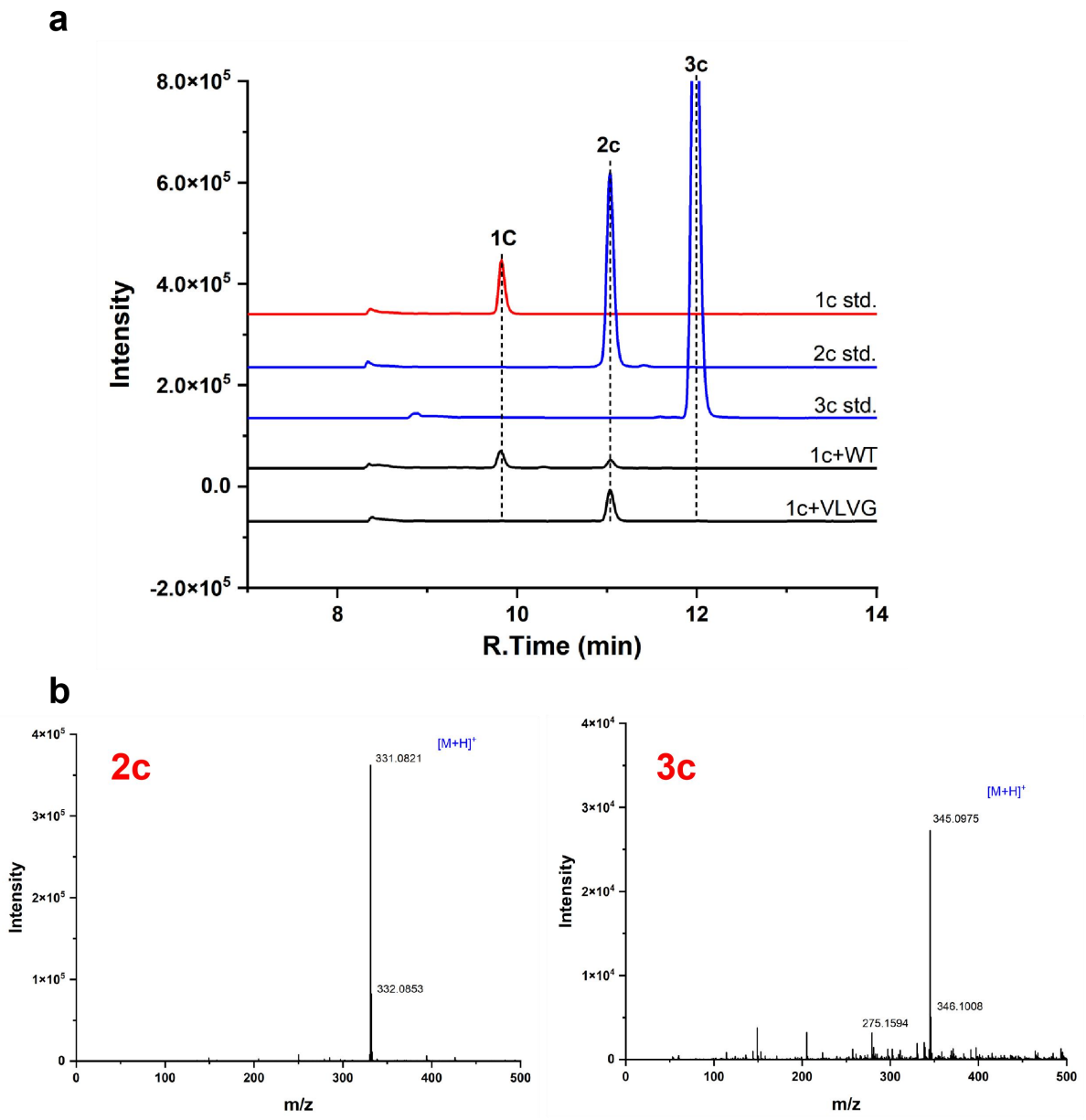

Supplementary Fig. 24 | HPLC-DAD and HRMS analysis of 1c methylation by *Ate*HMT mutants. a, HPLC chromatogram showing substrate **1c** and its methylated products **2c** and **3c**. **b**, Representative positive ion HRMS spectra for products **2c** and **3c**. Molecular weights: **1c** =316; **2c** = 330; **3c** = 344. Detection was performed at 369 nm.

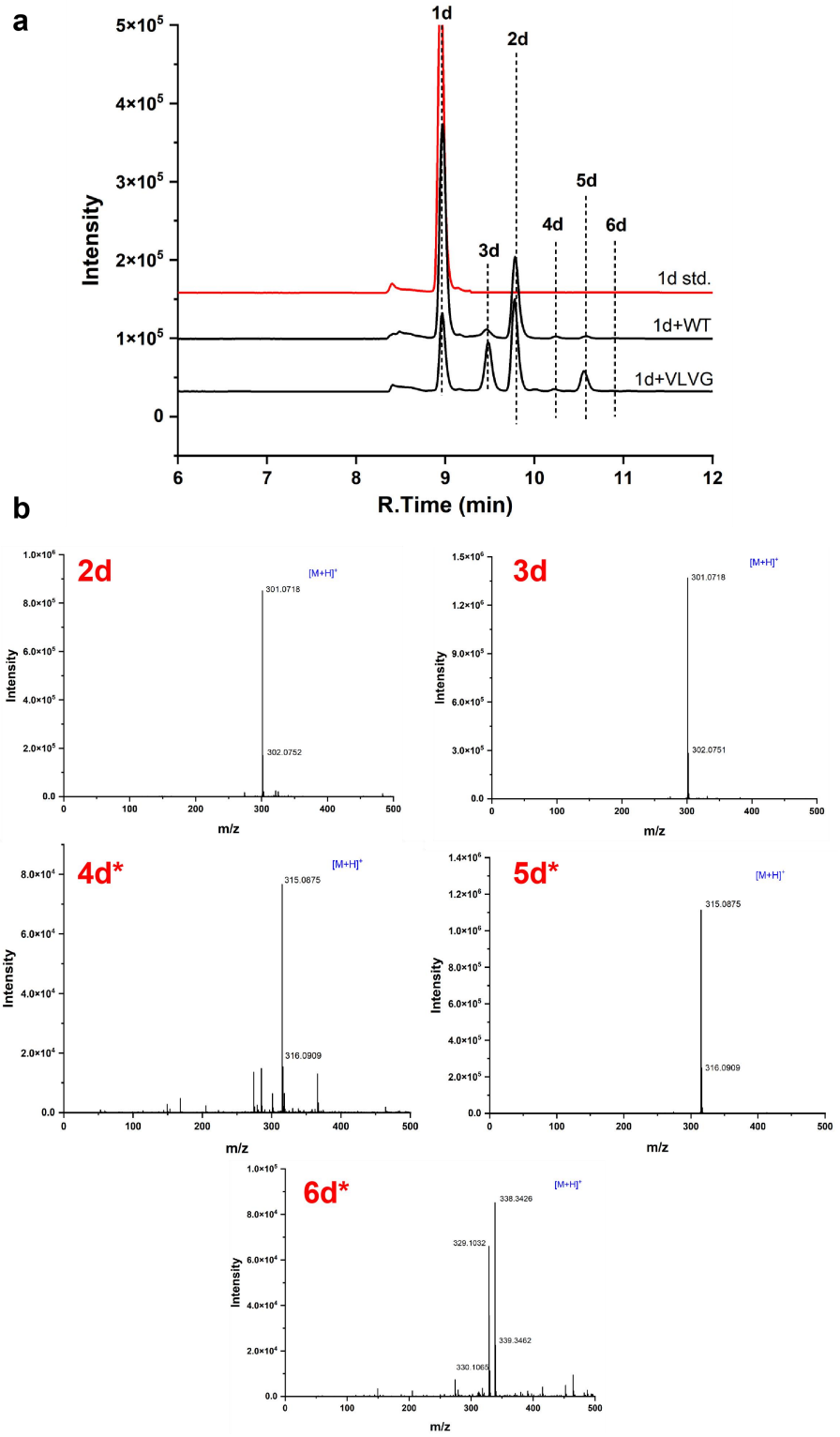

Supplementary Fig. 25 | HPLC-DAD and HRMS analysis of 1d methylation by *Ate*HMT mutants. a, HPLC chromatogram showing substrate **1d** and its methylated products **2d**, **3d**, **4d**, **5d**, and **6d**. **b**, Representative positive ion HRMS spectra for products **2d**, **3d**, **4d**, **5d**, and **6d**. Molecular weights: **1d** =286; **2d**, **3d** = 300; **4d**, **5d** = 314, **6d** =328. Detection was performed at 360 nm. * indicates products that were not fully characterized.

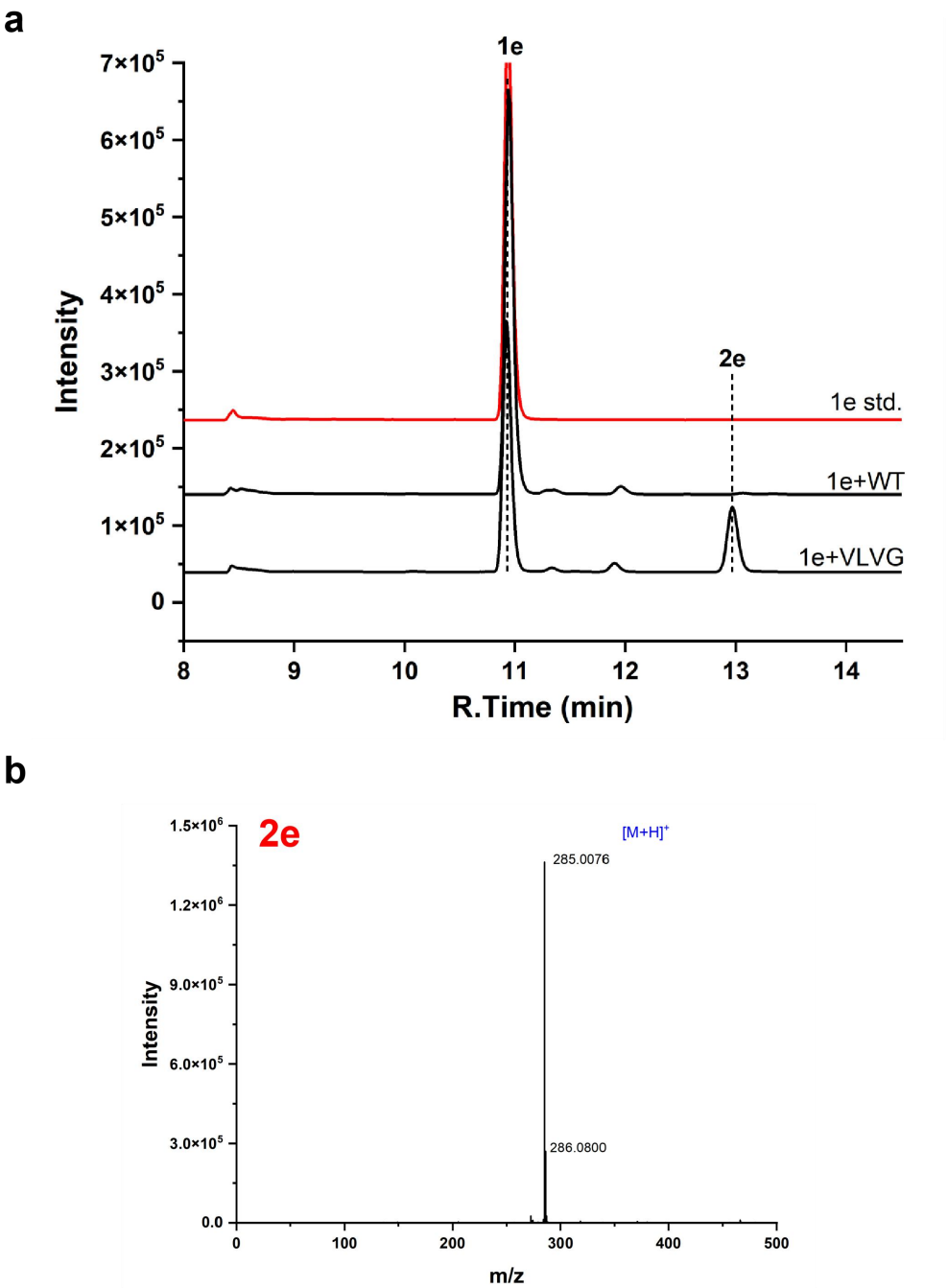

Supplementary Fig. 26 | HPLC-DAD and HRMS analysis of 1e methylation by *Ate*HMT mutants. a, HPLC chromatogram showing substrate **1e** and its methylated product **2e**. **b**, Representative positive ion HRMS spectra for products **2e**. Molecular weights: **1e** =270; **2e** = 284. Detection was performed at 350 nm.

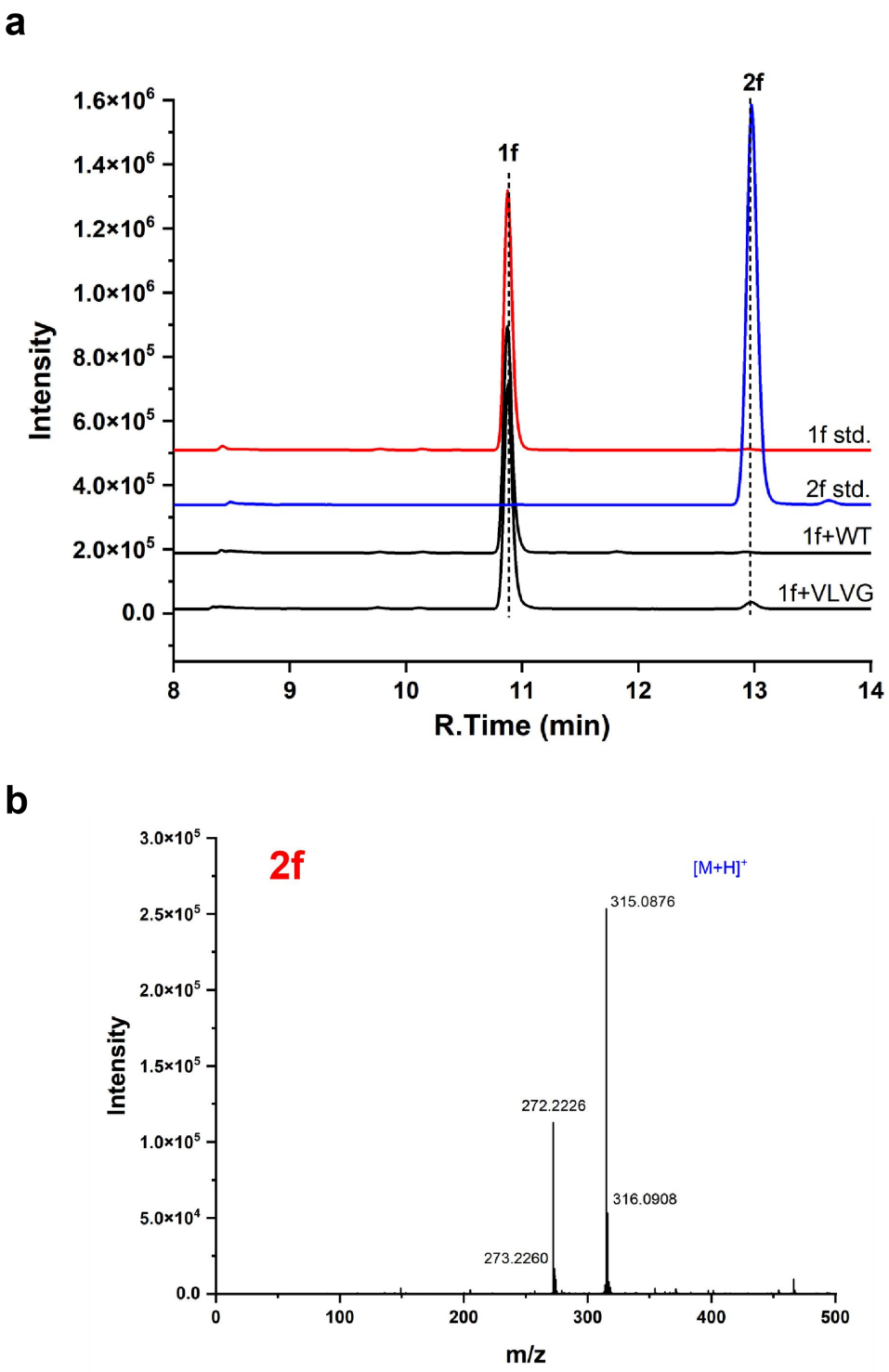

Supplementary Fig. 27 | HPLC-DAD and HRMS analysis of 1f methylation by *Ate*HMT mutants. a, HPLC chromatogram showing substrate **1f** and its methylated product **2f**. **b**, Representative positive ion HRMS spectra for products **2f**. Molecular weights: **1f** =300; **2f** = 314. Detection was performed at 365 nm.

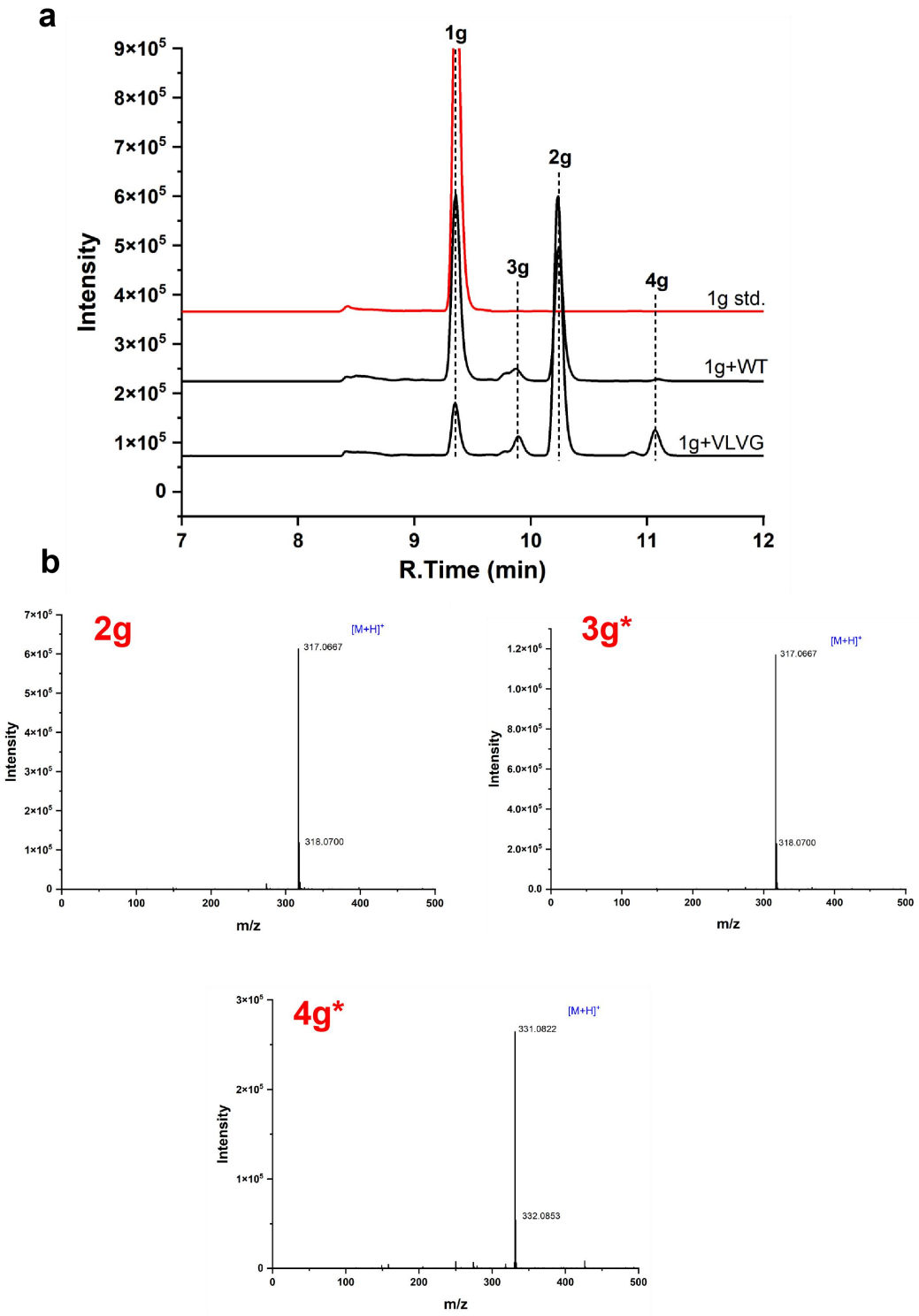

Supplementary Fig. 28 | HPLC-DAD and HRMS analysis of 1g methylation by *Ate*HMT mutants. a, HPLC chromatogram showing substrate **1g** and its methylated products **2g**, **3g**, and **4g**. **b**, Representative positive ion HRMS spectra for products **2g**, **3g**, and **4g**. Molecular weights: **1g** =302; **2g**, **3g** = 316; **4g** = 330. Detection was performed at 371 nm. * indicates products that were not fully characterized..

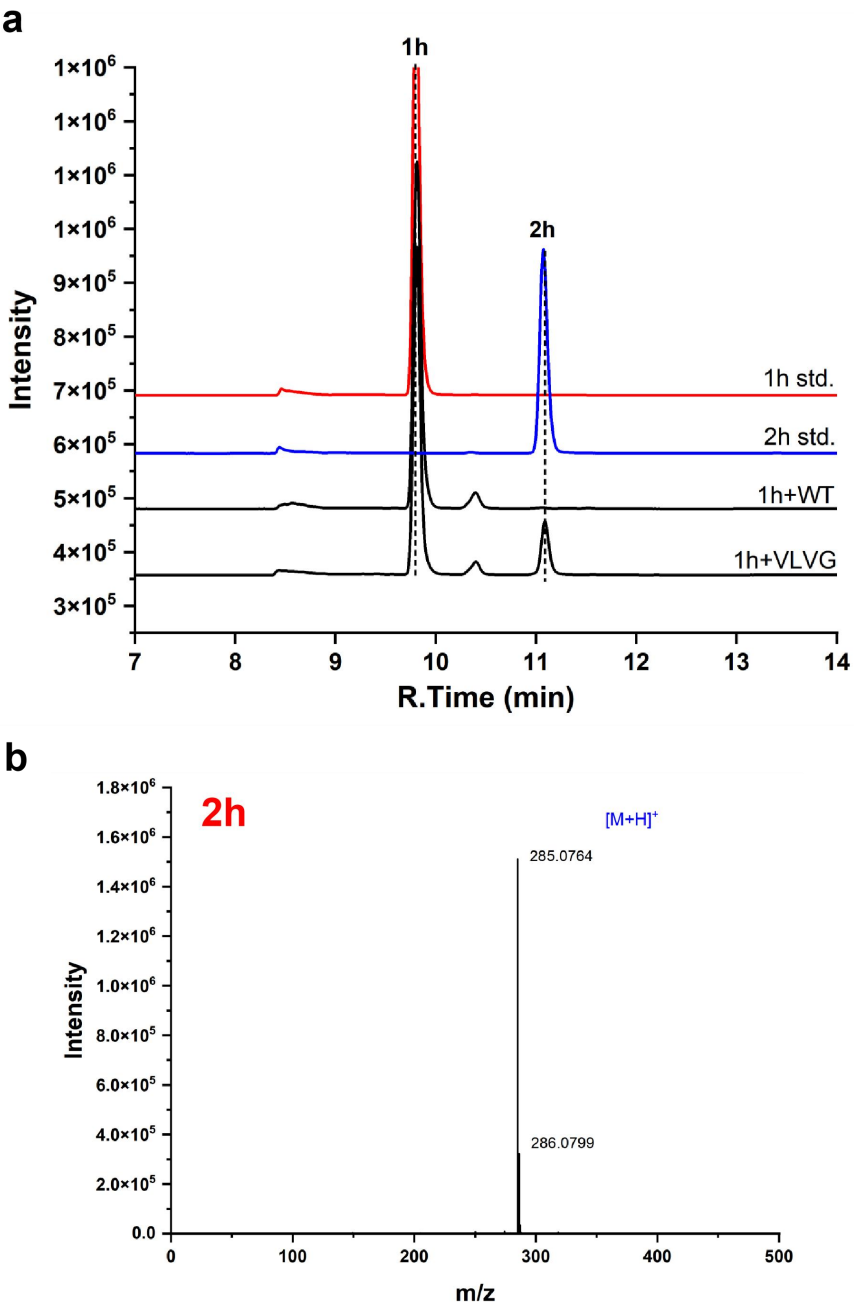

Supplementary Fig. 29 | HPLC-DAD and HRMS analysis of 1h methylation by *Ate*HMT mutants. a, HPLC chromatogram showing substrate **1h** and its methylated products **2h**. **b**, Representative positive ion HRMS spectra for products **2h**. Molecular weights: **1h** =270; **2h** = 284. Detection was performed at 337 nm.

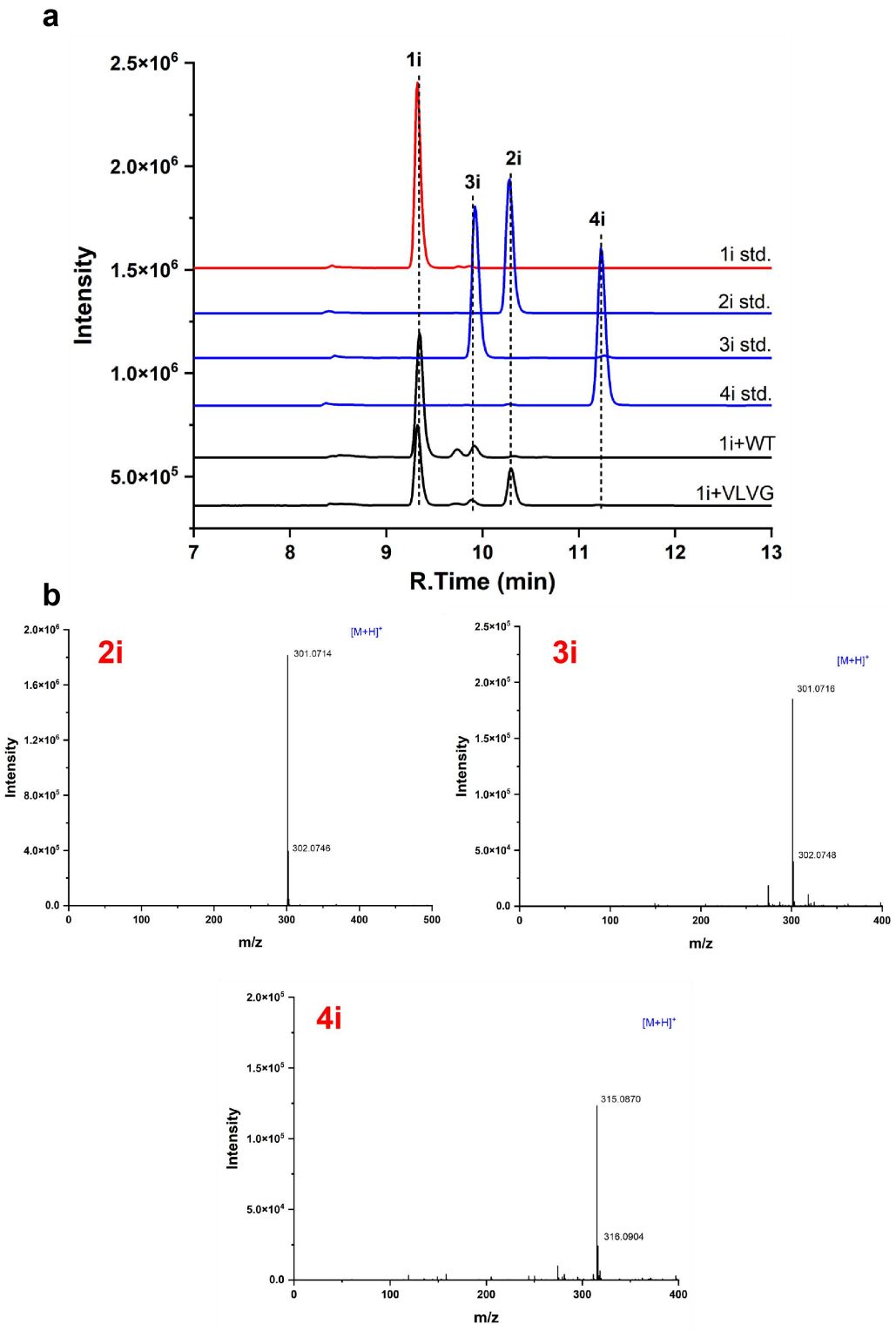

Supplementary Fig. 30 | HPLC-DAD and HRMS analysis of 1i methylation by *Ate*HMT mutants. a, HPLC chromatogram showing substrate **1i** and its methylated products **2i**, **3i**, and **4i**. **b**, Representative positive ion HRMS spectra for products **2i**, **3i**, and **4i**. Molecular weights: **1i** =286; **2i**, **3i** = 300; **4i** = 314. Detection was performed at 346 nm.

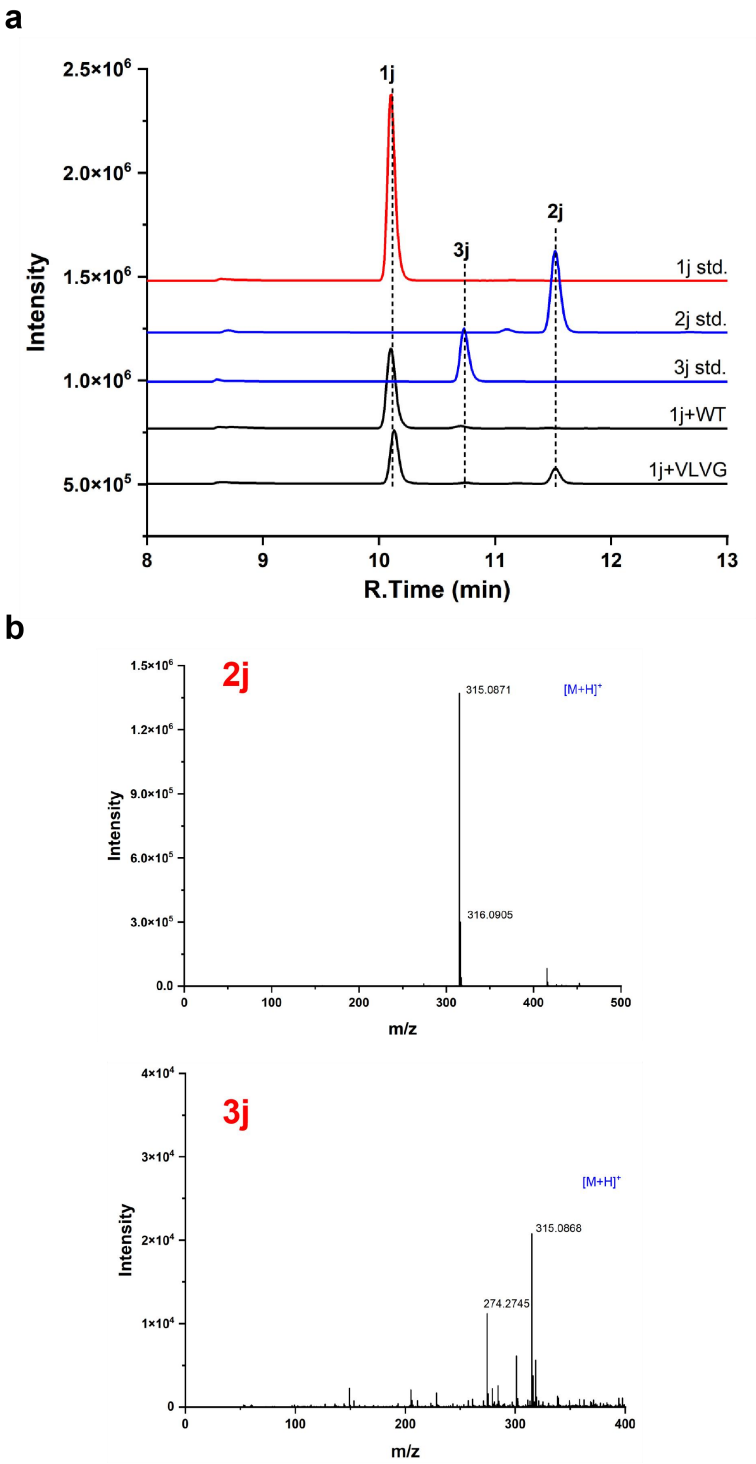

Supplementary Fig. 31 | HPLC-DAD and HRMS analysis of 1j methylation by *Ate*HMT mutants. a, HPLC chromatogram showing substrate **1j** and its methylated products **2j** and **3j**. **b**, Representative positive ion HRMS spectra for products **2j**, and **3j**. Molecular weights: **1j** =300; **2j** = 314; **3j** = 328. Detection was performed at 345 nm.

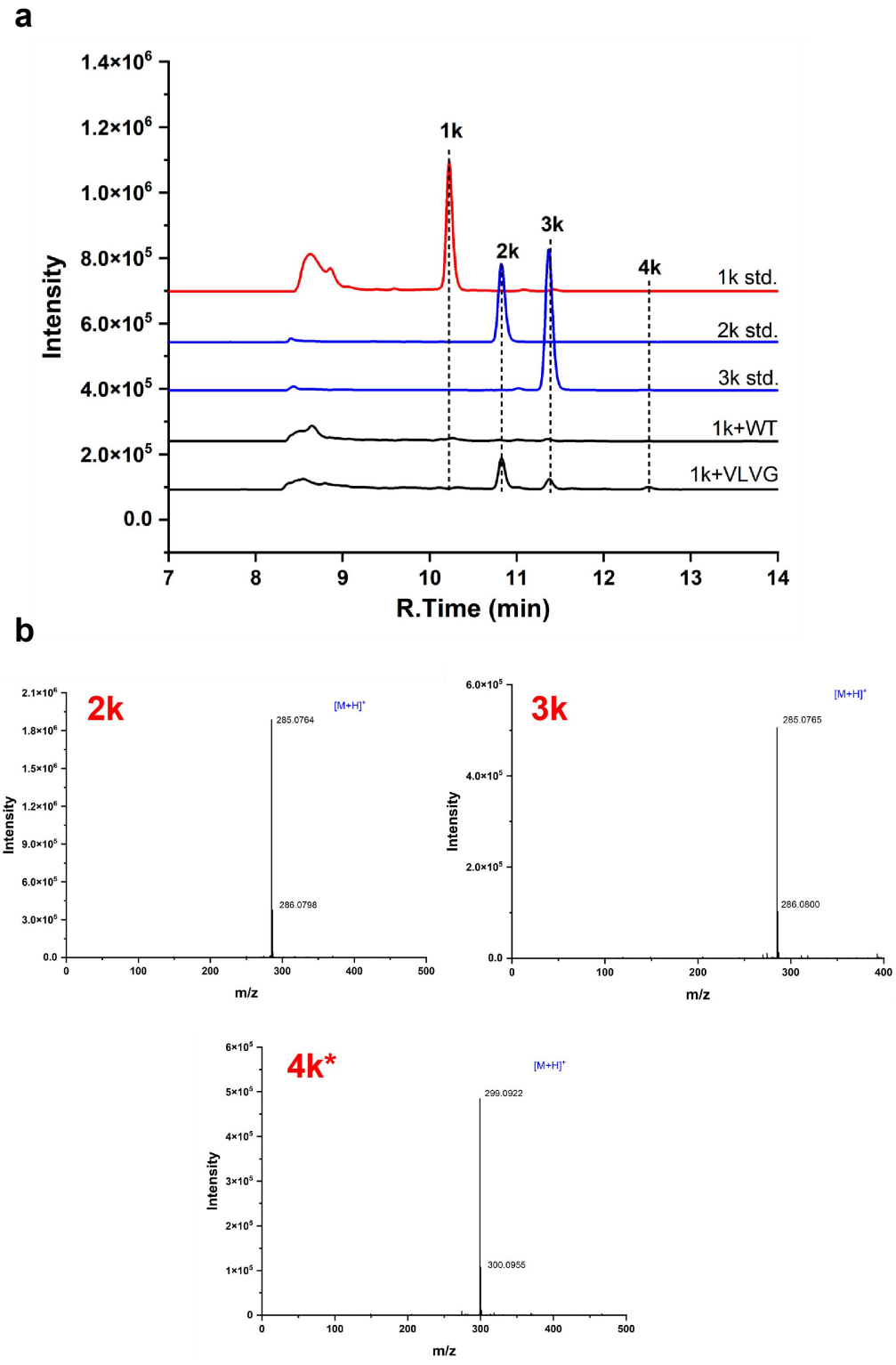

Supplementary Fig. 32 | HPLC-DAD and HRMS analysis of 1k methylation by *Ate*HMT mutants. a, HPLC chromatogram showing substrate **1k** and its methylated products **2k**, **3k**, and **4k**. **b**, Representative positive ion HRMS spectra for products **2k**, **3k**, and **4k**. Molecular weights: **1k** =270; **2k**, **3k** = 284; **4k** = 298. Detection was performed at 275 nm. * indicates products that were not fully characterized.

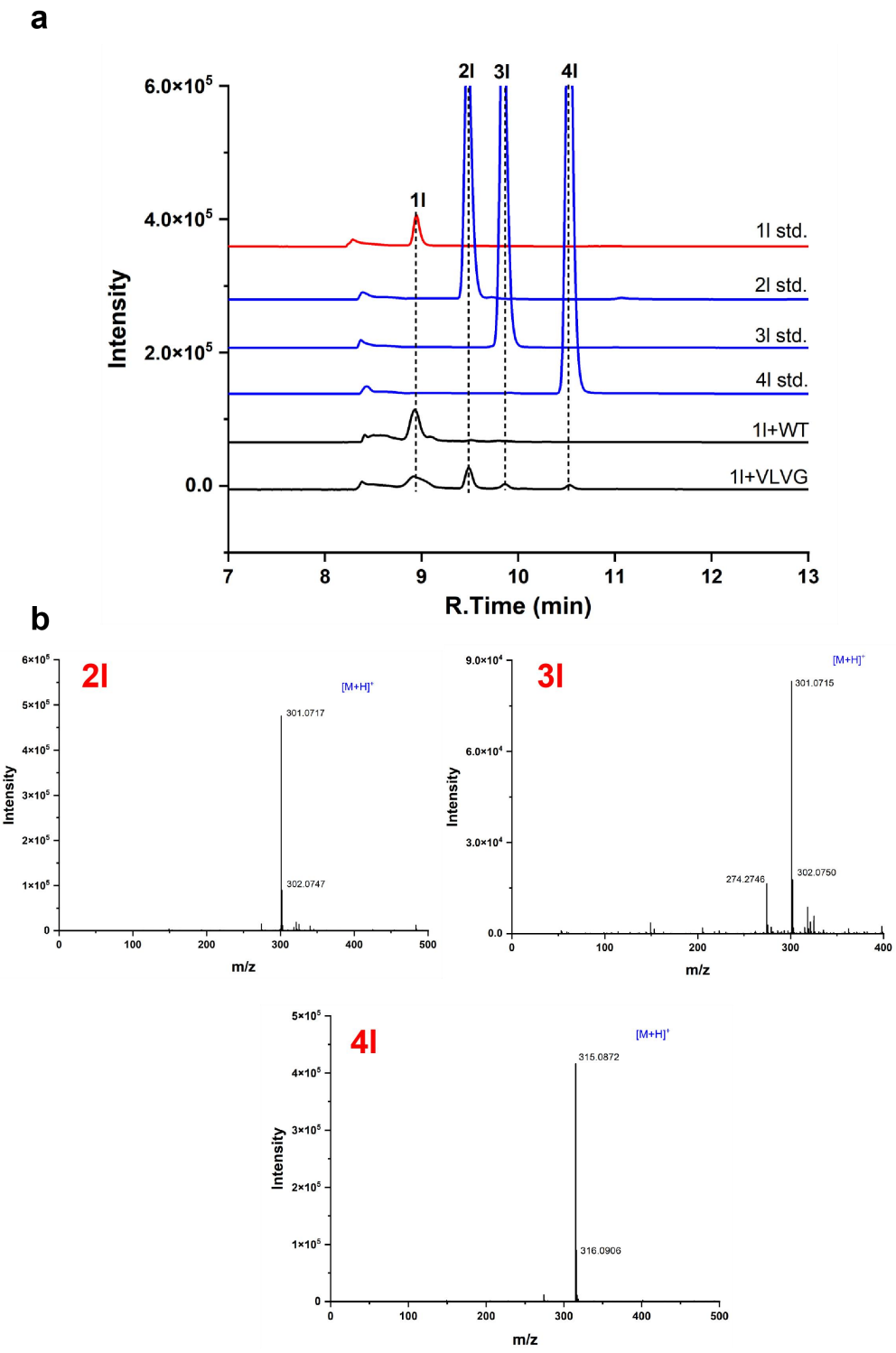

Supplementary Fig. 33 | HPLC-DAD and HRMS analysis of 1l methylation by *Ate*HMT mutants. a, HPLC chromatogram showing substrate **1l** and its methylated products **2l**, **3l**, and **4l**. **b**, Representative positive ion HRMS spectra for products **2l**, **3l**, and **4l**. Molecular weights: **1l** =286; **2l**, **3l** = 300; **4k** = 314. Detection was performed at 337 nm.

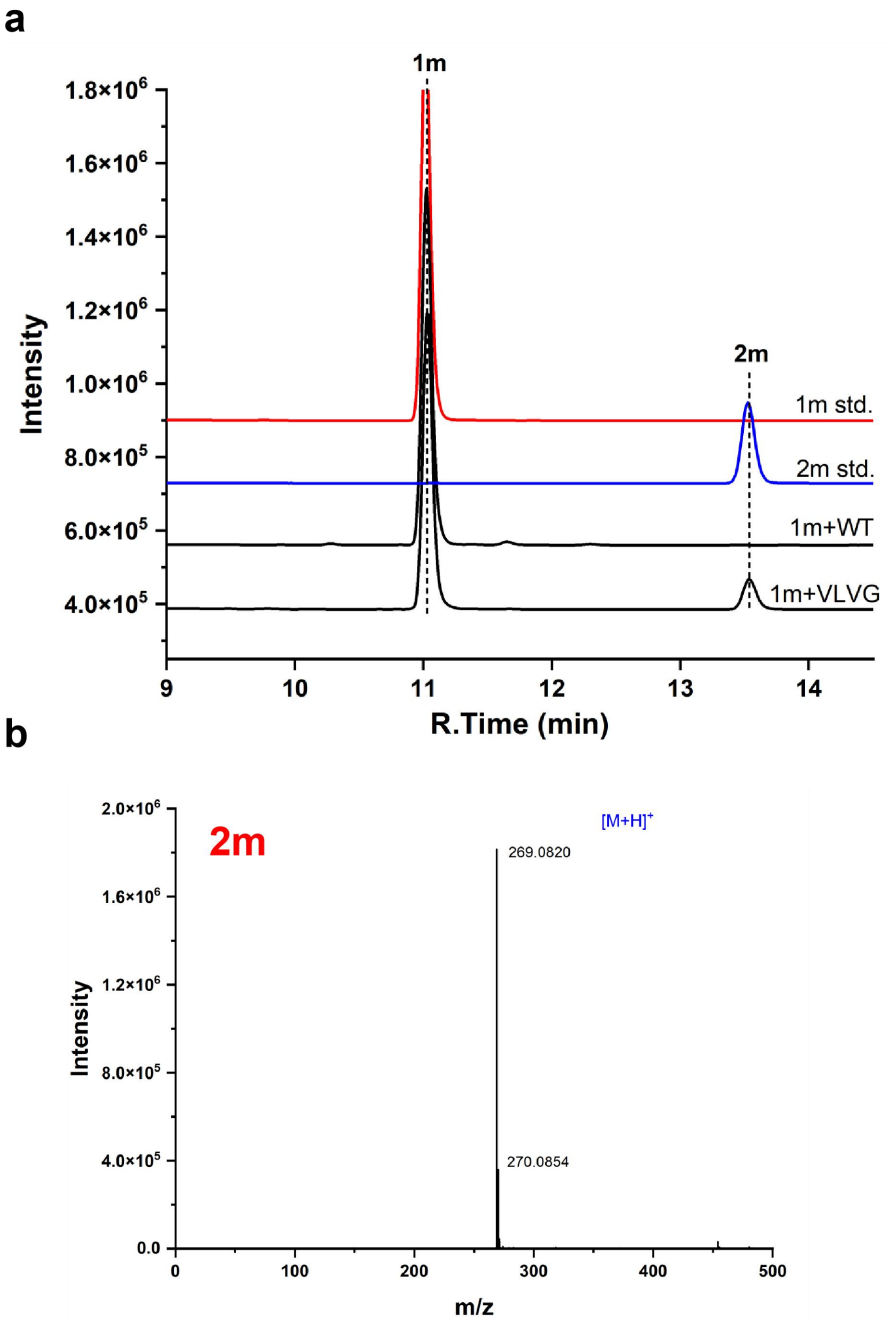

Supplementary Fig. 34 | HPLC-DAD and HRMS analysis of 1m methylation by *Ate*HMT mutants. a, HPLC chromatogram showing substrate **1m** and its methylated products **2m**. **b**, Representative positive ion HRMS spectra for products **2m**. Molecular weights: **1m** =254; **2m** = 268. Detection was performed at 267 nm.

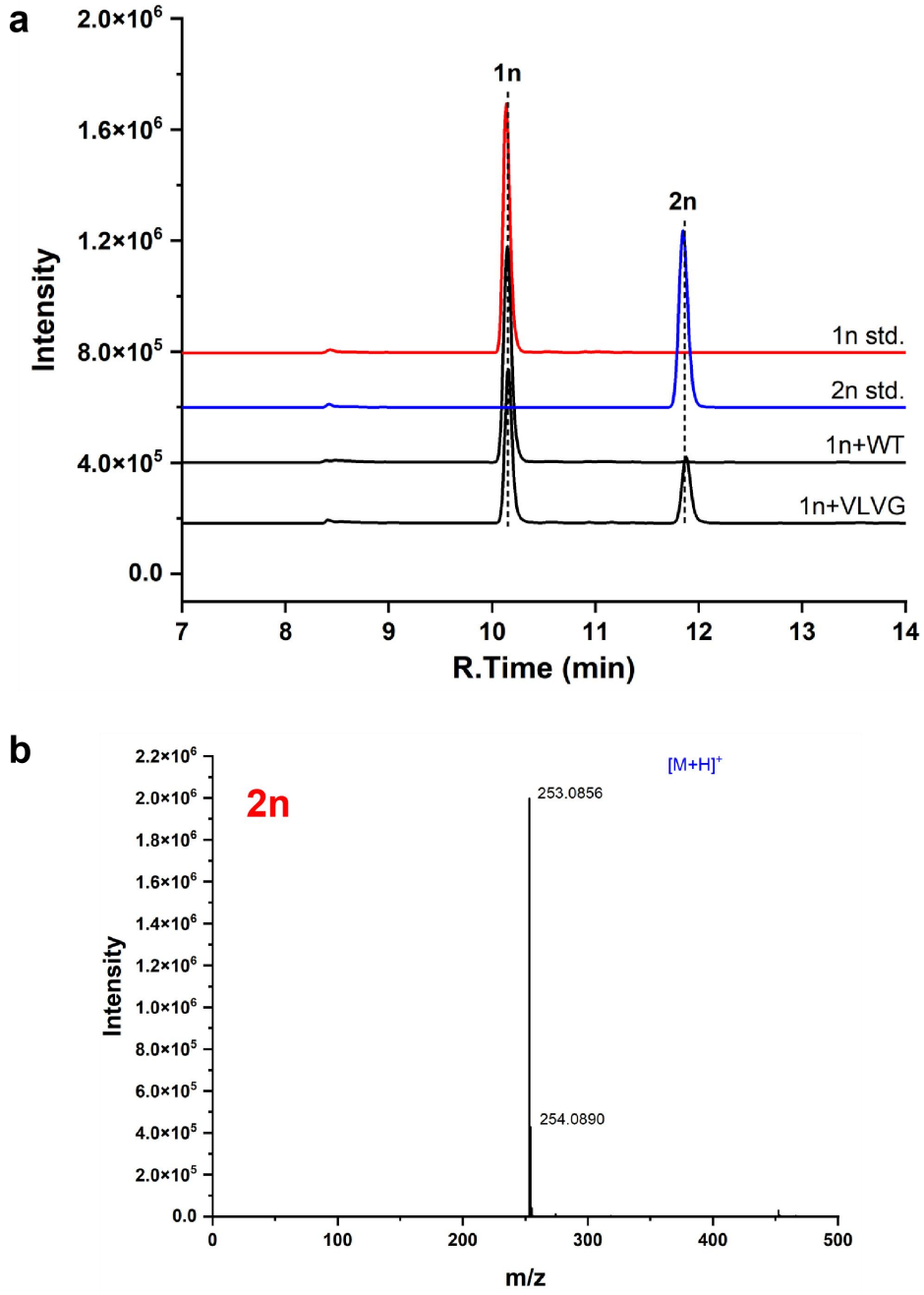

Supplementary Fig. 35 | HPLC-DAD and HRMS analysis of 1n methylation by *Ate*HMT mutants. a, HPLC chromatogram showing substrate **1n** and its methylated products **2n**. **b**, Representative positive ion HRMS spectra for products **2n**. Molecular weights: **1n** =238; **2n** = 252. Detection was performed at 309 nm.

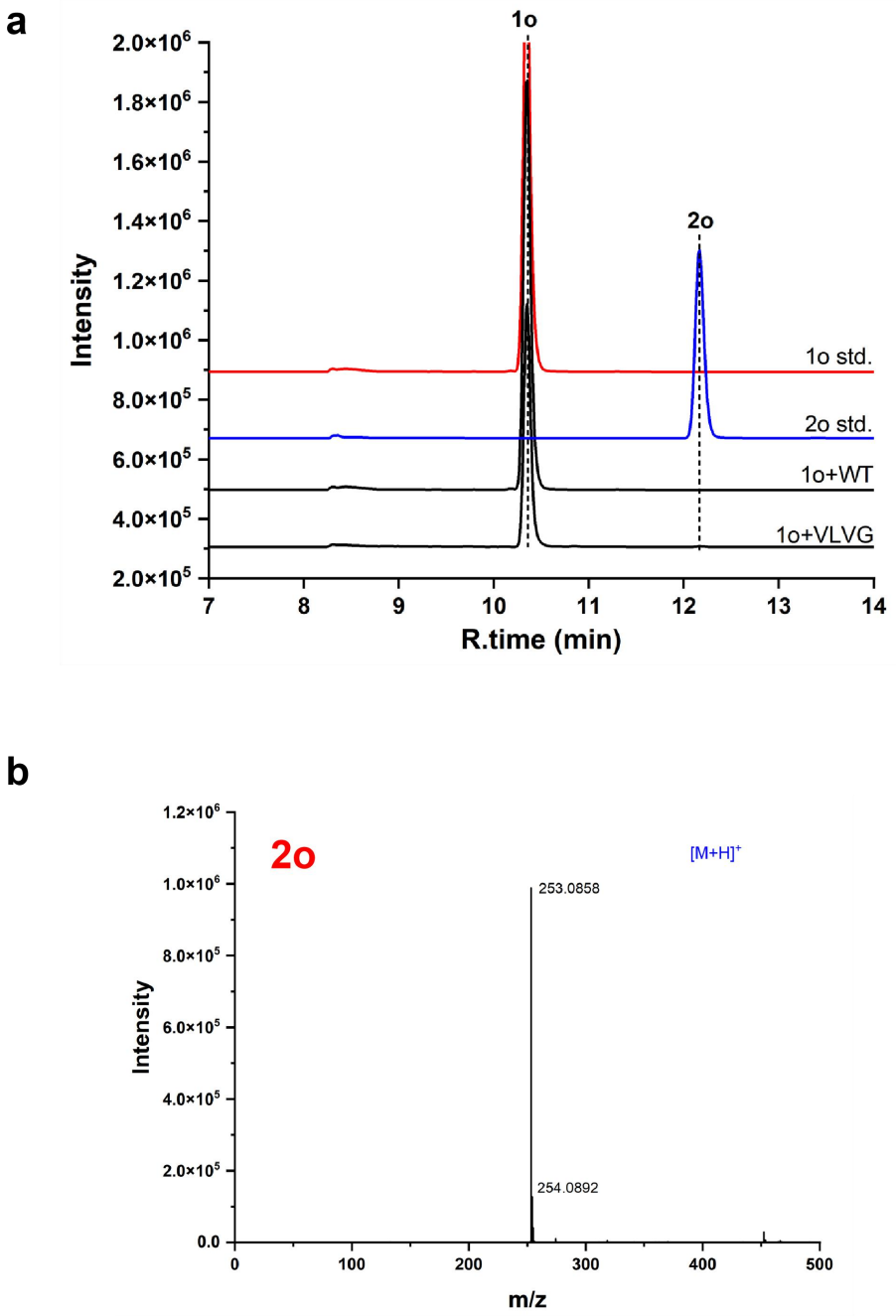

Supplementary Fig. 36 | HPLC-DAD and HRMS analysis of 1o methylation by *Ate*HMT mutants. a, HPLC chromatogram showing substrate **1o** and its methylated products **2o**. **b**, Representative positive ion HRMS spectra for products **2o**. Molecular weights: **1o** =238; **2o** = 252. Detection was performed at 269 nm.

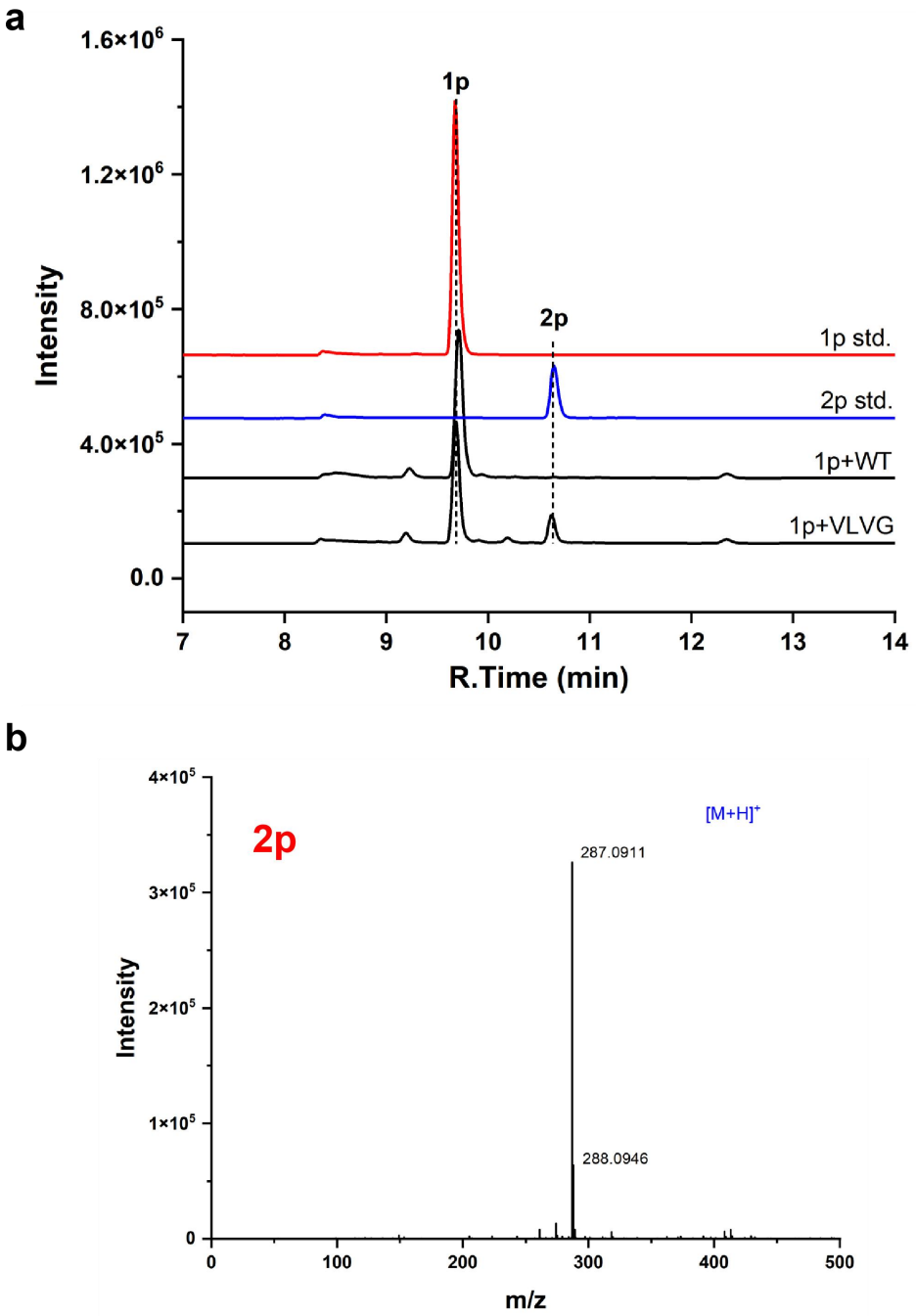

Supplementary Fig. 37 | HPLC-DAD and HRMS analysis of 1p methylation by *Ate*HMT mutants. a, HPLC chromatogram showing substrate **1p** and its methylated products **2p**. **b**, Representative positive ion HRMS spectra for products **2p**. Molecular weights: **1p** =272; **2p** = 286. Detection was performed at 288 nm.

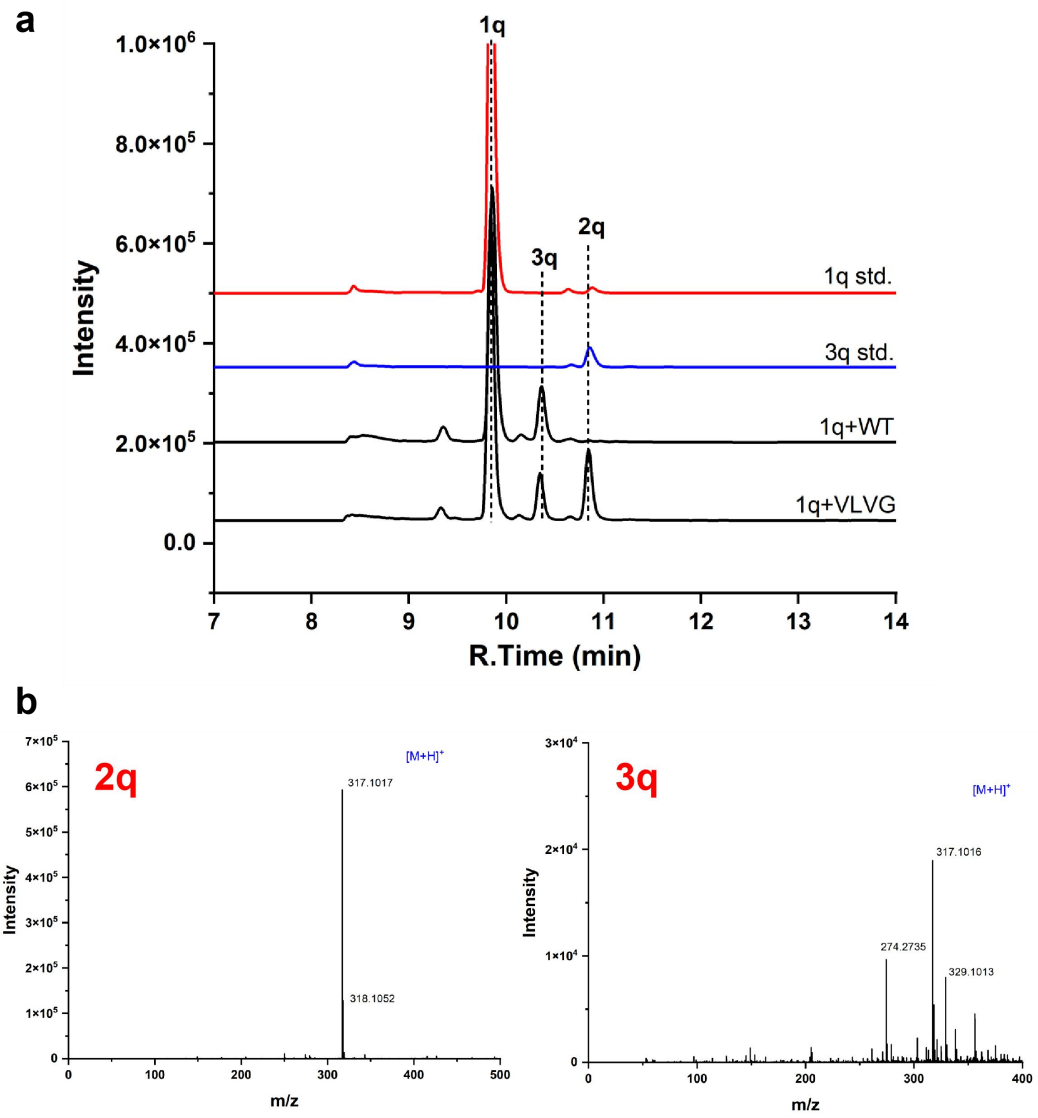

Supplementary Fig. 38 | HPLC-DAD and HRMS analysis of 1q methylation by *Ate*HMT mutants. a, HPLC chromatogram showing substrate **1q** and its methylated products **2q**, and **3q**. **b**, Representative positive ion HRMS spectra for products **2q**, and **3q**. Molecular weights: **1q** =302; **2q**, **3q** = 316. Detection was performed at 287nm.

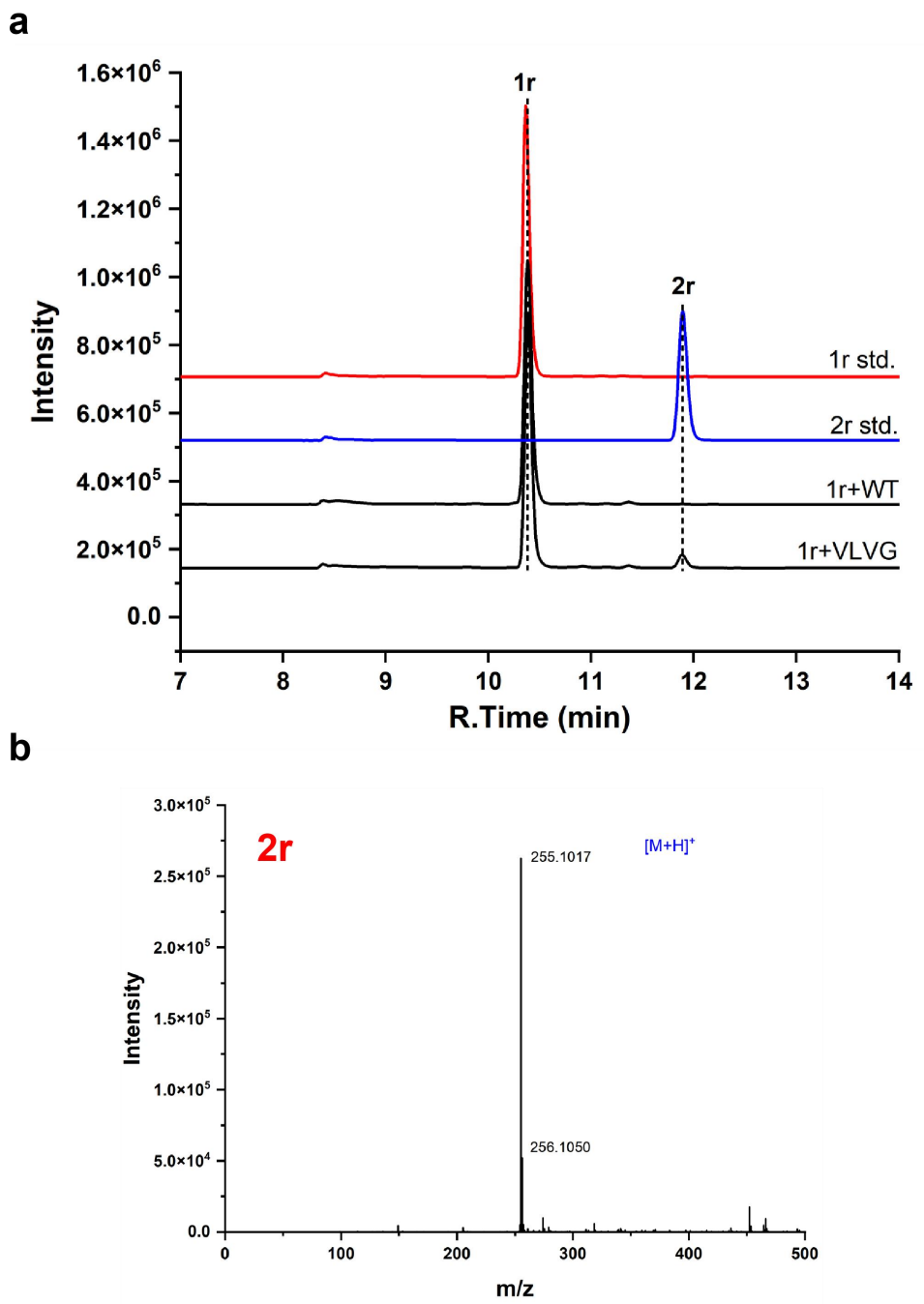

Supplementary Fig. 39 | HPLC-DAD and HRMS analysis of 1r methylation by *Ate*HMT mutants. a, HPLC chromatogram showing substrate **1r** and its methylated products **2r**. **b**, Representative positive ion HRMS spectra for products **2r**. Molecular weights: **1r** =240; **2r** = 254. Detection was performed at 274 nm.

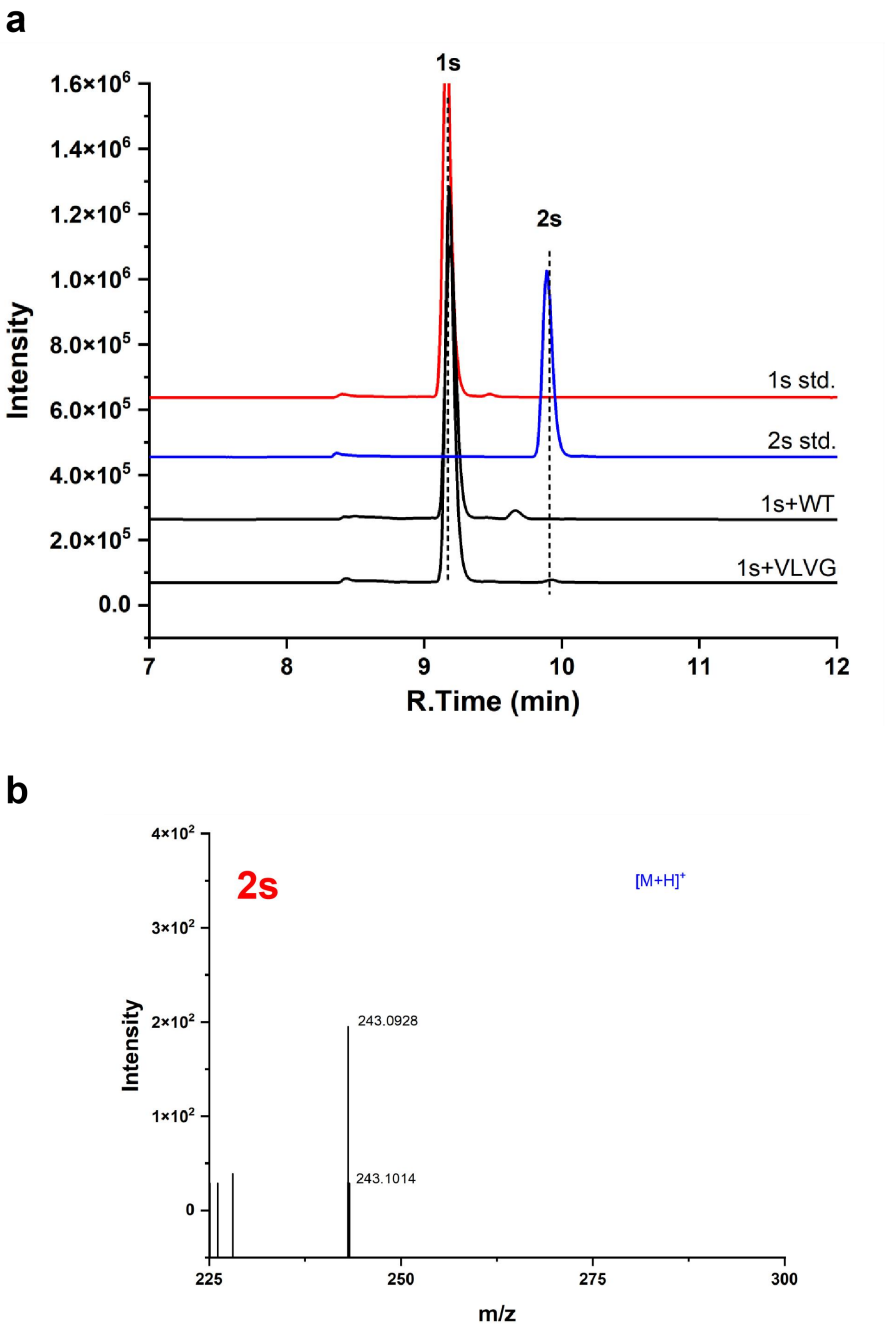

Supplementary Fig. 40 | HPLC-DAD and HRMS analysis of 1s methylation by *Ate*HMT mutants. a, HPLC chromatogram showing substrate **1s** and its methylated products **2s**. **b**, Representative positive ion HRMS spectra for products **2s**. Molecular weights: **1s** =228; **2s** = 242. Detection was performed at 300 nm.

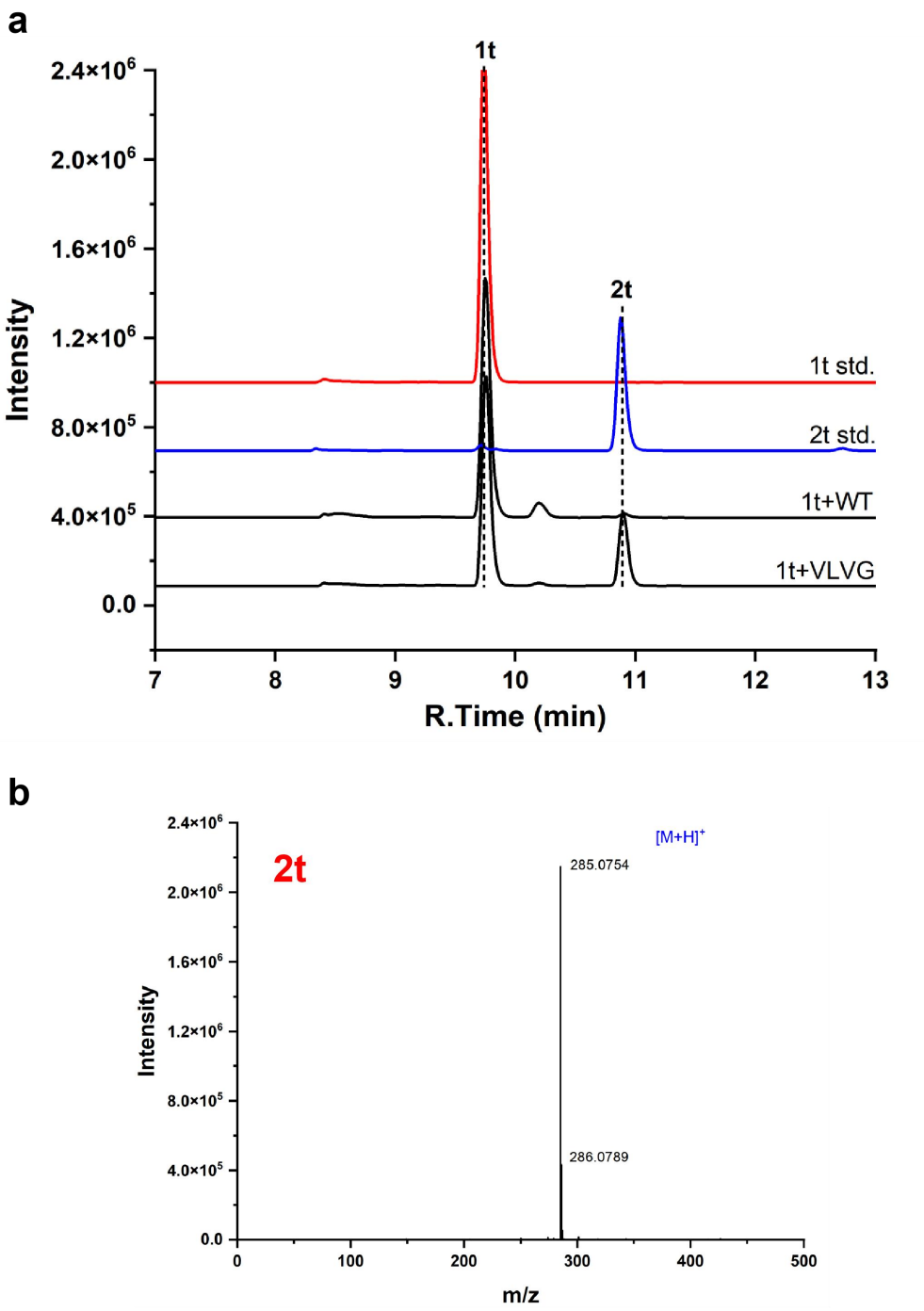

Supplementary Fig. 41 | HPLC-DAD and HRMS analysis of 1t methylation by *Ate*HMT mutants. a, HPLC chromatogram showing substrate **1t** and its methylated products **2t**. **b**, Representative positive ion HRMS spectra for products **2t**. Molecular weights: **1t** =270; **2t** = 284. Detection was performed at 260 nm.

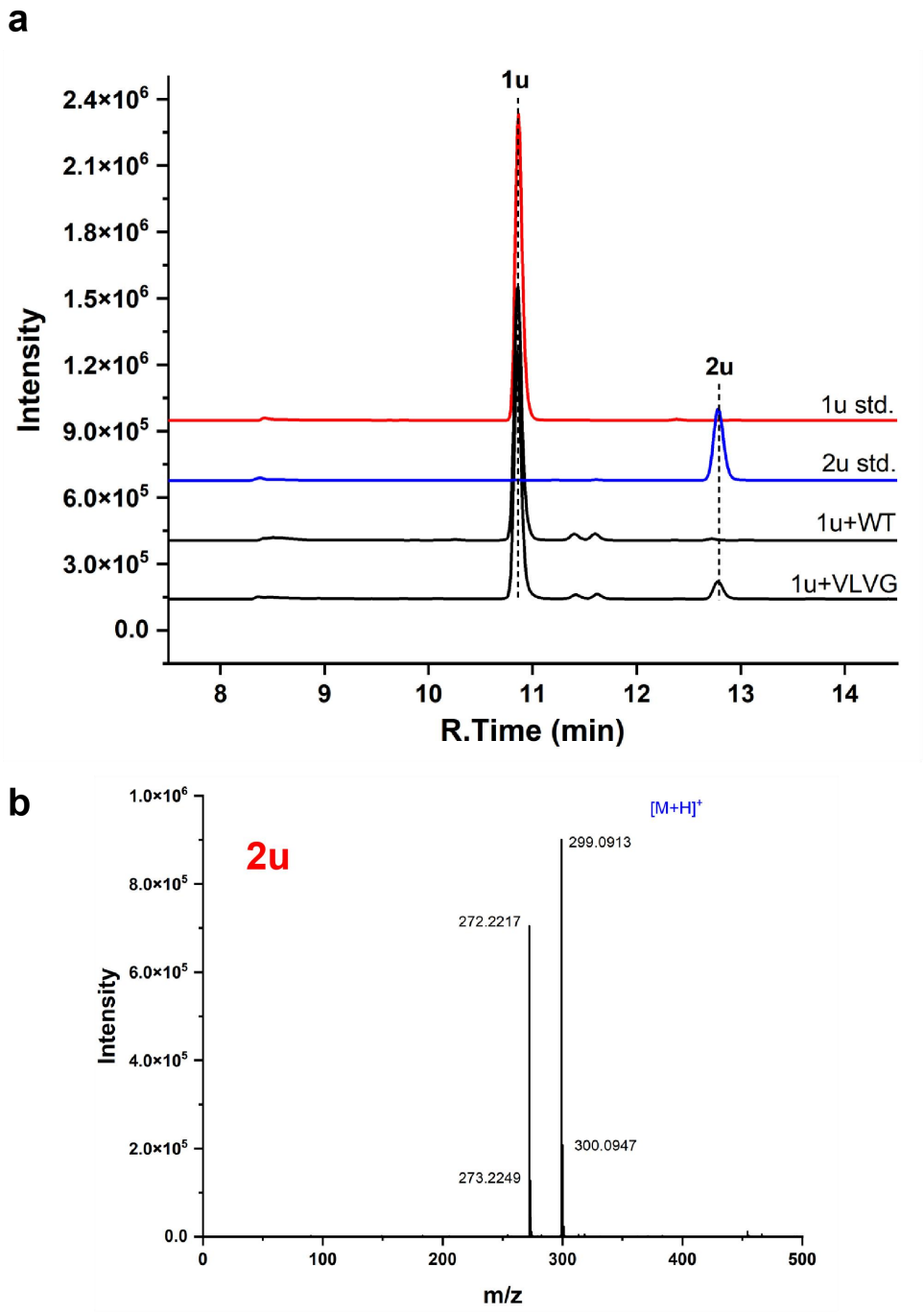

Supplementary Fig. 42 | HPLC-DAD and HRMS analysis of 1u methylation by *Ate*HMT mutants. a, HPLC chromatogram showing substrate **1u** and its methylated products **2u**. **b**, Representative positive ion HRMS spectra for products **2u**. Molecular weights: **1u** =284; **2u** = 298. Detection was performed at 260 nm.

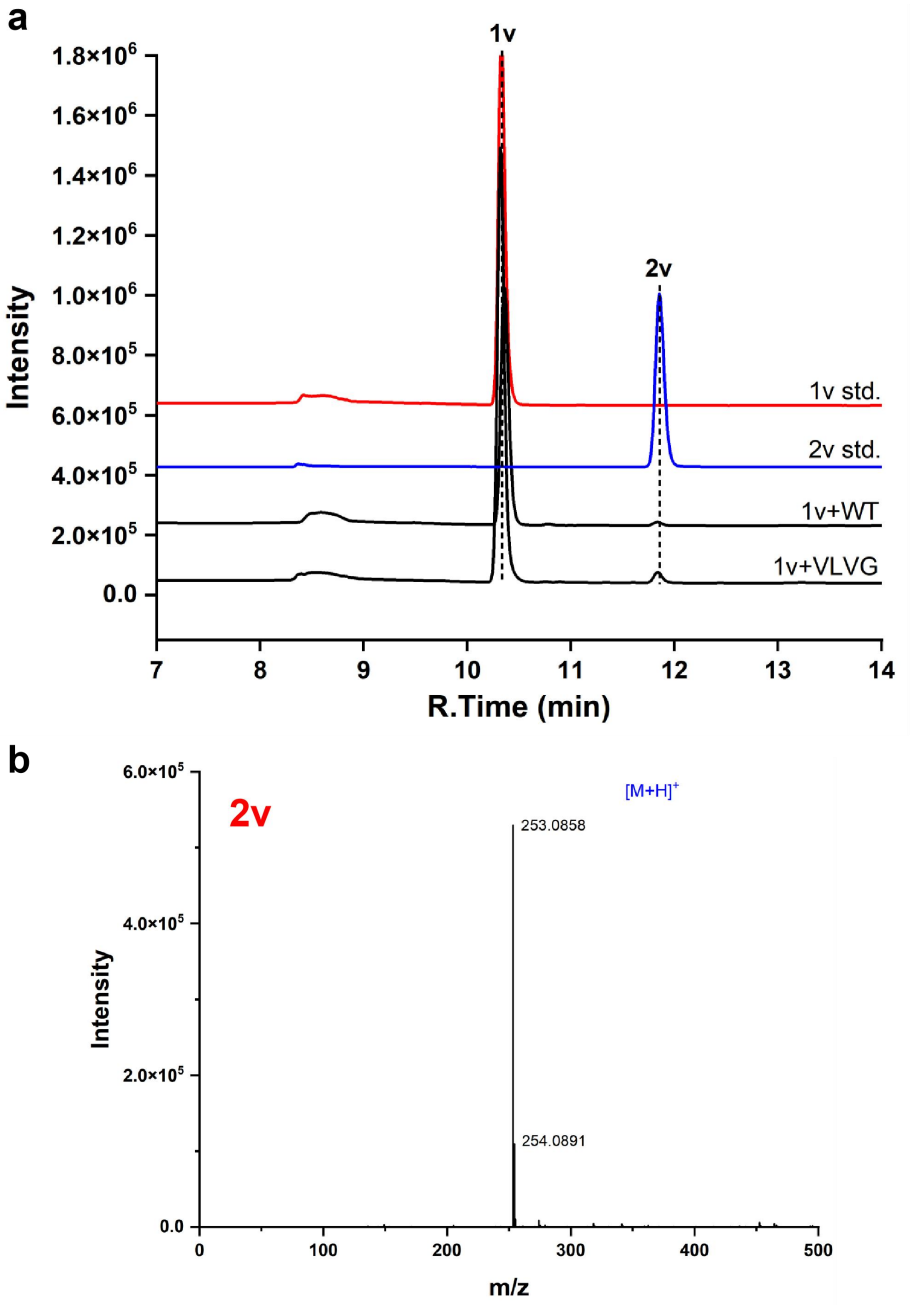

Supplementary Fig. 43 | HPLC-DAD and HRMS analysis of 1v methylation by *Ate*HMT mutants. a, HPLC chromatogram showing substrate **1v** and its methylated products **2v**. **b**, Representative positive ion HRMS spectra for products **2v**. Molecular weights: **1v** =238; **2v** = 252. Detection was performed at 246 nm.

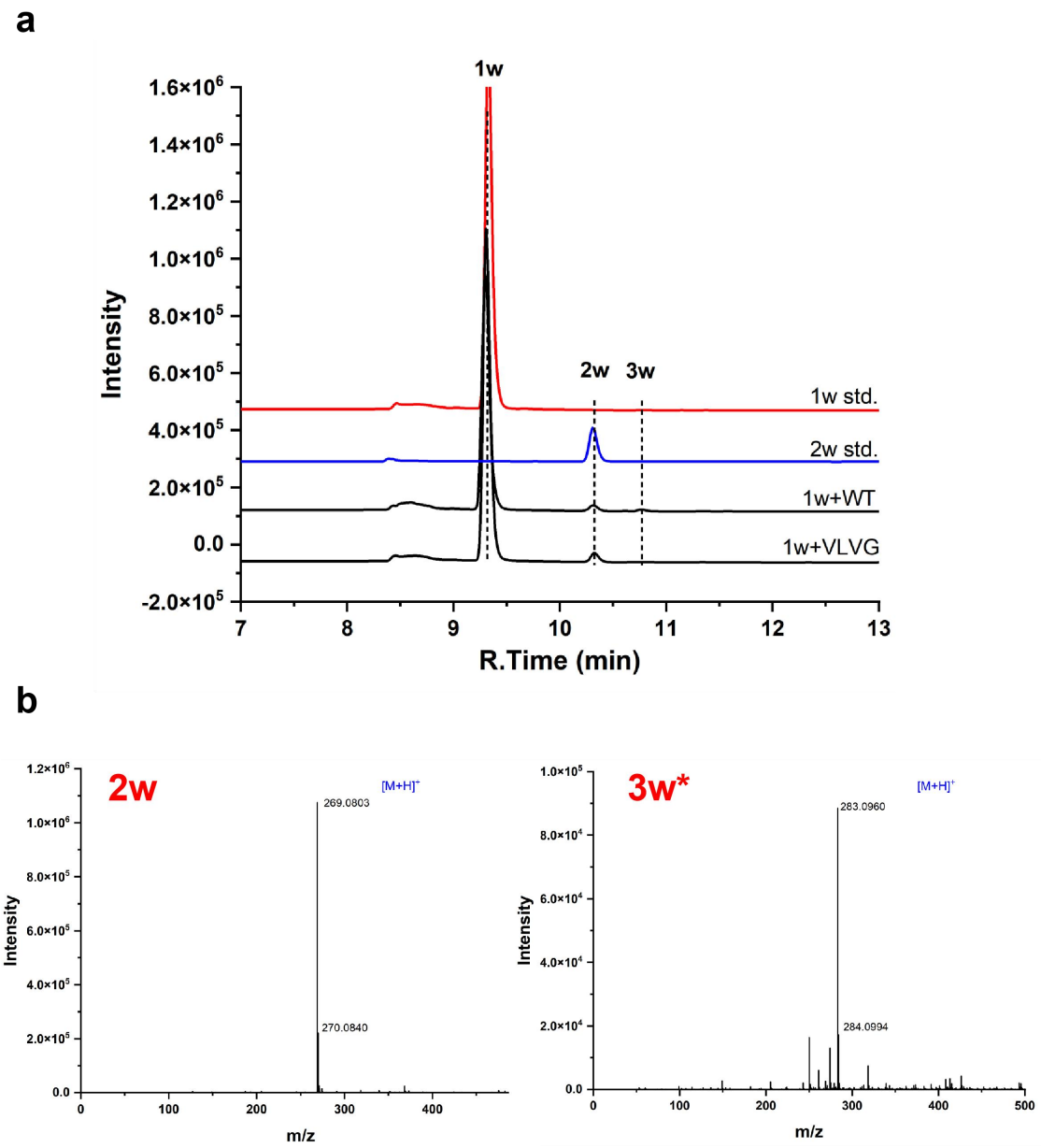

Supplementary Fig. 44 | HPLC-DAD and HRMS analysis of 1w methylation by *Ate*HMT mutants. a, HPLC chromatogram showing substrate **1w** and its methylated products **2w** and **3w**. **b**, Representative positive ion HRMS spectra for products **2w** and **3w**. Molecular weights: **1w** =254; **2w** = 268, **3w** = 282. Detection was performed at 248 nm. * indicates products that were not fully characterized.

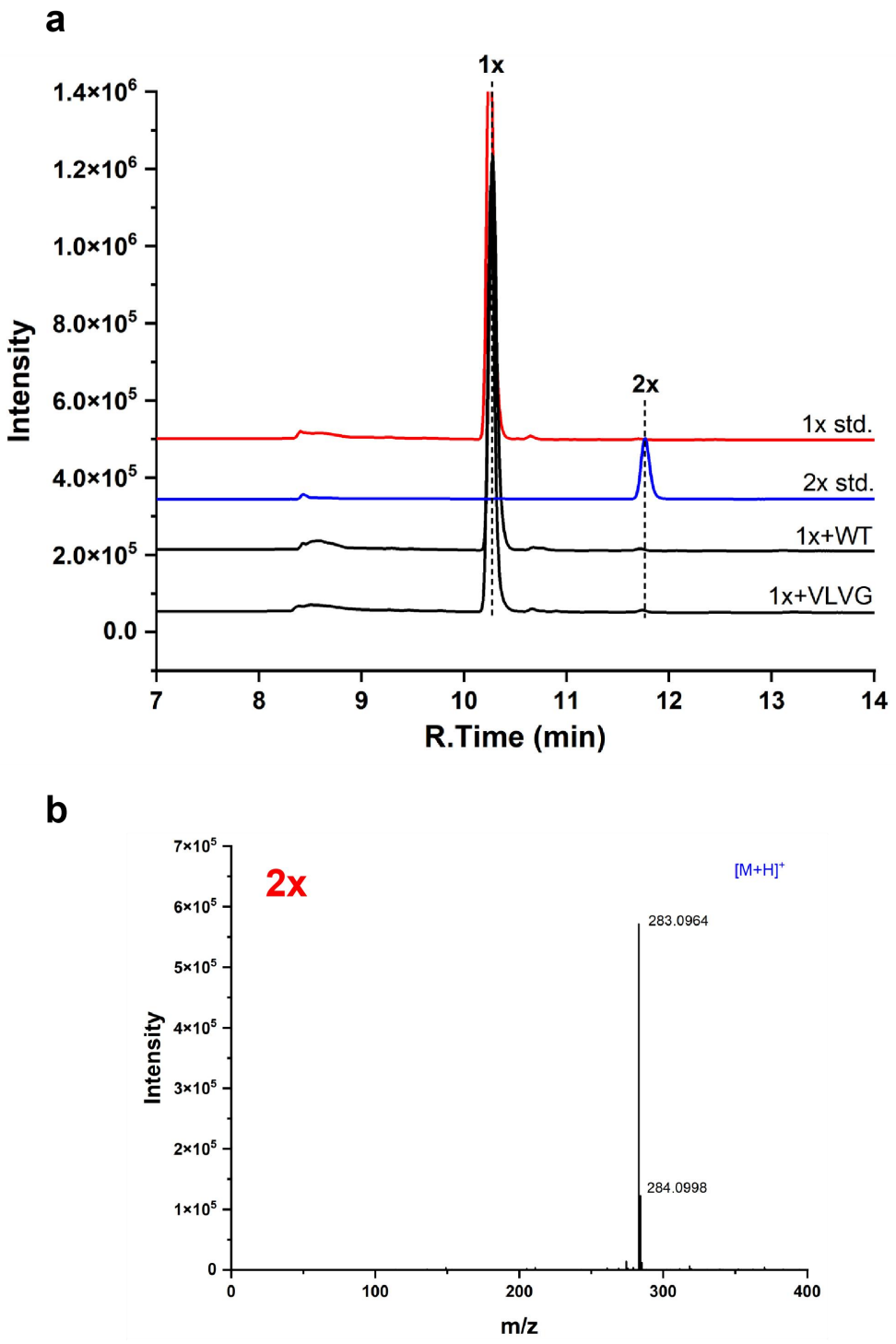

Supplementary Fig. 45 | HPLC-DAD and HRMS analysis of 1x methylation by *Ate*HMT mutants. a, HPLC chromatogram showing substrate **1x** and its methylated products **2x**. **b**, Representative positive ion HRMS spectra for products **2x**. Molecular weights: **1x** =268; **2x** = 282. Detection was performed at 249 nm.

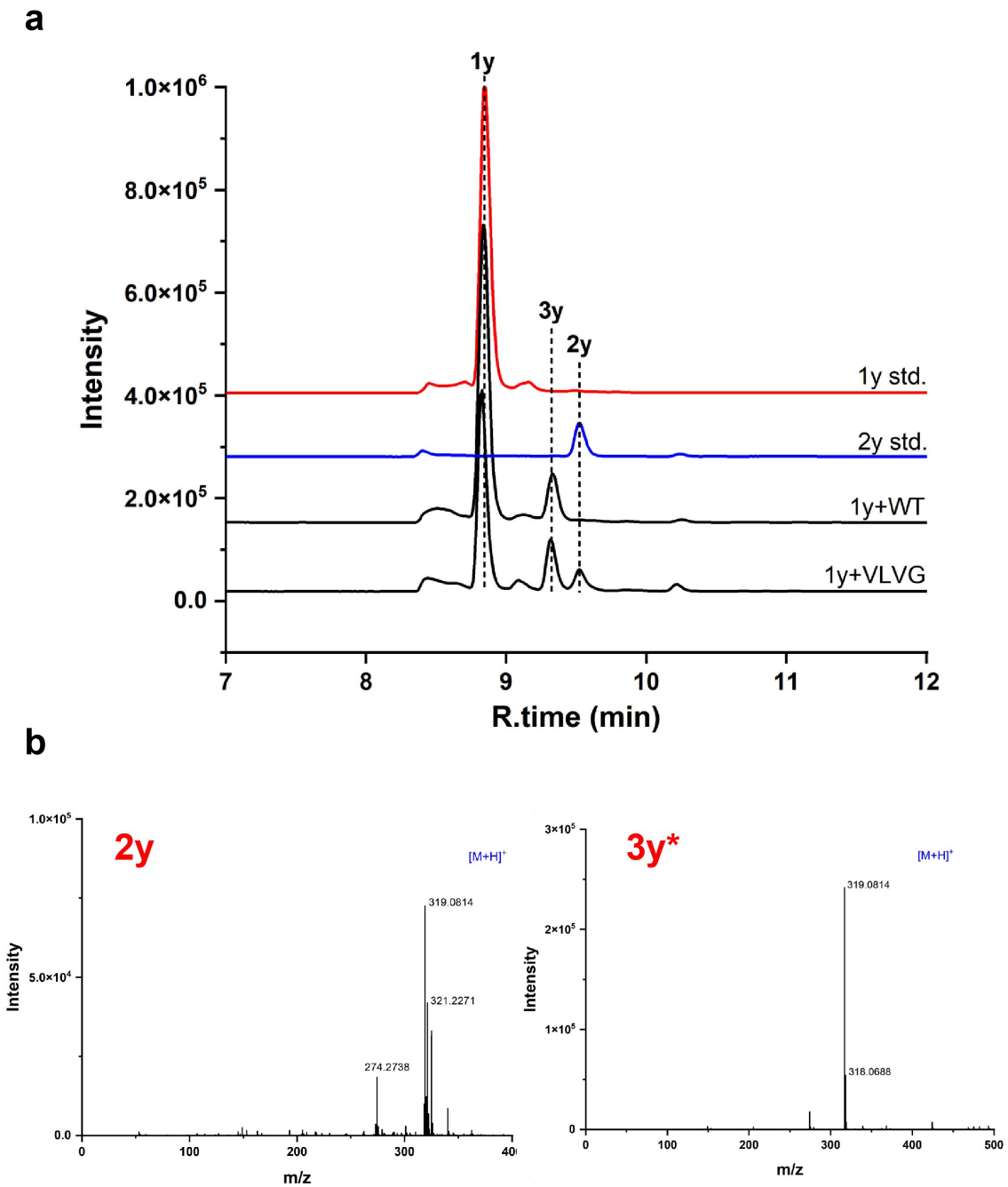

Supplementary Fig. 46 | HPLC-DAD and HRMS analysis of 1y methylation by *Ate*HMT mutants. a, HPLC chromatogram showing substrate **1y** and its methylated products **2y** and **3y**. **b**, Representative positive ion HRMS spectra for products **2y** and **3y**. Molecular weights: **1y** =304; **2y**, **3y** = 318. Detection was performed at 289 nm. * indicates products that were not fully characterized.

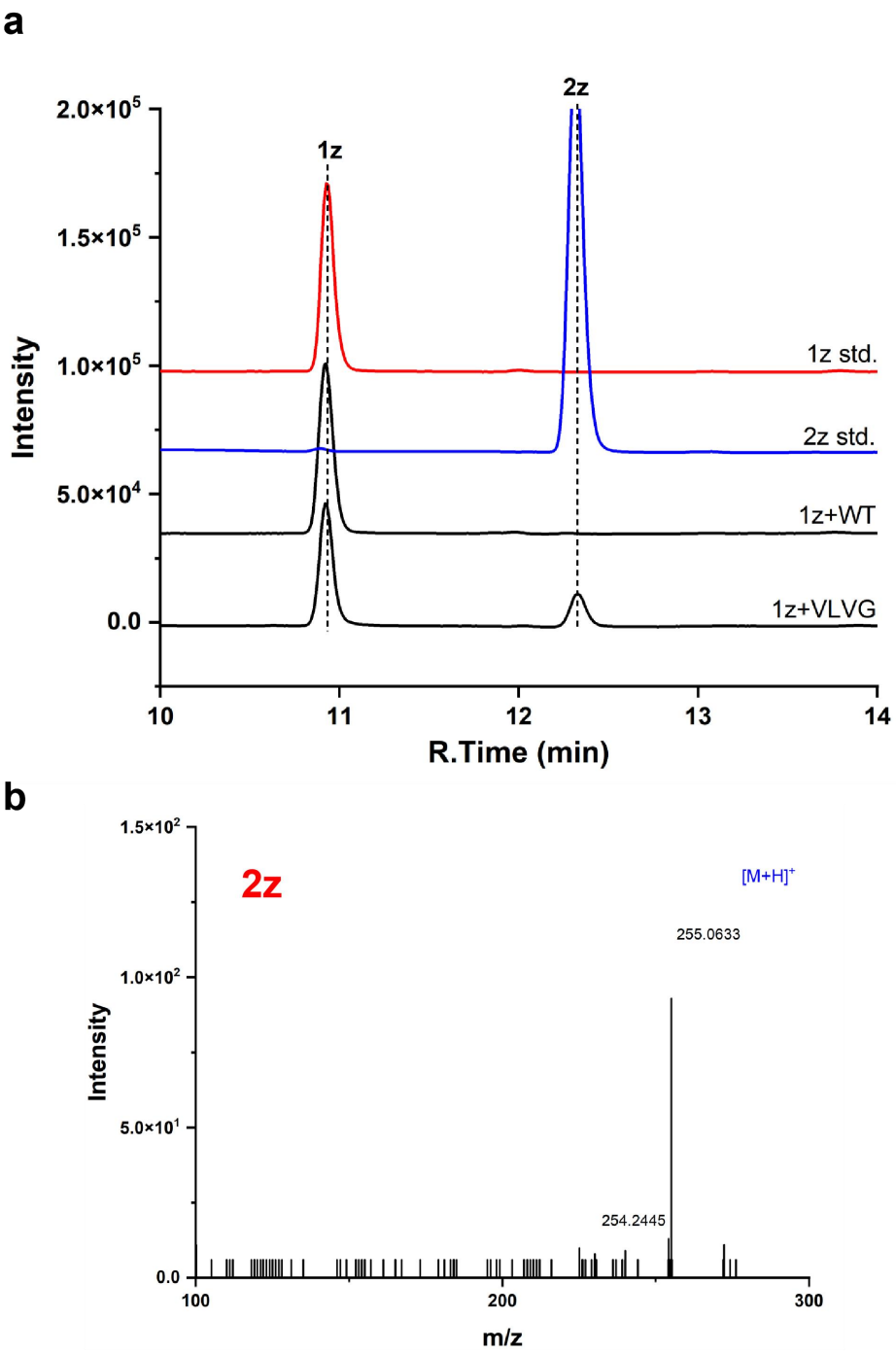

Supplementary Fig. 47 | HPLC-DAD and HRMS analysis of 1z methylation by *Ate*HMT mutants. a, HPLC chromatogram showing substrate **1z** and its methylated products **2z**. **b**, Representative positive ion HRMS spectra for products **2z**. Molecular weights: **1z** =240; **2z** = 254. Detection was performed at 350 nm.

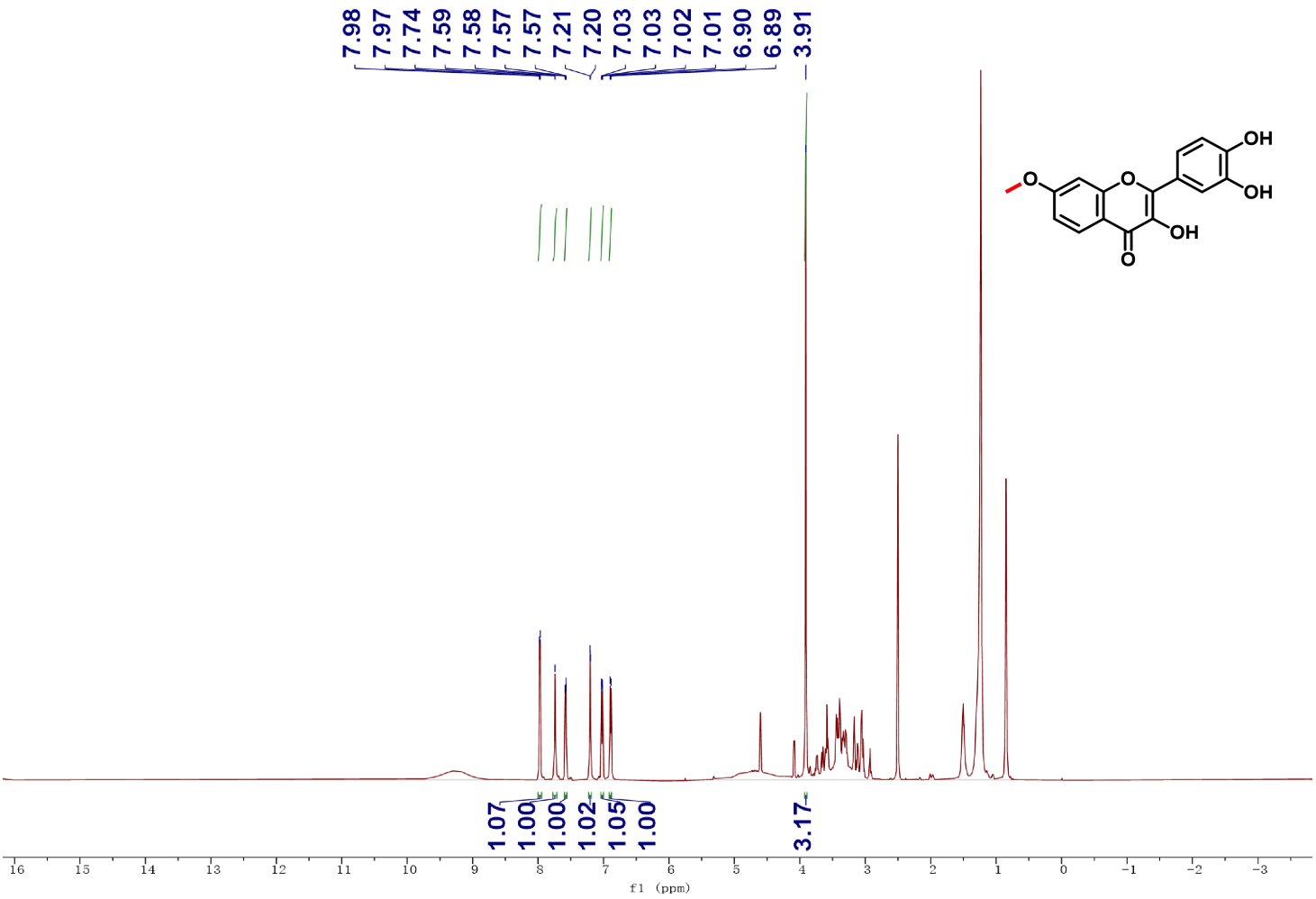

Supplementary Fig. 48 | ^{1}H NMR spectrum of 2d (400 MHz, DMSO-d_6).[5]

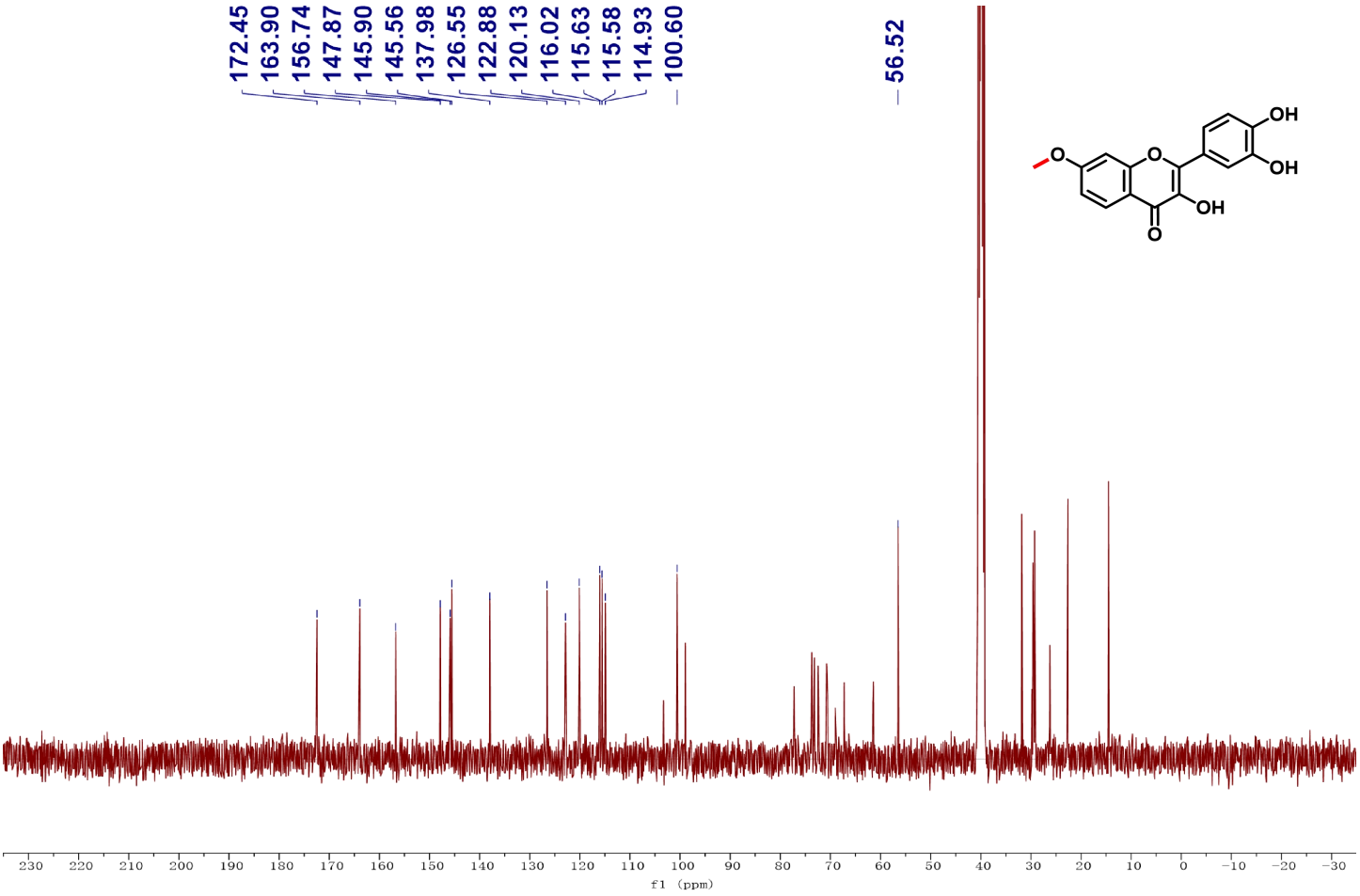

Supplementary Fig. 49 | ^{13}C NMR spectrum of 2d (101 MHz, DMSO-d_6).

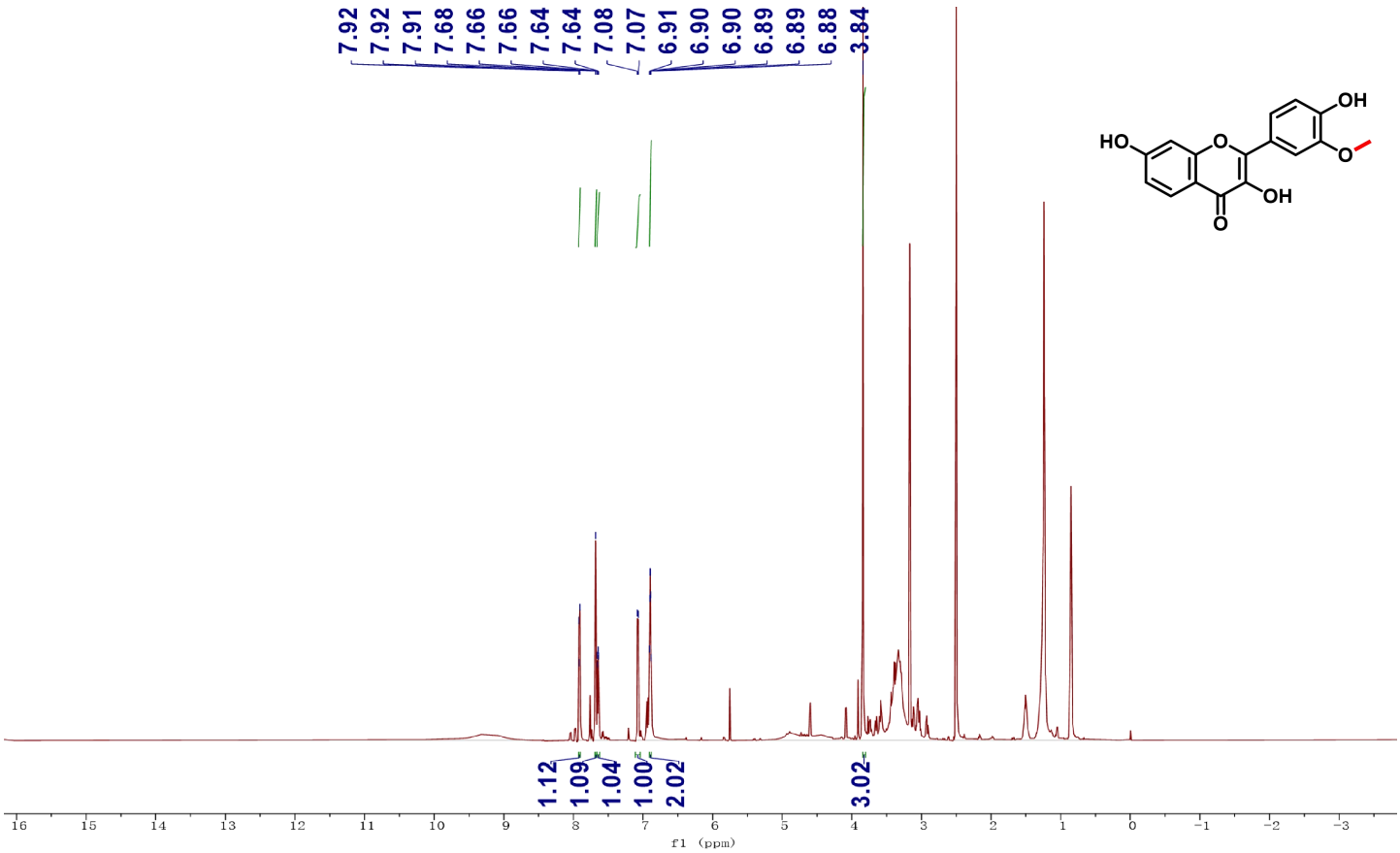

Supplementary Fig. 50 | ^{1}H NMR spectrum of 3d (600 MHz, DMSO-d_6).[6]

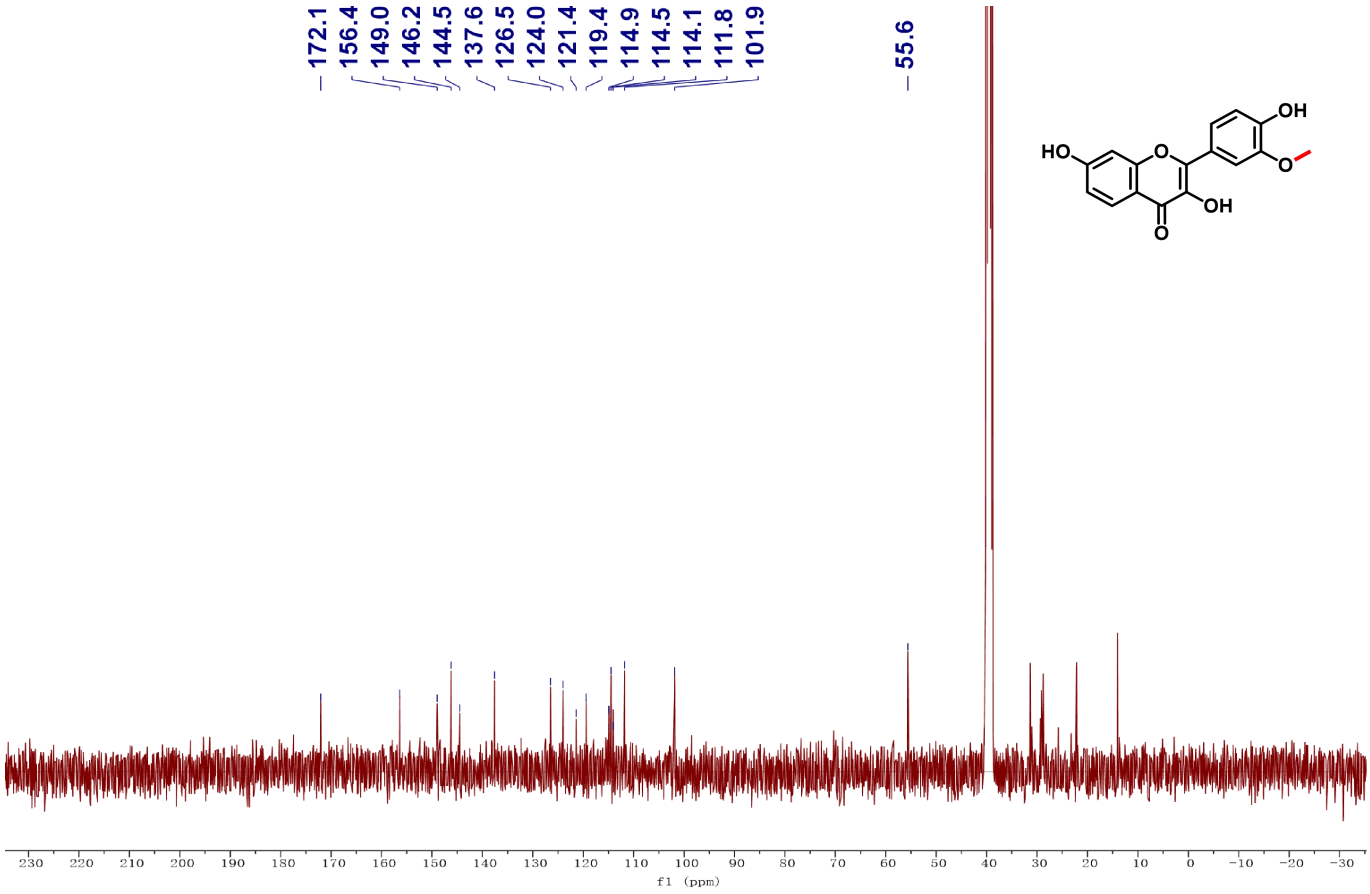

Supplementary Fig. 51 | ^{13}C NMR spectrum of 3d (101 MHz, DMSO-d_6).

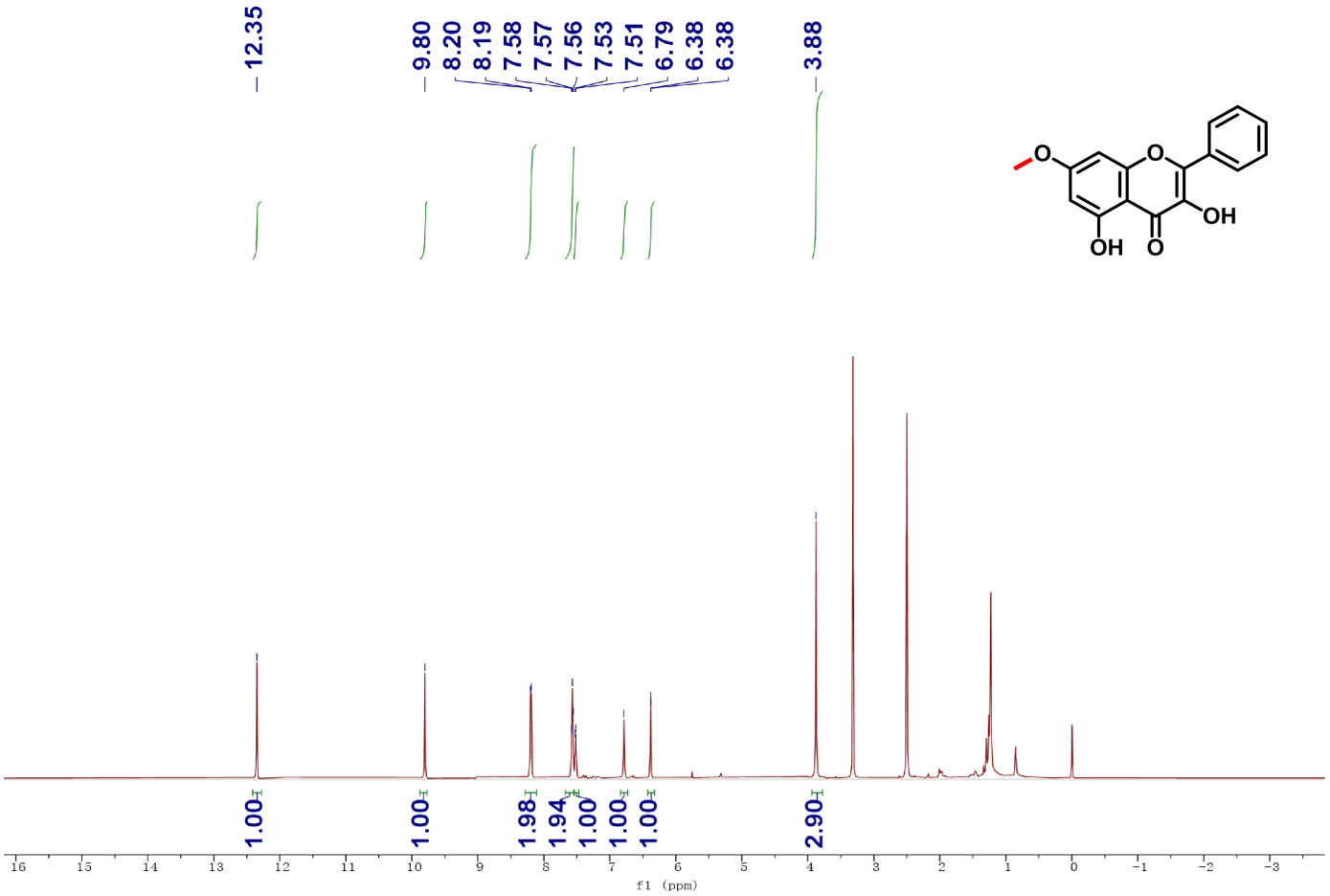

Supplementary Fig. 52 | ^{1}H NMR spectrum of 2e (400 MHz, DMSO-d_6).[7]

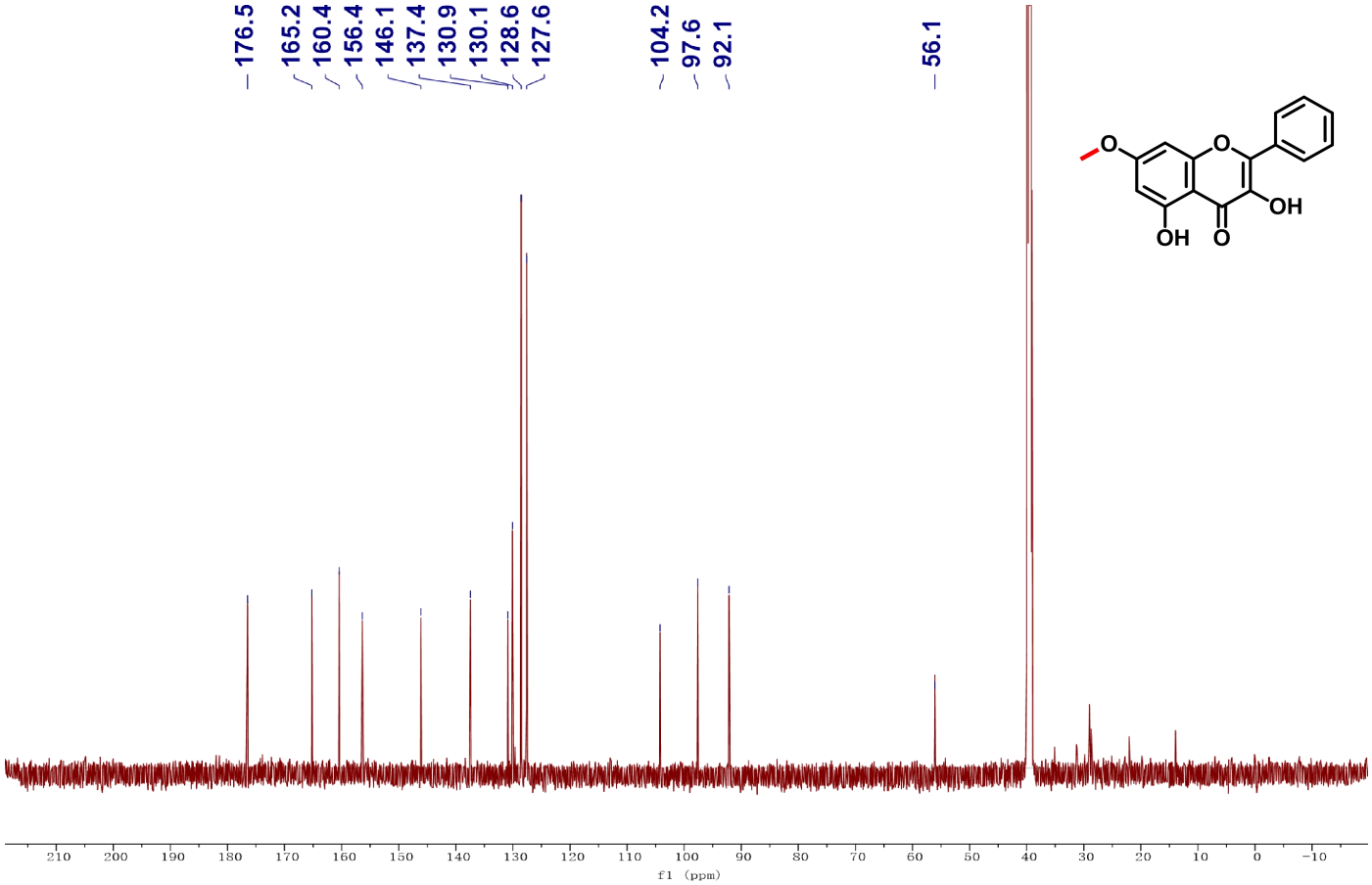

Supplementary Fig. 53 | ^{13}C NMR spectrum of 2e (151 MHz, DMSO-d_6).

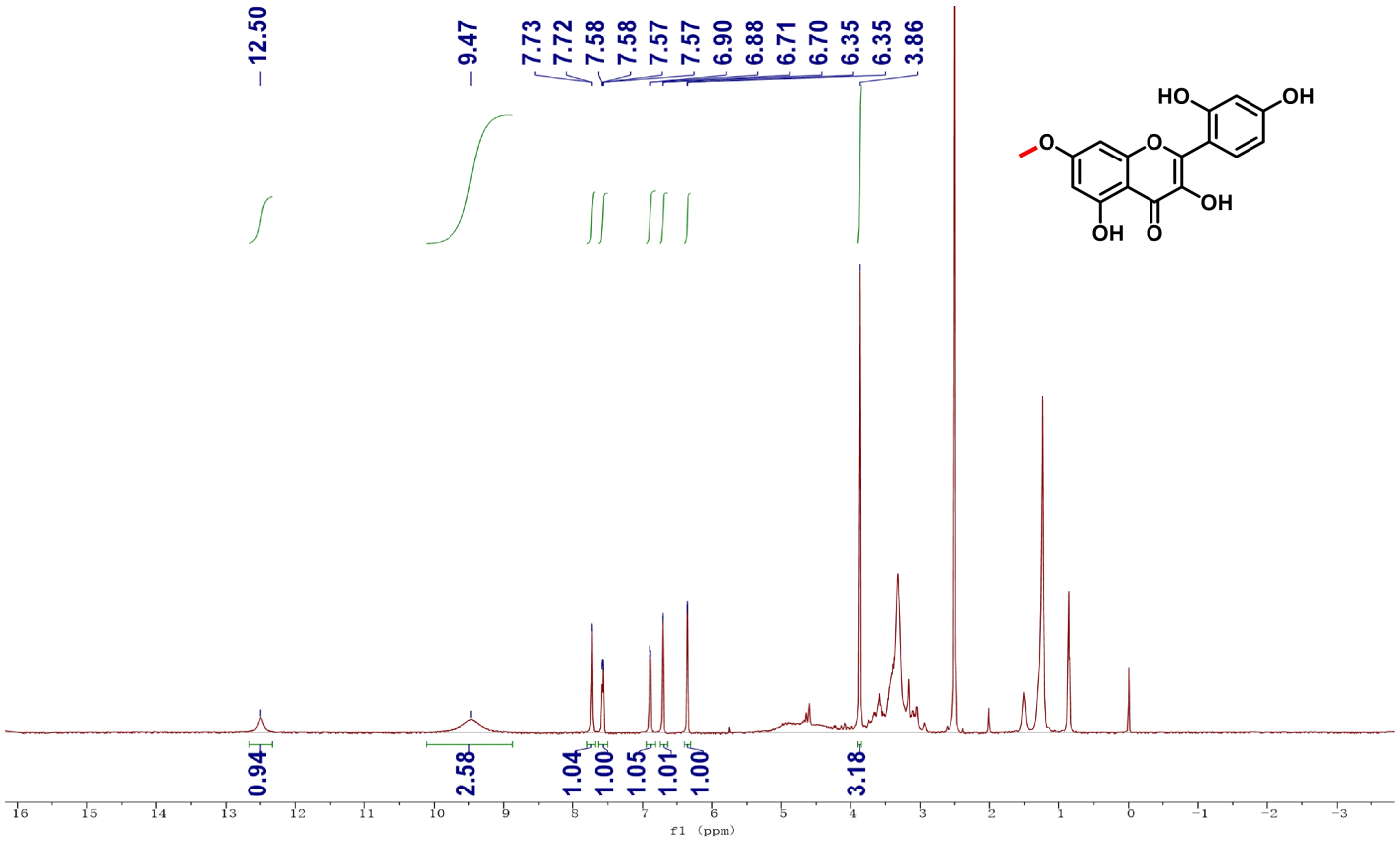

Supplementary Fig. 54 | ^{1}H NMR spectrum of 2g (400 MHz, DMSO-d_6).

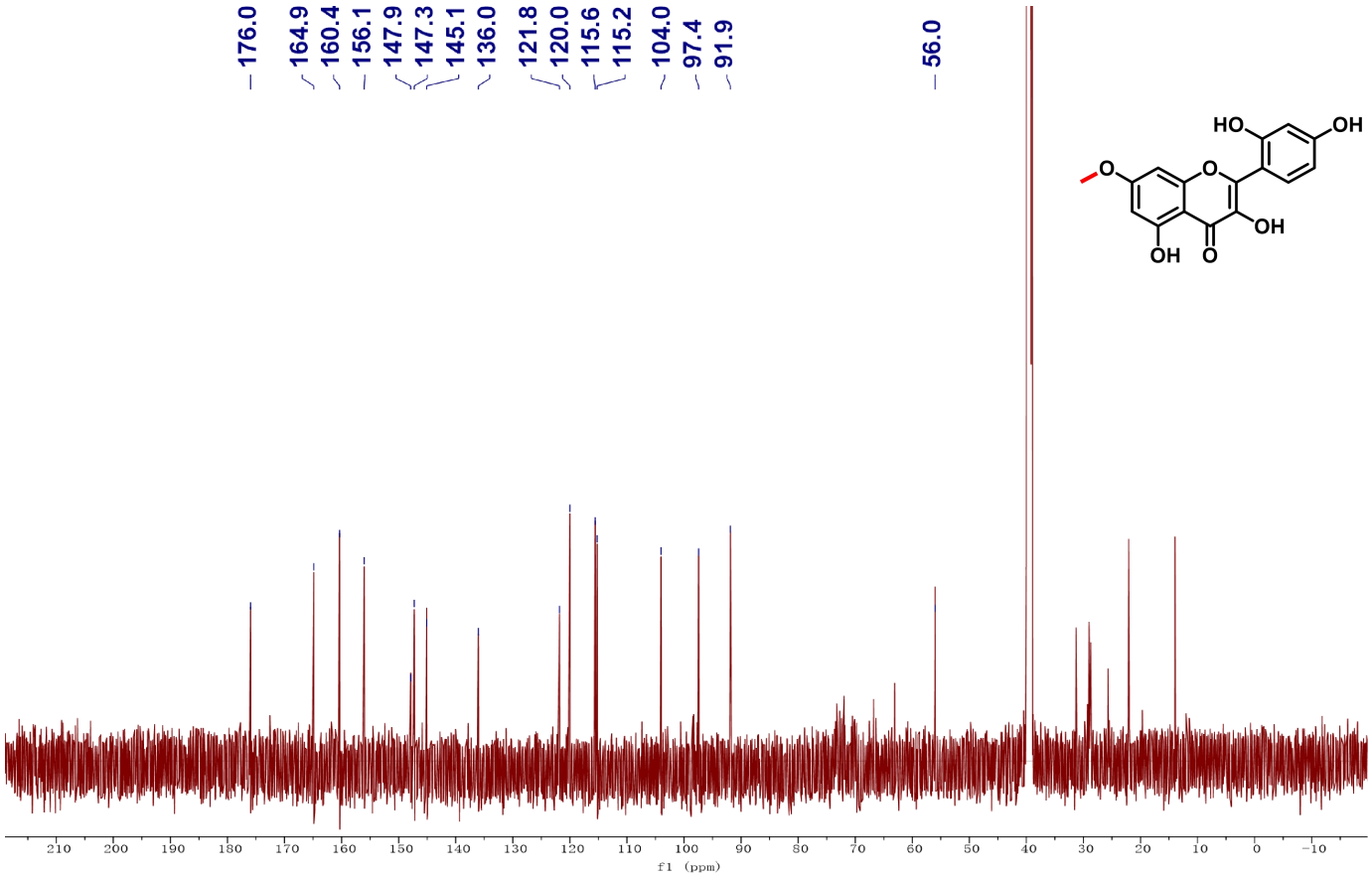

Supplementary Fig. 55 | ^{13}C NMR spectrum of 2g (151 MHz, DMSO-d_6).

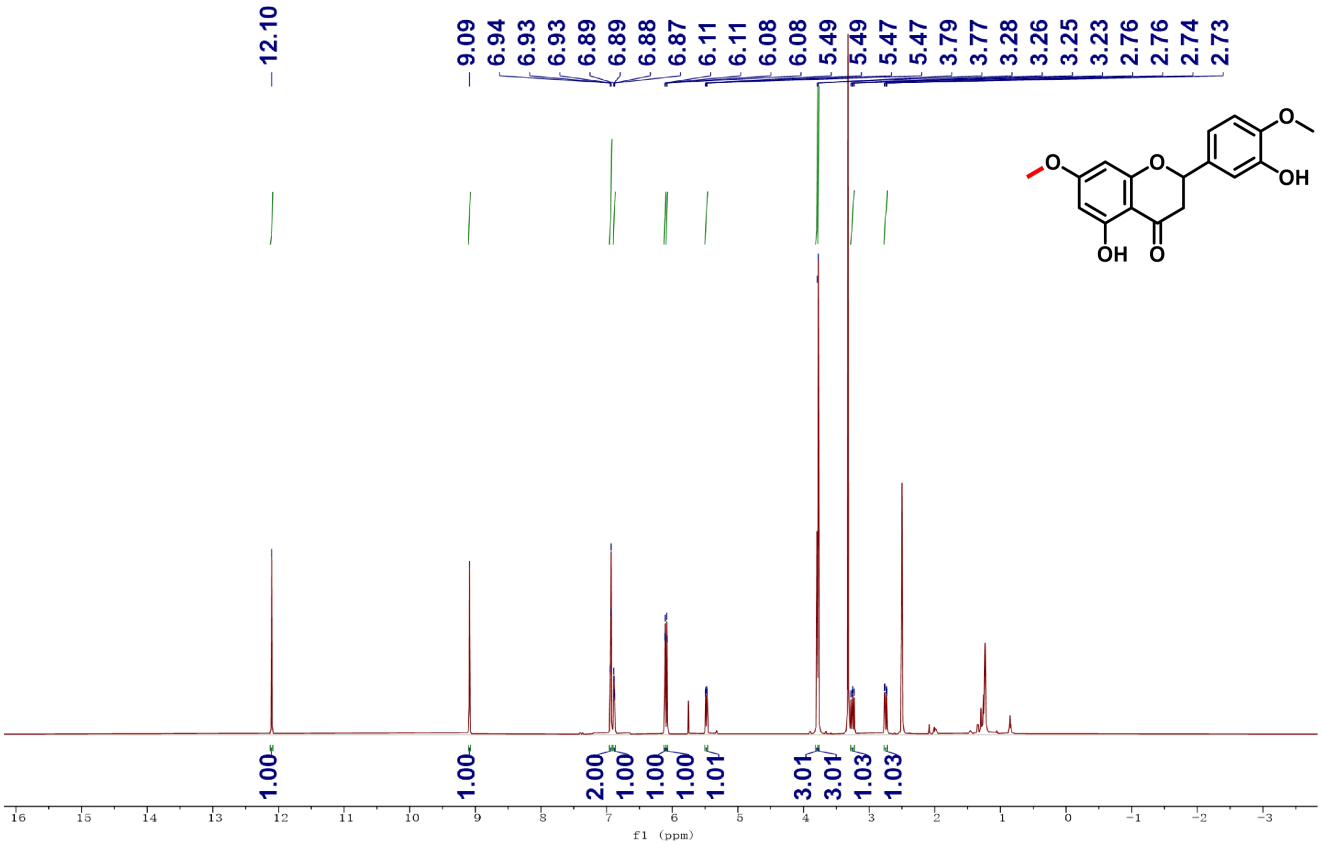

Supplementary Fig. 56 | ^{1}H NMR spectrum of 2q (600 MHz, DMSO-d_6).[8]

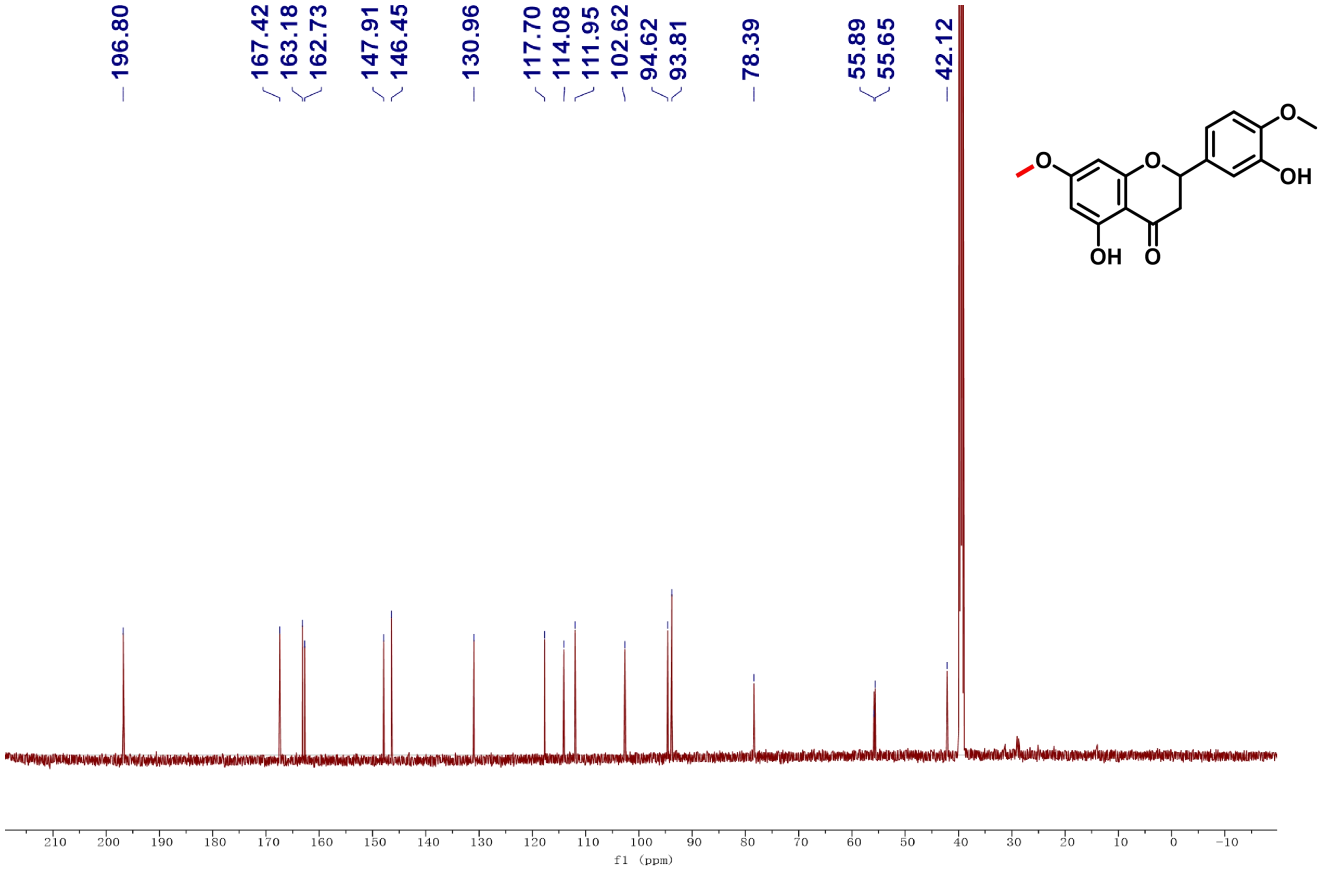

Supplementary Fig. 57 | ^{13}C NMR spectrum of 2q (151 MHz, DMSO-d_6).

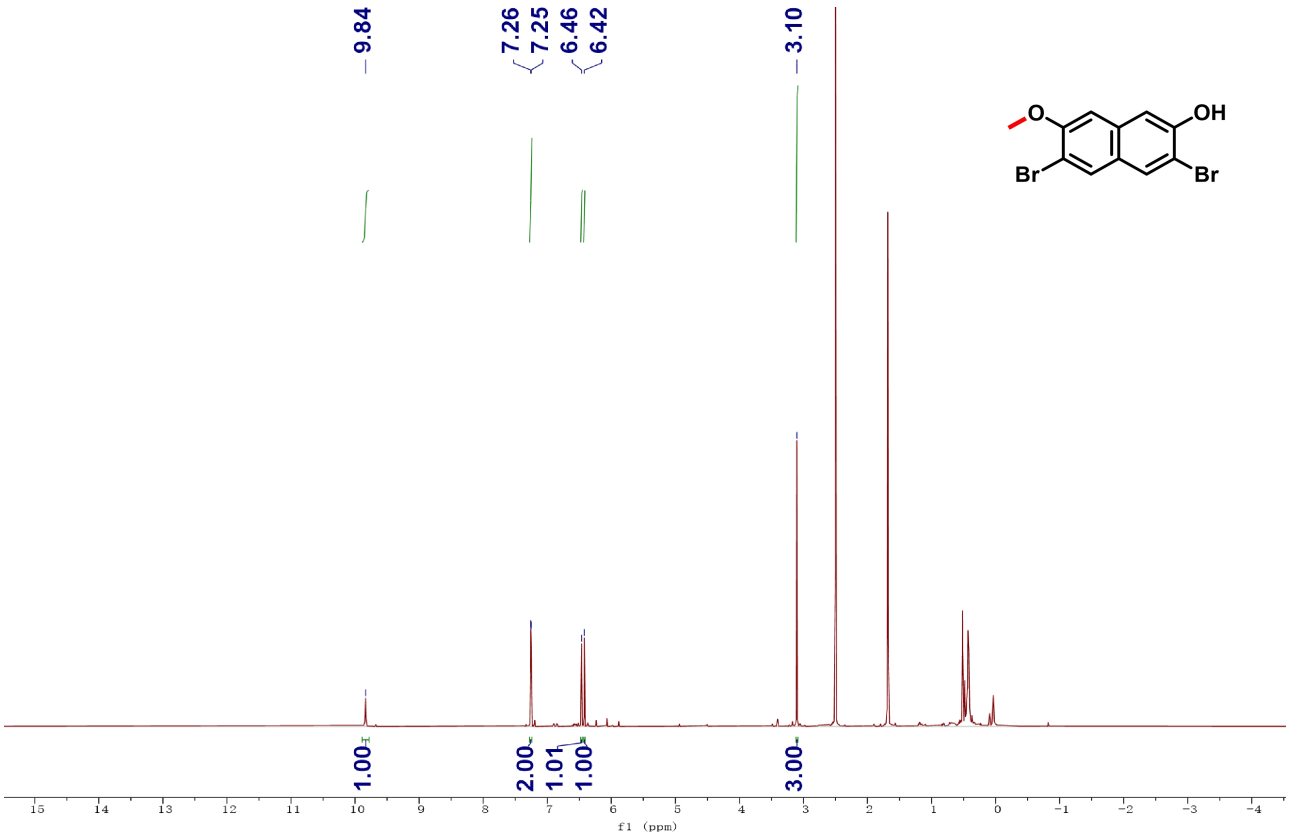

Supplementary Fig. 58 | ^{1}H NMR spectrum of 2B (600 MHz, DMSO-d_6).

Characterization of methylated products

2d: **^{1}H NMR** (600 MHz, DMSO-d_6) δ 7.97 (d, J = 8.9 Hz, 1H), 7.74 (s, 1H), 7.58 (dd, J = 8.4, 2.1 Hz, 1H), 7.22 – 7.19 (m, 1H), 7.02 (dd, J = 8.8, 2.3 Hz, 1H), 6.89 (d, J = 8.4 Hz, 1H), 3.91 (s, 3H). **^{13}C NMR** (101 MHz, DMSO-d_6) δ 172.45, 163.90, 156.74, 147.87, 145.90, 145.56, 137.98, 126.55, 122.88, 120.13, 116.02, 115.63, 115.58, 114.93, 100.60, 56.52.

3d: **^{1}H NMR** (600 MHz, DMSO-d_6) δ 7.94 – 7.88 (m, 1H), 7.68 (d, J = 2.2 Hz, 1H), 7.65 (dd, J = 8.5, 2.2 Hz, 1H), 7.08 (d, J = 8.6 Hz, 1H), 6.90 (dq, J = 5.8, 3.0, 2.6 Hz, 2H), 3.84 (d, J = 3.7 Hz, 3H). **^{13}C NMR** (101 MHz, DMSO-d_6) δ 172.06, 156.40, 148.96, 146.19, 144.51, 137.58, 126.49, 124.01, 121.40, 119.41, 114.92, 114.49, 114.08, 111.81, 101.86, 55.61.

2e: **^{1}H NMR** ^{1}H NMR (600 MHz, DMSO-d_6) δ 12.35 (s, 1H), 9.80 (s, 1H), 8.20 (d, J = 7.7 Hz, 2H), 7.57 (t, J = 7.5 Hz, 2H), 7.52 (d, J = 7.2 Hz, 1H), 6.79 (s, 1H), 6.38 (d, J = 2.0 Hz, 1H), 3.88 (s, 3H). **^{13}C NMR** (151 MHz, DMSO-d_6) δ 176.48, 165.21, 160.41, 156.37, 146.15, 137.45, 130.88, 130.08, 128.55, 127.60, 104.23, 97.62, 92.14, 56.09.

2g: **^{1}H NMR** (600 MHz, DMSO-d_6) δ 12.50 (s, 1H), 9.47 (s, 3H), 7.83 – 7.68 (m, 1H), 7.61 – 7.52 (m, 1H), 6.89 (d, J = 8.5 Hz, 1H), 6.74 – 6.63 (m, 1H), 6.35 (d, J = 2.3 Hz, 1H), 3.86 (s, 3H). **^{13}C NMR** (151 MHz, DMSO-d_6) δ 175.96, 164.88, 160.36, 156.06, 147.89, 147.29, 145.10, 136.04, 121.83, 120.01, 115.57, 115.22, 104.00, 97.44, 91.88, 56.01.

2q: **1H NMR** (600 MHz, DMSO-d_6) δ 12.10 (s, 1H), 9.09 (s, 1H), 6.96 – 6.91 (m, 2H), 6.88 (dd, J = 8.3, 2.1 Hz, 1H), 6.11 (d, J = 2.3 Hz, 1H), 6.08 (d, J = 2.3 Hz, 1H), 5.48 (dd, J = 12.5, 3.1 Hz, 1H), 3.79 (s, 3H), 3.77 (s, 3H), 3.25 (dd, J = 17.1, 12.5 Hz, 1H), 2.75 (dd, J = 17.1, 3.2 Hz, 1H). **^{13}C NMR** (151 MHz, DMSO-d_6) δ 196.80, 167.42, 163.18, 162.73, 147.91, 146.45, 130.96, 117.70, 114.08, 111.95, 102.62, 94.62, 93.81, 78.39, 55.89, 55.65, 42.12.

2B: **^{1}H NMR** (600 MHz, DMSO-d_6) δ 9.84 (s, 1H), 7.26 (d, J = 2.9 Hz, 2H), 6.46 (s, 1H), 6.42 (s, 1H), 3.10 (s, 3H).

Protein Sequences

1. The sequence of *Ate*HMT-WT

MPPKAVAPQEMLDTLGKYQGDRVFDGWEELWQKGGDCLPWDRGVPNPALEDTLLQKRAILGGPTTTDAQGHMRRKKALV
PGCGRGVDVLLLASFGYDAYGLEYSAAAVAQCKQEEAKNGDKYPVRDAEIGRGKLVFVRGDFFKNDWLEALQLPLNCFDLI
YDYTFFCALNPSMRPDWALRHTQLLAPSPNGNLICLEFPRHKDPSKPGPPWGSSSEAYMEHLSHPGEKIPYDSSGRCKSDPLR
ETSELGLERVAYWQPARTHEVGKDAEGEIQDRVSVWRRR

2. The sequence of *Ate*HMT-C167A

MPPKAVAPQEMLDTLGKYQGDRVFDGWEELWQKGGDCLPWDRGVPNPALEDTLLQKRAILGGPTTTDAQGHMRRKKALV
PGCGRGVDVLLLASFGYDAYGLEYSAAAVAQCKQEEAKNGDKYPVRDAEIGRGKLVFVRGDFFKNDWLEALQLPLNCFDLI
YDYTFFAALNPSMRPDWALRHTQLLAPSPNGNLICLEFPRHKDPSKPGPPWGSSSEAYMEHLSHPGEKIPYDSSGRCKSDPLR
ETSELGLERVAYWQPARTHEVGKDAEGEIQDRVSVWRRR

3. The sequence of *Ate*HMT-VLVG

MPPVLVAPQEVLDTLGKYQGDRVFDGWEELWQKGGDCLPWDRGVPNPALEDTLLQKRAILGGPTTTDAQGHMRRKKALVP
GCGRGVDVLLLASFGYDAYGLEYSAAAVAQCKQEEAKNGDKYPVRDAEIGRGKLVFVRGDFFKNDWLEALQLPLNCFDLIY
DYTFFCALNPSMRPDWALRHTQLLAPSPNGNLICLEFPRHKDPSKPGPPWGSSSEAYMEHLSHPGEKIPYDSSGRCKSDPLRE
TSELGLERVAYWQPARTHEGGKDAEGEIQDRVSVWRRR

4. The sequence of *Aam*HMT-WT

MPPKAVAPQEVLDTLGKYQGDKVFDGWEELWKKGGDCLPWDRGIPNPALEDTLVQRRAILGGPITTDEQGNVHRKKALVPG
CGRGVDVLLLASFGYDAYGLEYSTSAVEECKQEETRNGDKYPVRDAKIGRGKITFVQGDFFQNNWLEALRLPMNCFDLTYD
YTFFCALNPSMRPDWALRHTQLLAPSPHGNLICLEFPRHKDPSKPGPPWGSSSEAYMEHLSHPGEKIPYDSNGRCKSDPLREIS
EQGLERVAHWQPVRTHEVGKDADGEIQDRVSVWRRR

5. The sequence of *Aho*HMT-WT

MSGPDKAAIQRKVMDTLAKYQGDNYVDGWAELWNSTEHLPWDKGAPHPALEDTLTQQRATIGGPLATDAQGKTYRKKAL
VPGCGRGVDVLLLASFGYDAYGLEYSDAAVKKCESEAAQNGDRYPVRDAEVGRGKITFVQGDFFKNDWLERLQLPLNCFD
LIYDYTFLCALNPTMRPNWALRHTQLLAPSPRGNLICLEFPRHKDPAQQGPPWGLSSEAYMEHLSHPGEKIPYDAQGRCKMD
PLREPSEHGLERVAYWQPARTHEGGKDENGVVQDRVSIWRHR

6. The sequence of *Abr*HMT-WT

MQQKVRDTLAKYQGDNYVDGWAELWDKNENLPWDKGVPNPALEDTLIQQRATVGGPIATDAQGATYRKKALVPGCGRGV
DVLLLASFGYDAYGLEYSDAAVNICESEAAQNGDKYPVRDAGIGRGKIAFVQGDFFKNDWLESLQLPLNCFDLIYDYTFFCA
LNPTMRPNWALRHTQLLAPSPRGNLICLEFPRHKDPTQQGPPWGVSSEAYMEHLSHPGEQIPYDAQGRCKMDPLREPSEHGL
ERVAYFQPAQTHEGGKDSNGVVQDRVSIWRHR

7. The sequence of *Ale*HMT-WT

MDSDKATMQRKVRDTLAKYQGDDYIDGWAELWDKNDNLPWDKGIPNPALEDALTQQRATLGGPIATDAQGATYRKKALVP
GCGRGVDVLLLASFGYDAYGLEYSDAALKICESEAAQNGDKYPVRDSGIGRGKIAFVQGDFFKNDWLESLQLPLNCFDLIYD
YTFFCALNPTMRPNWALRHTQLLAPSPCGNLICLEFPRHKDPTQQGPPWGVSSEAYMEHLSHPGEQIPYDAQGRCKMDPLRE
PSEHGLERVAYFQPARTHEGGKDSNGVVQDRVSVWRHR

8. The sequence of *Ati*HMT-WT

MDSDKATMQRKVRDTLAKYQGDDYVDGWAELWDKNENLPWDKGIPNPALEDTLIQQRATVGGPIATDAQGATYRKKALVP
GCGRGVDVLLLASFGYDAYGLEYSDAAVKICESEAAQNGDKYPVRDAGIGRGKIAFVQGDFFKNDWLESLQLPLECFDLIYD
YTFFCALNPTMRPSWALRHTQLLAPSPRGNLICLEFPRHKDPTQQGPPWGVSSEAYMEHLSHPGEQIPYDDQGRCKMDPLRE
PSEHGLERVAYFQPARTHEGGKDSNGVVQDRVSIWRHR

9. The sequence of *Afi*HMT-WT

MQRKVRDTLAKYQGDDYVDGWAELWDKNENLPWDKGIPNPALEDTLIQQRATVGGPIATDAQGATYRKKALVPGCGRGV
DVLLLASFGYDAYGLEYSDAAVNICESEAAQNGDKYPVRDAGIGRGKIAFVQGDFFKNDWLESLQLPLNCFDLIYDYTFFCA
LNPTMRPNWALRHTQLLAPSPRGNLICLEFPRHKDPTQQGPPWGVSSEAYMEHLSHPGEQIPYDAQGRCKMDPLREPSEHGL
ERVAYFQPAQTHEGGKDSNGVVQDRVSIWRHR

10. The sequence of *Auv*HMT-WT

MATPDRATMQRNVRDTLARYQGDDYVDGWAELWNKNENLPWDKGIPNPALEDTLTQQRATLGGPIATDAQGATYRKKALV
PGCGRGVDVLLLASFGYDAYGLEYSDAAVKNCENEAAQNGDKYPVRDAGIGRGKIAFVQGDFFKNDWMESLQIPPNCFDLI
YDYTFFCALNPMMRPSWALRHTQLLAPSPRGNLICLEFPRHKDPTQQGPPWGVSSEAYMEHLSHPGEQIPYDAQSRCKMDPL
REPSEHGLERVAYFQPARTHEGGKDSNGVVQDRVSIWRHR

11. The sequence of *Ain*HMT-WT

MATPDRATMQRNVRDTLARYQGDDYVDGWAELWNKNENLPWDKGIPNPALEDTLIQQRATLGGPIATDAQGATYRKKALV
PGCGRGVDVLLLASFGYDAYGLEYSDAAVKICENEAAQNGDKYPVRDAGIGRGKIAFVQGDFFKNDWLKSLQIPPNCFDLIY
DYTFFCALDPTMRPSWALRHTQLLAPSPRGNLICLEFPRHKDPTQQGPPWGVSSEAYMEHLSHPGEQIPYDAQSRCKMDPLR
EPSEHGLERVAYFQPARTHEGGKDSNGVVQDRVSIWRHR

12. The sequence of *Aja*HMT-WT

MATPDRATMQRNVRDTLARYQGDDYVHGWAELWNKNENLPWDKGIPNPALEDTLIQQRATLGGPIATDAQGATYRKKALV
PGCGRGVDVLLLASFGYDAYGLEYSDAAVKNCENEAAQNGDKYLVRDAGIGRGKIAFVQGDFFKNDWLESLQTPPNCFDLI
YDYTFFCALDPTMRPSWALRHTQLLAPSPRGNLICLEFPRHKDPTQQGPPWGVSSEAYMEHLSHPGEQIPYDAQSRCKMDPL
REPSEHGLERVAYFQPARTHEGGKDSNGVVQDRVSIWRHR

13. The sequence of *Avi*HMT-WT

MATPDRATMQRNVRDTLARYQGDDYVHGWAELWNKNENLPWDKGIPNPALEDTLIQQRATLGGPIATDAQGATYRKKALV
PGCGRGVDVLLLASFGYDAYGLEYSDAAVKNCENEAAQNGDKYLVRNAGIGRGKIAFVQGDFFKNDWLESLQTPPNCFDLI
YDYTFFCALDPTMRPSWALRHTQLLAPSPRGNLICLEFPRHKDPTQQGPPWGVSSEAYMEHLSHPGEQIPYDAQSRCKMDPL
REPSEHGLERVAYFQPARTHEGGKDSNGVVQDRVSIWRHR

13. The sequence of *Acl*HMT-WT

MSTPSLIPSGVHEVLAKYKDGNYVDGWAELWDKSKGDRLPWDRGFPNPALEDTLIQKRAIIGGPLGQDAQGKTYRKKALVP
GCGRGVDVLLLASFGYDAYGLEYSATAVDVCQEEQAKNGDQYPVRDAEIGQGKITFVQGDFFEDTWLEKLNLTRNCFDVIY
DYTFFCALNPSMRPQWALRHTQLLADSPRGHLICLEFPRHKDPSVQGPPWGSASEAYRAHLSHPGEEIPYDASRQCQFDSSKA
PSAQGLERVAYWQPERTHEVGKNEKGEVQDRVSIWQRPPQSSL

14. The sequence of *Acl*HMT-Mut

MSTVLLIPSGVHEVLAKYKDGNYVDGWAELWDKSKGDRLPWDRGFPNPALEDTLIQKRAIIGGPLGQDAQGKTYRKKALVP
GCGRGVDVLLLASFGYDAYGLEYSATAVDVCQEEQAKNGDQYPVRDAEIGQGKITFVQGDFFEDTWLEKLNLTRNCFDVIY
DYTFFCALNPSMRPQWALRHTQLLADSPRGHLICLEFPRHKDPSVQGPPWGSASEAYRAHLSHPGEEIPYDASRQCQFDSSKA
PSAQGLERVAYWQPERTHEGGKNEKGEVQDRVSIWQRPPQSSL

15. The sequence of *Aho*HMT-Mut

MSGPDVLAIQRKVMDTLAKYQGDNYVDGWAELWNSTEHLPWDKGAPHPALEDTLTQQRATIGGPLATDAQGKTYRKKALV
PGCGRGVDVLLLASFGYDAYGLEYSDAAVKKCESEAAQNGDRYPVRDAEVGRGKITFVQGDFFKNDWLERLQLPLNCFDLI
YDYTFLCALNPTMRPNWALRHTQLLAPSPRGNLICLEFPRHKDPAQQGPPWGLSSEAYMEHLSHPGEKIPYDAQGRCKMDPL
REPSEHGLERVAYWQPARTHEGGKDENGVVQDRVSIWRHR

16. The sequence of *Ati*HMT-Mut

MDSDVLTMQRKVRDTLAKYQGDDYVDGWAELWDKNENLPWDKGIPNPALEDTLIQQRATVGGPIATDAQGATYRKKALVP
GCGRGVDVLLLASFGYDAYGLEYSDAAVKICESEAAQNGDKYPVRDAGIGRGKIAFVQGDFFKNDWLESLQLPLECFDLIYD
YTFFCALNPTMRPSWALRHTQLLAPSPRGNLICLEFPRHKDPTQQGPPWGVSSEAYMEHLSHPGEQIPYDDQGRCKMDPLRE
PSEHGLERVAYFQPARTHEGGKDSNGVVQDRVSIWRHR

17. The sequence of *Ale*HMT-Mut

MDSDVLTMQRKVRDTLAKYQGDDYIDGWAELWDKNDNLPWDKGIPNPALEDALTQQRATLGGPIATDAQGATYRKKALVP
GCGRGVDVLLLASFGYDAYGLEYSDAALKICESEAAQNGDKYPVRDSGIGRGKIAFVQGDFFKNDWLESLQLPLNCFDLIYD
YTFFCALNPTMRPNWALRHTQLLAPSPCGNLICLEFPRHKDPTQQGPPWGVSSEAYMEHLSHPGEQIPYDAQGRCKMDPLRE
PSEHGLERVAYFQPARTHEGGKDSNGVVQDRVSVWRHR

18. The sequence of *Aam*HMT-Mut

MPPVLVAPQEVLDTLGKYQGDKVFDGWEELWKKGGDCLPWDRGIPNPALEDTLVQRRAILGGPITTDEQGNVHRKKALVPG
CGRGVDVLLLASFGYDAYGLEYSTSAVEECKQEETRNGDKYPVRDAKIGRGKITFVQGDFFQNNWLEALRLPMNCFDLTYD
YTFFCALNPSMRPDWALRHTQLLAPSPHGNLICLEFPRHKDPSKPGPPWGSSSEAYMEHLSHPGEKIPYDSNGRCKSDPLREIS
EQGLERVAHWQPVRTHEGGKDADGEIQDRVSVWRRR

Supplementary References

1 Li, Z., Wen, X., Bolotova, S. B. & Seebeck, F. P. Short-circuiting the SAM-cycle in escherichia coli. *J. Am. Chem. Soc.* **147**, 47690-47700 (2025).

2 Schmidberger, J. W., James, A. B., Edwards, R., Naismith, J. H. & O'Hagan, D. Halomethane biosynthesis: Structure of a SAM-dependent halide methyltransferase from arabidopsis thaliana. *Angew. Chem. Int. Ed.* **49**, 3646-3648 (2010).

3 Wen, X., Leisinger, F., Leopold, V. & Seebeck, F. P. Synthetic reagents for enzyme-catalyzed methylation. *Angew. Chem. Int. Ed.* **61**, e202208746 (2022).

4 Chovancova, E. *et al.* Caver 3.0: A tool for the analysis of transport pathways in dynamic protein structures. *PLOS Comput. Biol.* **8**, e1002708 (2012).

5 Wang, X. *et al.* Design, synthesis and bioactivity evaluation of fisetin derivatives as potential anti-inflammatory agents against lps-induced acute lung injury. *Biorg. Med. Chem.* **49**, 116456 (2021).

6 Zhang, J., Fu, X.-L., Yang, N. & Wang, Q.-A. Synthesis and cytotoxicity of chalcones and 5-deoxyflavonoids. *Sci. World J.* **2013**, 649485 (2013).

7 Ko, H. *et al.* Galangin 3-benzyl-5-methylether derivatives function as an adiponectin synthesis-promoting peroxisome proliferator-activated receptor γ partial agonist. *Biorg. Med. Chem.* **54**, 116564 (2022).

8 Shan *et al.* Semisynthesis of five bioactive flavonoids from hesperidin. *Chin. J. Org. Chem.* **28**, 1024-1028 (2008).